Journal of Environmental Chemical Engineering 13 (2025) 115174

Contents lists available at ScienceDirect

Journal of Environmental Chemical Engineering

journal homepage: www.elsevier.com/locate/jece

Recent advances in the preparation and applications in separation processes of electrospun nanofiber-based materials

Guoqiang Li [a,h,*], Waldemar Jankowski [a], Joanna Kujawa [a], Baturalp Yalcinkaya [b], Fatma Yalcinkaya [c], Diána Balogh-Weiser [d,g], Gergő Tóth [e], Ferenc Ender [f,g], Norman Sepsik [f], Wojciech Kujawski [a,*]

[a] Faculty of Chemistry, Nicolaus Copernicus University in Toruń, 7 Gagarina Street, 87-100 Toruń, Poland
[b] Department of Material Science, Faculty of Mechanical Engineering, Technical University of Liberec, Studenstká 1402/2, Liberec 461 17, Czech Republic
[c] Institute for Nanomaterials, Advanced Technologies and Innovation, Technical University of Liberec, Studentská 1402/2, Liberec 461 17, Czech Republic
[d] Department of Organic Chemistry and Technology, Budapest University of Technology and Economics, Műegyetem rkp. 3., Budapest 1111, Hungary
[e] Department of Physical Chemistry and Materials Science, Budapest University of Technology and Economics, Műegyetem rkp. 3., Budapest 1111, Hungary
[f] Department of Electron Devices, Budapest University of Technology and Economics, Műegyetem rkp. 3., Budapest 1111, Hungary
[g] Spinsplit LlC., Szőlőskert Street 0182/135, 2220, Hungary
[h] Institute of Chemical Technology and Engineering, Faculty of Chemical Technology, Poznan University of Technology, Berdychowo 4, Poznan 60-965, Poland

List of abbreviations: 17-FAS, trimethoxy (1H,1H,2H,2H-heptadecafluorodecyl) silane; 2D, two-dimensional; 3D, three-dimensional; AFM, atomic force microscopy; AGMD, air gap membrane distillation; A-MNM, atrazine molecularly imprinted nanofibrous membrane; APAN, aminated polyacrylonitrile; APTES, 3-aminopropyltriethoxysilane; ATO, antimony tin oxide; BSA, bovine serum albumin; BT-DG, guanidinium-based ionic covalent organic framework; CA, cellulose acetate; CA, citric acid; CAB, cellulose acetate butyrate; CB, carbon black; CEW, chicken egg white; CH, collagen hydrolysate; CNF, carbon nanofiber; CNFs, carbon nanofibers; COFs, covalent organic frameworks; CS, carbon sphere; Ch, chitosan; CTA, cellulose triacetate; CTAB, cetyltrimethylammonium bromide; DAG, diaminoglyoxime; DCM, dichloromethane; DCMD, direct contact membrane distillation; DETA, diethylenetriamine; DMAc, dimethylacetamide; DMF, dimethylformamide; DMG, dimethylglyoxime; DMSO, dimethyl sulfoxide; DSC, differential scanning calorimetry; DTPA, diethylenetriaminepentaacetic acid; EC, ethyl cellulose; ECNFs, electrospun carbon nanofibers; ELD, electroless deposition; ENMs, electrospun nanofiber membranes; ES, electrospinning; FDTS, 1H,1H,2H,2H-perfluorodecyltrichlorosilane; FCS, freeze-dried chitosan; FE, filtration efficiency; FG, fluorinated graphite; FO, forward osmosis; GA, glutaraldehyde; G-C_3N_4, Graphitic carbon nitride; Ge, gelatine; GO, graphene oxide; GO-OCNTs, graphene oxide and oxidized carbon nanotubes; Hal-HH2, amine-grafted halloysite nanotube; HB-Den, hyper-branched dendritic; HFIP, hexafluoroisopropanol; HFP, hexafluoropropylene; HKUST, Hong Kong University of Science and Technology; HOFs, hydrogen-bonded organic frameworks; HPEI, hyperbranched polyethylenimine; ICP, internal concentration polarization; IONP, ultra-small nanoparticle; IP, interfacial polymerization; iPP, isotactic polypropylene; KTS, potassium tin sulfide; LDH, layered double hydroxides; M, molecular weight; MCF-5, mesocellular silica foam; MD, membrane distillation; MED, multi-effect distillation; MEK, methyl ethyl ketone; MFD, multi-flash distillation; MO, *Moringa oleifera*; MOFs, metal organic frameworks; MPD, *M*-phenylenediamine; MWCNTs, multi-walled carbon nanotubes; NaCl, sodium chloride; NCMs, nanofibrous composite membranes; NF, nanofiltration; NPs, nanoparticles; PA, polyamide; PA6, polyamide 6; PAA, polyacrylic acid; PAH, polyallylamine hydrochloride; PAN, polyacrylonitrile; PANi, polyaniline; PCA, poly citric acid; PCL, polycaprolactone; PDA, polydopamine; PDMS, polydimethylsiloxane; PDTS, 1H,1H,2H,2H-perfluorodecyl-triethoxysilane; PEG, polyethylene glycol; PEI, polyethyleneimine; PEI, poly(ethyleneimine); PEN, poly(arylene ether nitrile); PEO, poly(ethylene oxide); PES, polyethersulfone; PET, poly (ethylene terephthalate); PS, polyester; PFBA, perfluorobutanoic acid; PFBS, perfluorobutanesulfonic acid; PFO, pseudo-first-order; PFOA, perfluorooctanoic acid; PFOS, perfluorooctanesulfonic acid; PH, poly(vinylidene fluoride-*co*-hexafluoropropylene); PLA, polylactic acid; PLGA, poly(lactic-*co*-glycolic) acid; PM, particulate matter; PMIA, poly(m-phenylene isophthalamide); PMMA, poly(methyl methacrylate); PNIPAAm/PNIPAM, poly(N-isopropylacrylamide); POSS, polyhedral oligomeric silsesquioxanes; POTS, 1H,1H,2H,2H-perfluorooctyltriethoxysilane; PPD, p-phenylenediamine; P-PLLA, porous poly (L-lactic acid); PPy, polypyrrole; PS, persulfate; PS, polystyrene; PSf, polysulfone; PSO, pseudo-second-order; PTFE, polytetrafluoroethylene; PUR/PU, polyurethane; PVA, polyvinyl alcohol; PVC, polyvinyl chloride; PVDF, polyvinylidene fluoride; PVDF-HFP, polyvinylidene fluoride-*co*-hexafluoropropylene; PVP, polyvinylpyrrolidone; RO, reverse osmosis; SA, sodium alginate; SDBS, sodium dodecylbenzene sulfonate; SDMD, solar-driven membrane distillation; SDS, sodium dodecyl sulfate; SEBS, styrene block copolymer polystyrene-b-(ethylene-*co*-butene)-b-styrene; SEM, scanning electron microscopy; SERS, surface-enhanced Raman spectroscopy; SF, silk fibroin; SP, sodium periodate; SPES, sulfonated polyethersulfone; SPME, solid phase microextraction; SSAS, poly(sodium styrene sulfonate–*co*–acrylonitrile–*co*–styrene); TA, tannin; TA, tannic acid; TEA, triethylamine; TEM, transmission electron microscopy; TEOS, tetraethyl orthosilicate; TFA, trifluoroacetic acid; TFNC, thin-film nanofibrous composite; Tg, glass transition temperature; TMC, 1,3,5-trimesoylchloride; TMOS, tetramethyl orthosilicate; TNPs, TiO_2 nanoparticles; TPU, thermoplastic polyurethane; UF, ultrafiltration; VD, vapor deposition; WCA, water contact angle; XRD, X-ray diffraction; ZIF, zeolitic imidazolate framework; ZP, zwitterionic phosphate; β-CD, β-cyclodextrin.

* Corresponding authors at: Faculty of Chemistry, Nicolaus Copernicus University in Toruń, 7 Gagarina Street, Toruń 87-100, Poland.
E-mail addresses: guoqiang.li@put.poznan.pl (G. Li), wkujawski@umk.pl (W. Kujawski).

https://doi.org/10.1016/j.jece.2024.115174
Received 20 October 2024; Received in revised form 12 December 2024; Accepted 18 December 2024
Available online 22 December 2024

ARTICLE INFO

Keywords:
Electrospinning technique
Nanofibers
Surface modification
Adsorption
Separation
Desalination

ABSTRACT

Electrospinning has shown its versatility and feasibility for the fabrication of nanofiber based materials which possess various advantages in separation processes. Electrospun nanofibers exhibited interconnectivity between pores, high specific surface area and ratio of surface area to volume. Therefore, the application of electrospun nanofiber materials in tackling the environmental challenges has drawn great attention in academia and industry. This review provides the current advancement of electrospun nanofiber based materials and applications in separation processes. Firstly, the fundamentals of electrospinning, the key factors of electrospinning process and the characterization methods for nanofibers were introduced. Then the modification methods for electrospun nanofiber-based materials were discussed. Next, the applications of electrospun nanofiber-based materials in separation processes, e.g., water treatment processes, desalination, air filtration, and the separation of biological compounds were comprehensively reviewed and critically discussed. Last but not least, despite the advancements in the fabrication and application of electrospun nanofiber-based materials, the scale-up the electrospun nanofiber production in industry still faces several problems which must be further addressed.

1. Introduction

Among various environmental challenges, water scarcity and air pollution have attracted great attention, owing to the continuous growth of the global population and the fast advancement of urbanization and industrialization. The need for pure air and water has grown dramatically [1,2]. Human life and health are at risk owing to the fine particulate matter (PM) in the air. PMs mainly consist of dust, sulfates, ammonia, nitrates, sodium chloride, black carbon, and water [1]. Particularly, PM 2.5 has a lengthy airborne residence time, and small particle size, which makes it more harmful to human's respiratory system [1]. Therefore, it is important to develop air filters for protection from air pollutants. The improper disposal of wastewater from various discharge sources, such as industrial sectors, agricultural activities, and mining, has deteriorated water quality, resulting in many health problems [3]. The separation of pollutants such as heavy metals, dyes, organic contaminants, medical compounds, and biological compounds from water environment is crucial to obtain potable and safe water [4–6]. Additionally, the desalination of seawater is another promising way to deal with water scarcity. Membrane distillation has been used in seawater desalination [7]. Membrane-based separation methods and adsorption have been studied and used in wastewater treatment processes owing to their smaller carbon footprint and cost-effectiveness [8].

The nanofiber is defined as a type of nanomaterial fiber with cross-sectional diameters that are less than 100 nm [9]. Electrospun nanofiber materials have obtained a lot of attention in wastewater treatment, seawater desalination, and air filtration owing to their advantages, such as smaller and controllable fiber diameter, high surface area and porosity, elevated ratio of surface area to volume, ease of surface functionalization, and desirable connectivity of inner pores [10–14]. In the wastewater treatment process, nanofibrous membranes work more effectively for surface adsorption of pollutants, owing to their elevated ratio of surface area to volume and tunable functionality [2]. What is more, nanofibrous membranes demonstrated higher flux at low pressure and lower fouling tendency than the conventional membranes [2]. In comparison to the commercial membranes, electrospun nanofibrous membranes fabricated from the same polymers showed higher permeability and antiwetting properties in membrane distillation since they have higher hydrophobicity, highly porous interconnected structure, and higher surface roughness [15,16]. In the air filtration process, electrospun nanofibrous membranes showed high filtration efficiency and low air resistance owing to their three-dimensional (3D) structure, desirable pore connectivity, and the strong interface effect [10,17–23]. Electrospun nanofibers can also be used as adsorbents to remove pollutants from wastewater in adsorption processes. Nanofiber adsorbents demonstrated higher adsorption capacity, faster adsorption rate, and easier regeneration and recyclability than conventional adsorbents [24,25].

This work provides a critical review on the preparation, modification and applications in the separation processes of electrospun nanofibers from 2020 to 2023. The significance of this work shed light on the fabrication, modification, and utilization of electrospun nanofibers and nanofibrous membranes in the separation processes, especially in the water treatment processes, membrane distillation processes, and air filtration processes. Most importantly, there is a great potential for the large-scale production of electrospun nanofibers and their scale-up applications in separation processes.

2. Fundamentals of fabrication of electrospun nanofibers

2.1. What is electrospinning?

In the fields of material science and engineering, electrospinning is an important technique for fabricating nanofibers. It involves ejecting a charged polymer solution or melt through a nozzle and stretching it into fine fibers under the influence of an electric field [26]. These nanofibers exhibit a high surface-area-to-volume ratio, making them valuable for applications such as filtration processes [27], tissue engineering [28], energy storage [29] and drug delivery [30]. Moreover, electrospinning is a versatile technique, compatible with a wide range of materials, including polymers, ceramics [31], and composites [32]. The process also allows for precise tuning of the structure and properties of the resulting nanofibers, rendering it suitable for various industrial and biomedical applications. Additionally, electrospinning holds significant potential for scaling up to mass production, making it a promising technology for commercial use [33].

2.2. Types of electrospinning set-up

2.2.1. Fundamental electrospinning apparatus

The electrospinning technique is based on transforming polymer solutions into ultra-thin fibers with diameters reaching the nanoscale, done by applying an electrical force. The apparatus required for this process is notably basic and easy to procure, consisting of a syringe with a needle from which the solution is pumped, a grounded conductive collector, and a high voltage source. The application of this high voltage reshapes the droplet of polymer solution at the needle's end into a conical structure as a result of the electrostatic forces at play, named the "Taylor cone" after Sir Geoffrey Ingram Taylor, a British physicist who first described the phenomenon in the 1960s [34]. This intense electrical field initiates and drives the electrospinning, manipulating the dimensions of the jetting solution from the needle tip to achieve an equilibrium of forces [35].

Advancements in technology and a rising interest have spurred the development of various electrospinning methods that cater to large-scale production of differentiated fiber characteristics. This expansion has greatly enhanced the portfolio of electrospun materials, thus widening the spectrum of their applications. In sections to follow, we will explore cutting-edge alterations to the electrospinning apparatus, focusing on the collector and spinneret modifications. Fig. 1 illustrates

the typically used electrospinning systems in the laboratory and industrial scale. Besides to the obvious difference in the size of the equipment, it could be noted that the commonly applied voltage (up to 40 kV vs. 140 kV), and the number of emitters (up to 10 vs. 6000) also differ. In the case of scale-up machines, emitters are usually built up from a wire with lot of tips, and the collector is a rotating cylinder.

2.2.2. Melt electrospinning

Melt electrospinning (Fig. 2) is a variation of electrospinning that allows fiber manufacturing to be done not only with polymer solutions but also with polymer melts. This particular approach is a significant subset of electrospinning, offering advantages in avoiding certain drawbacks of solution electrospinning [36]. Additionally, this method enables the formation of nanofibers from polyolefins [37] like polyethylene [38] and polypropylene [39], which lack appropriate solvents at ambient temperatures, as well as from complex polymer blends that are challenging when it comes to identifying a mutual solvent. The primary constraint of melt electrospinning is that it typically results in fibers with discernibly larger diameters when compared to those produced by solution electrospinning [40]. Consequently, research into melt electrospinning has been somewhat constrained.

2.2.3. Bubble electrospinning

Introduced in 2007 [42], bubble electrospinning largely relies on the characteristics of bubbles, specifically their size, generated on the surface of a polymer solution. This technique is regarded as part of the needleless electrospinning technologies and diverges from the traditional technique by generating polymer bubbles in place of the Taylor cone to form polymeric fibers. Instead of relying on the surface tension of a droplet, polymer bubbles are created, and the inherent surface tension is overcome. The typical bubble electrospinning apparatus (Fig. 3) facilitates the creation of polymer bubbles using substantial air pressure provided by an air pump. Concurrently, an electric charge from a high-voltage power source is applied to surmount the bubbles' surface tension. At a specific voltage threshold, several jets exit from these bubbles, and a collector is positioned to gather the resulting fibers. Controlling the number, size, shape, and consistency of the bubbles that arise on the polymer solution's surface represents a challenge in this technique [43].

2.2.4. 3D electrospinning technologies

Traditional electrospinning is instrumental in creating two-dimensional (2D) nanofiber mats or membranes that are crucial for various uses. Moreover, by refining and evolving this classic technique, electrospinning has considerable potential to fabricate 3D nanofibrous frameworks that boast enhanced qualities. To date, several techniques have been developed to prepare 3D electrospun nanofibers, including methods such as wet electrospinning [45], coaxial-wet electrospinning [46], template-based electrospinning [47], incorporation of porogens within electrospinning [48], use of a cold collection plate [49], emulsion electrospinning, and centrifugal spinning [50]. The introduction of a significant third dimension in 3D structures garners advantages like increased surface area, a greater number of connected pores or channels, and augmented porosity.

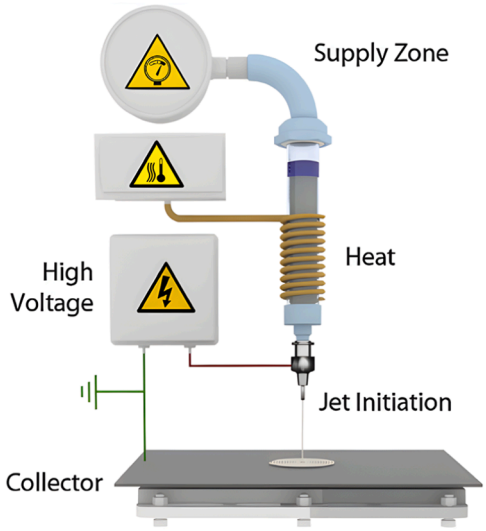

Fig. 2. Illustrated scheme of a melt electrospinning apparatus. The figure highlights key components, including the supply zone, heat source, high voltage power supply, and collector, essential for the jet initiation and fiber formation processes.
Reproduced with permission from ref. [41]. Copyright 2016 Elsevier.

2.2.5. Wet electrospinning

Wet electrospinning involves the deposition of a polymer solution on a non-solvent liquid coagulant (Fig. 4). It yields 3D nanofiber scaffolds

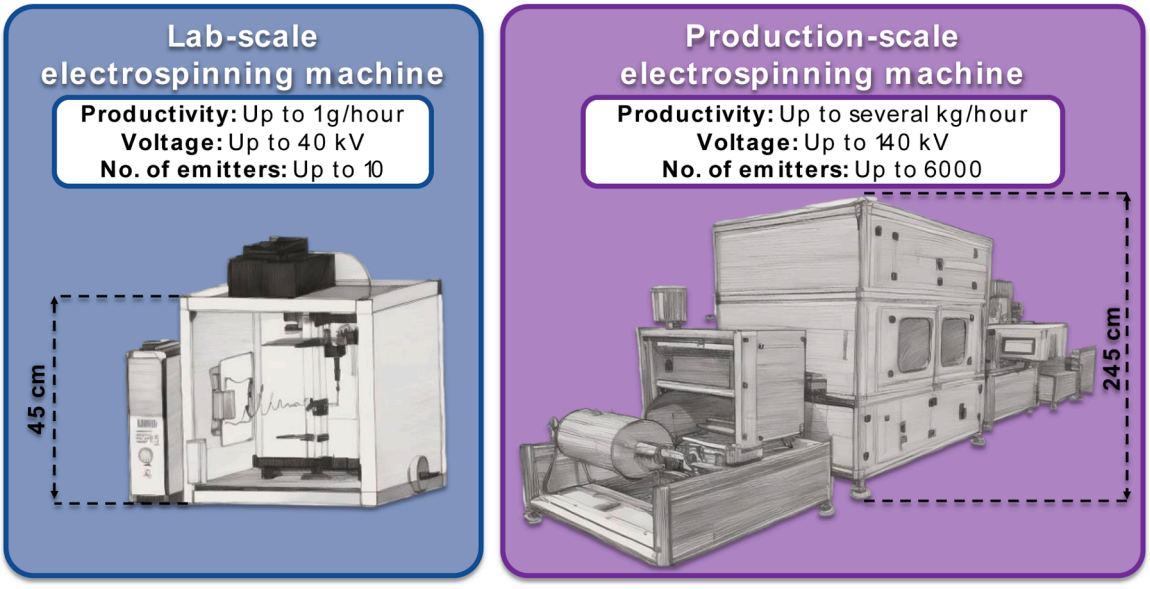

Fig. 1. Schematic illustration of typical electrospinning equipment at laboratory scale (left side) and industrial scale (right side).

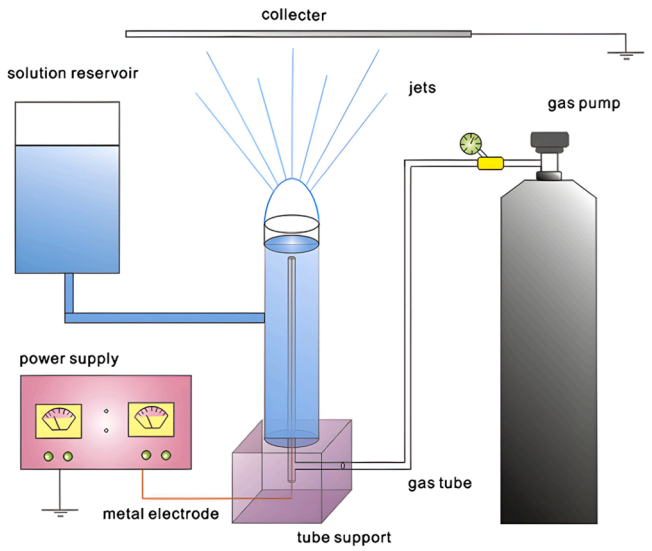

Fig. 3. Schematic illustration of the bubble electrospinning apparatus, highlighting its essential components. This setup enables the generation of multiple jets from a bubble formed at the solution's surface.
Reproduced with permission from ref. [44]. Copyright 2009 Elsevier.

with enhanced properties such as higher porosity and increased surface area. The procedure typically entails a polymer solution housed within a syringe connected with a pump, which administers the solution at a controlled flow rate while subjecting it to high voltage to induce fiber formation. These fibers are submerged in a coagulation bath, acting as a collector, where the solution solidifies to generate elongated fibers ranging between 30 to 600 μm in diameter [51].

2.2.6. *Template-based electrospinning*

Template-based electrospinning is a technology that uses a template, such as one made by 3D printing (Fig. 5) [47], to direct the development of electrospun fibers. Template-based electrospinning demonstrates some advantages, including the ability to create complex fiber structures and patterns, improved control over fiber alignment and orientation, and the potential for integrating functional materials within the fiber network [53].

2.2.7. *Cold-plate electrospinning*

The fundamental idea of cold-plate electrospinning is to use a temperature-controlled cold plate as the collector for the electrospun fibers. This process allows for the simultaneous formation of ice crystals and the collection of nanofibers, resulting in a more porous and flexible scaffold than conventional electrospinning procedures. The cold plate is

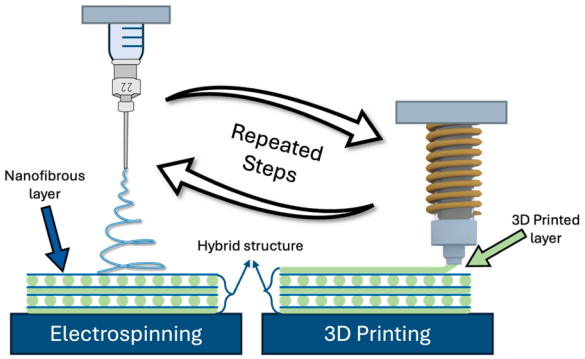

Fig. 5. Illustration of template-based electrospinning integrated with 3D printing technology. The approach enables the creation of complex fiber structures and patterns, improved alignment and orientation of fibers. The illustration is adapted from the article titled "New 3D Printing Technique Unleashes New Surgical Mesh Designs and Properties".
Published on 3D4Makers.com (Copyright 2023, 3D4Makers.com), based on the work of Sterk et al. [54].

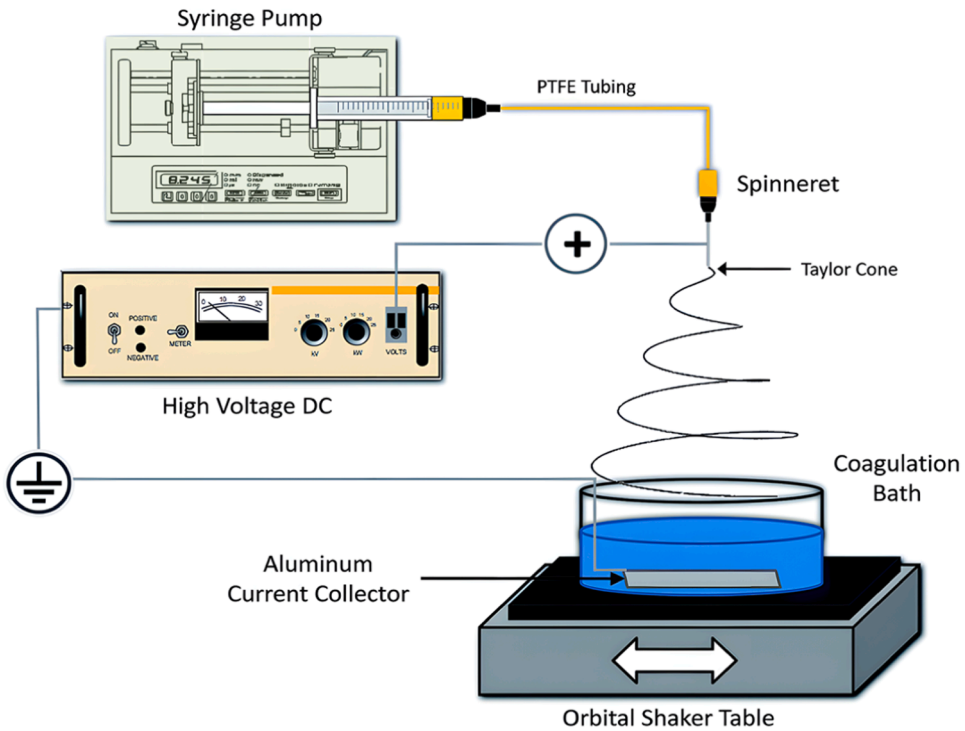

Fig. 4. Schematic representation of the key components of a wet electrospinning setup, illustrating the syringe pump, spinneret, high-voltage power supply, coagulation bath, current collector, and orbital shaker.
Reproduced with permission from ref. [52]. Copyright 2014 Royal Society of Chemistry.

kept at a temperature below the freezing point of the electrospinning precursor solution, causing it to solidify upon contact. This solidification process induces the formation of ice crystals, which supports the electrospun nanofibers. The fibers are subsequently deposited onto the ice crystals, resulting in a 3D nanofiber scaffold (Fig. 6) [49,50].

2.3. Modules of an electrospinning equipment

Among mandatory and optional electrospinning modules, the emitter and the collector modules are available in several forms, and they are essential to the nanofiber fabrication process.

2.3.1. Special emitters

The emitter, which allows polymer solution to be charged and dispensed, is crucial to every electrospinning setup. The most typical emitter is a flat-tipped metal nozzle. Typically, a flat tip is favored because it offers a level surface that facilitates the development of a stable Taylor cone and results in minimal fluctuation in the jet, in contrast with needles with chamfered tips [56].

2.3.1.1. Coaxial emitter. Coaxial electrospinning is a variation of the standard electrospinning process and is used for creating core-shell structured nanofibers [57]. This technique involves using two or more concentric needles, collectively called a coaxial spinneret (Fig. 7). Each needle accommodates a distinct polymer solution or melt; conventionally, the core solution traverses through the inner needle, while the shell solution is pumped through the outer needle.

2.3.1.2. Gas-jet coaxial emitter. Gas-jet, or gas-assisted coaxial electrospinning, represents a variation of the conventional coaxial electrospinning process that involves using a gas to assist in forming the coaxial structure and the ejection of the jet. The gas is introduced via the outer emitter needle to initiate the jet, sustain the continuity of the spinning jet, guide the electrospinning process, and enhance the rate of fiber deposition [59]. The introduction of gas through the inner needle to the electrospinning process also has the potential to boost nanofiber production efficiency significantly [60].

2.3.1.3. Multi needle emitters. Spinnerets with multiple needles (Fig. 8) are employed in electrospinning to generate a series of polymer solution jets, thus facilitating a greater nanofiber output rate than systems that utilize a single needle. These spinnerets come in diverse configurations, including patterns like equilateral hexagons, circles, V-shaped arrays, and straight lines, with varying needle counts for each array [61]. The advantages offered by these multi-needle systems include enhanced control over the nanofiber deposition on the collector and the capability to manufacture sheets of nanofibers with uniform characteristics [61]. Moreover, the integration of gas assistance in multi-needle electrospinning setups has been explored as a technique to significantly step up nanofiber production rates [62].

2.3.1.4. Needleless emitters. In the quest to amplify the productivity of the electrospinning process, several specialized emitters have been developed to replace traditional needle-based systems. Free-surface emitters, which substitute needles with geometrically arranged openings on a charged surface, have emerged as a novel category. This group encompasses diverse designs such as hollow tube spinnerets, flat and stepped spinnerets, and porous tube electrospinning, each contributing to an increased surface area for fiber formation. Another innovative approach involves bath emitters, which utilize rotating geometric shapes partially dipped in the precursor solution. These shapes adsorb the solution on their surfaces and, upon rotation, carry it closer to the collector where electrospinning occurs. This category includes various configurations like rotating wire, spiral coil, ring coil, cylinder, disc, and spherical ball electrospinning, each allowing continuous coating of the emitter with precursor and enabling sustained fiber production. Lastly, reservoir emitters take advantage of a filled precursor reservoir from which electrospinning commences as soon as spillover occurs. Techniques such as bowl-edge electrospinning and corona electrospinning from a sharp-edged circular spinneret fall under this classification, enabling consistent and uninterrupted fiber generation. Collectively, these advanced emitter designs significantly contribute to the upscaling

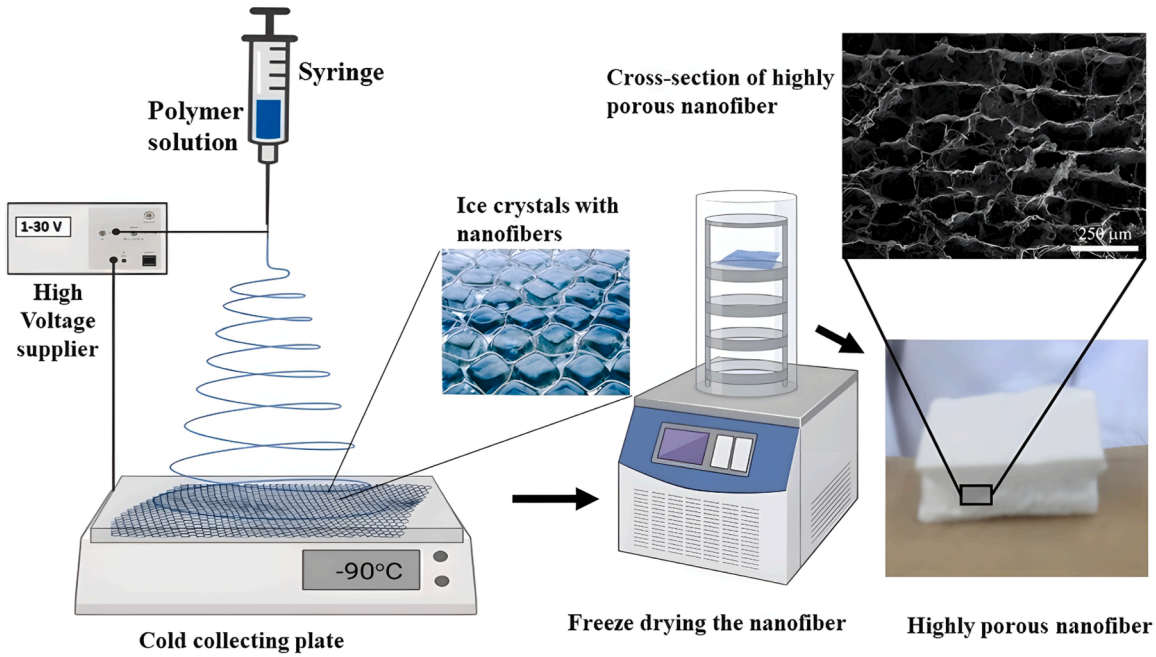

Fig. 6. Schematic representation of cold-plate electrospinning. The cold plate, maintained below the freezing point of the precursor solution, causes the solution to solidify upon contact, forming ice crystals that support the deposition of nanofibers. This method produces a porous and flexible 3D scaffold by freeze-drying the ice crystal-nanofiber composite, as shown in the cross-sectional SEM image and the final highly porous nanofiber structure.
Reproduced with permission from ref. [55]. Copyright 2023 Elsevier.

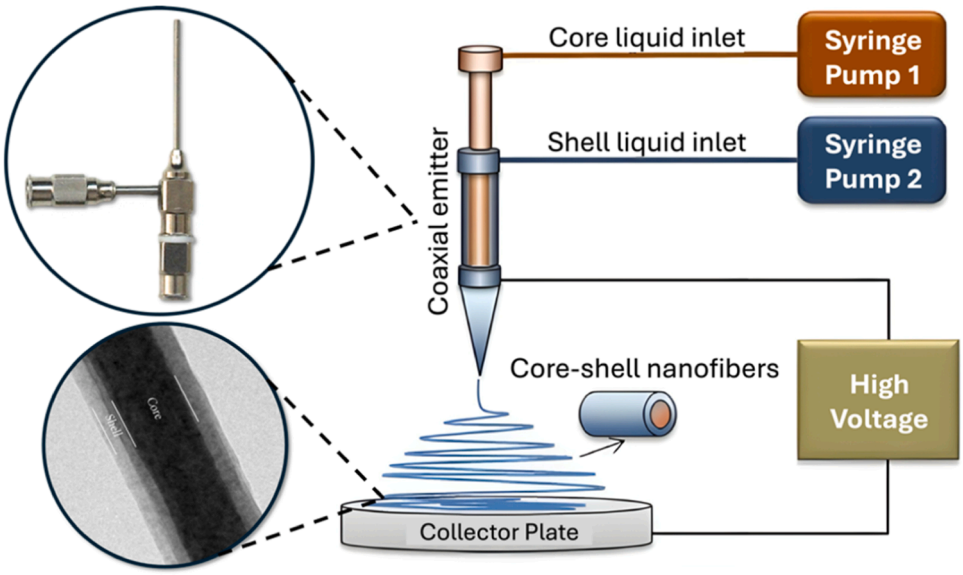

Fig. 7. Schematic representation of coaxial electrospinning, illustrating the use of a coaxial emitter to simultaneously extrude core and shell liquids from separate syringe pumps to produce core-shell nanofibers, as visualized on the collector plate. The magnified images show the coaxial emitter design and a TEM image of a core-shell nanofiber structure. (Reproduced with permission from ref. [58]. Copyright 2015 Springer).

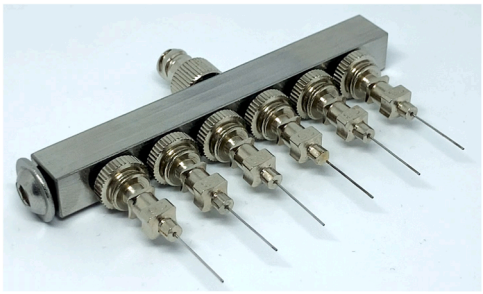

Fig. 8. Photograph of a multi needle emitter used for electrospinning. It is equipped with an array of aligned needles designed to enhance throughput and scalability in nanofiber production.

of electrospinning, thus addressing the need for high-throughput production of nanofibers [61]. Fig. 9 presents photographs of representative needleless emitters, illustrating diverse designs, all of which enable efficient large-scale nanofiber production.

2.3.1.5. Motorized moving emitter. The advent of moving emitters in electrospinning represents a significant advancement in the field aimed at optimizing the uniformity and quality of electrospun nanofibers. The dynamic movement of the emitter can play a crucial role in enhancing the homogeneity of the produced nanofibrous structures. As the emitter traverses, the ejected polymer jets are systematically deposited along the full extent of the collector, which is notably advantageous when employing rotating collectors and leads to an even distribution of the polymer material. Such uniformity manifests in a final product with improved consistency in thickness. Moreover, the emitter's locomotion elevates the electrospinning procedure's overall efficiency and output [67].

2.3.2. Special collectors

The plate collector stands as the most prevalent and rudimentary form of collector utilized in electrospinning processes, renowned for its straightforward design and general effectiveness. While this type of collector is entirely competent for a broad range of applications, it does present notable limitations, particularly in certain specialized fields. One of these drawbacks is the non-uniform thickness that often occurs along the radial axis of the electrospun product, which can be detrimental to applications requiring precise dimensional control. Another significant impediment is the random orientation and deposition of nanofibers on the collector surface, a factor that restricts its use in applications demanding highly ordered fiber structures. These inherent limitations have initiated the research and adoption of alternative, specialized collector types in the field of electrospinning.

2.3.2.1. Static collectors. Innovative approaches include the use of parallel electrodes to align fibers by creating an air gap that causes the electrospinning jet to oscillate, resulting in fibers that align neatly between the electrodes. The dynamics of this process have been observed through high-speed photography, revealing that fibers initially attach to one electrode before spanning across to the opposite one [68]. Subsequent adaptations to this method have produced diverse fiber architectures. Using a series of parallel electrodes has been effective in gathering intersecting nanofibers at their nexus [69]. Meanwhile, positioning two pointed edges in a linear arrangement with an intervening space has been effective in forming bundles of nanofibers. Alternatively, arranging these edges parallel to each other facilitates the assembly of a denser aligned fiber mesh. These various collector modifications have thus expanded the versatility of electrospun fiber structures [70].

These examples demonstrate that it is possible to achieve ordered nanofibrous structures by altering the electric field during electrospinning. By utilizing tailored electric fields, the trajectory of the jet can be precisely controlled. Based on this foundational principle, the adoption of specially designed collectors enables the manipulation of fiber layout, leading to enhanced structure control and the realization of highly organized nanofibrous assemblies.

2.3.2.2. Bath collectors. In electrospinning processes where the solution cannot adequately dry during its journey from the spinneret to the collector, a specialized setup becomes necessary. This situation is frequently encountered with specific water-soluble polymers, as their fibers may not achieve sufficient dryness upon reaching traditional solid collectors. To address this challenge, a coagulation bath collector is employed and strategically positioned at a defined distance from the needle tip similar to the setup presented in Fig. 4. As the fibers traverse and enter this liquid medium, they become immersed in a substance,

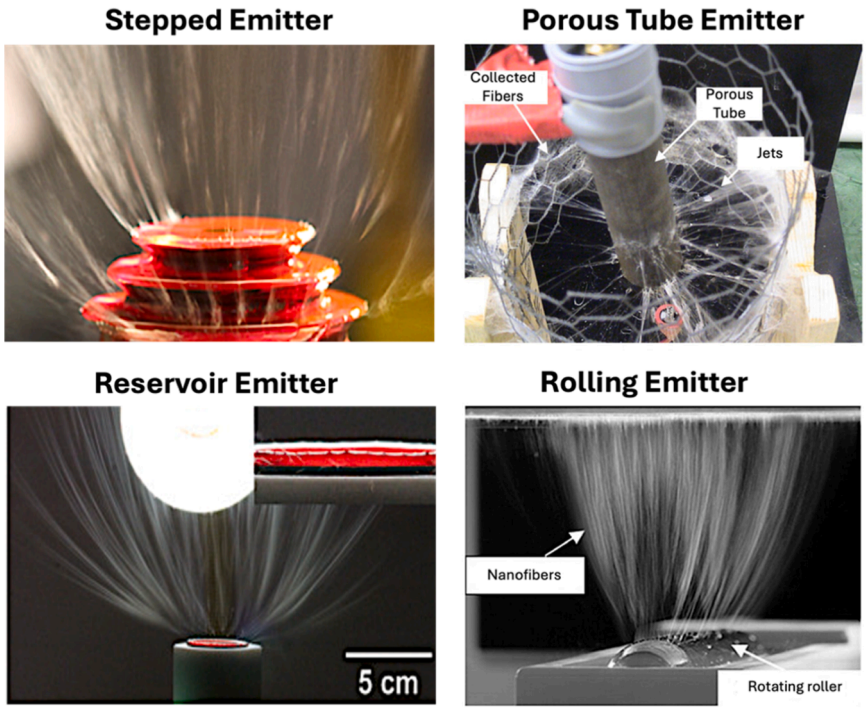

Fig. 9. Photographs of various needleless electrospinning emitters. (Top left) Stepped emitter, where fibers are generated from the edges of a stepped structure. (Top right) Porous tube emitter, showing multiple jets forming on the surface of a porous tube. (Bottom left) Reservoir emitter, utilizing a filled precursor reservoir from which electrospinning commences as spillover occurs. (Bottom right) Rolling emitter, demonstrating fiber formation from the rotating roller surface. These configurations allow for large-scale nanofiber production.
Reproduced with permission from ref. [63]. Copyright 2015 Elsevier. Reproduced with permission from ref. [64]. Copyright 2006 IOP Publishing. Reproduced with permission from ref. [65]. Copyright 2019 Elsevier. Reproduced with permission from ref. [66]. Copyright 2012 Wiley.

typically a non-solvent for the polymer, such as ethanol. This coagulation solution not only expedites the removal of water to prevent fiber fusion but also promotes the solidification and purification of the fibers [71]. Water can also be an excellent choice for the coagulation bath medium, as it is known to be insoluble in most non-polar polymers and thus may be used as an effective non-solvent for many polymers [72,73]. A simple adjustment to this arrangement is to agitate the water bath using a simple magnetic stirrer, resulting in a rotating bath that may be utilized to aid the creation of circumferentially aligned nanofibers [74].

2.3.2.3. Rotating collectors. Rotating collectors have marked a significant advancement in the field of electrospinning, proving superior to traditional static plate collectors. They enhance the production of nanofibers by enforcing a uniform thickness and orderly arrangement, primarily aligning the fibers along a single axis as opposed to the chaotic orientations seen with a static collection. A variety of forms, including mandrels, wire drums, disc-like wheels, conical shapes, and skeletal frames, are among the rotating structures often employed. Their pivotal role in the precise control of nanofiber alignment and uniform distribution is paramount, leading to the generation of structured nanofibrous materials characterized by consistent thickness and alignment [75,76]. Fig. 10 presents a typical rolling drum collector used for the production of oriented nanofibers.

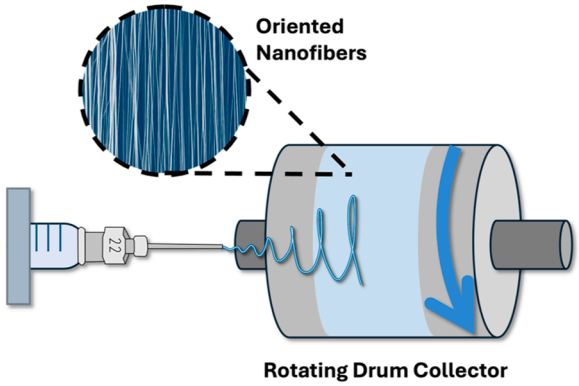

Fig. 10. Schematic representation of a rotating drum collector for electrospinning, designed to produce oriented nanofibers. The high-speed rotation of the drum aligns the fibers as they are deposited, resulting in the uniform and directional arrangement shown in the magnified view.

2.4. Influencing factors of the electrospinning process

In electrospinning technology, a diverse array of parameters can be delicately adjusted to generate various nanofiber architectures. These parameters neatly fall into three primary categories: precursor solution parameters, electrospinning process parameters, and environmental parameters. Among these three factors, environmental conditions have received comparatively less attention in research, primarily because effectively controlling them poses significant challenges. Additionally, isolating the study of environmental conditions proves challenging, as alterations in these conditions can impact other aspects of the process. For instance, elevating the temperature may lead to a decrease in solution viscosity, and a reduction in pressure can enhance solvent volatility. The two dominant sets of factors, such as precursor parameters and process parameters, are shown in Fig. 11. The precursor parameters and electrospinning process parameters show crucial effects on the structure and morphology, *e.g.* porosity, surface area, nanofiber diameter distribution, membrane thickness, and surface-area-to-volume ratios of electrospun nanofiber membranes, which affects the performance, *e.g.* flux and separation efficiency, of electrospun nanofiber membranes. The effects of precursor parameters and electrospinning process parameters on the properties of electrospun nanofibers

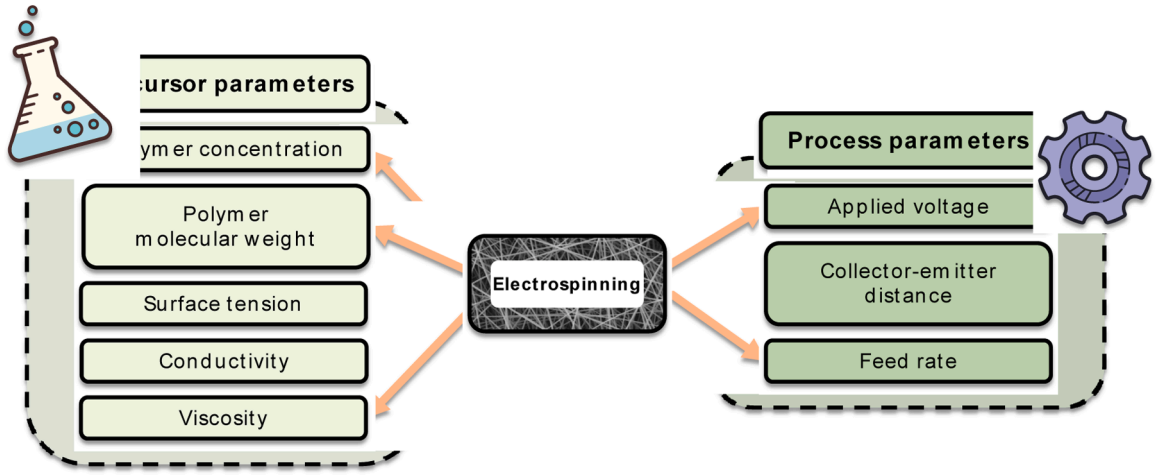

Fig. 11. The basic set of parameters in the electrospinning process, precursor parameters and process parameters.

will be briefly discussed in Sections 2.4.1 and 2.4.2, respectively.

2.4.1. Precursor solution parameters

Polymer concentration is one of the precursor features that is most important in maintaining the fibrous structure. It also affects other properties, including surface tension, solution viscosity, and electrical conductivity. A proper polymer concentration is crucial for producing uniform nanofibers and minimizing bead formation, as insufficient concentrations often result in the formation of beads due to inadequate viscoelasticity [77,78]. While increasing polymer concentration generally improves the viscoelastic performance of the solution, enabling it to better withstand the electrostatic forces during electrospinning and forming smooth fibers, it is important to note that other factors, including polymer type, molecular weight, and solvent system, also play a significant role. Furthermore, excessive polymer concentrations can lead to an undesirable increase in solution viscosity, which may prevent the disruption of the Taylor cone, ultimately compromising the electrospinning process. Thus, an optimal polymer concentration must be carefully selected to balance these effects and achieve the desired nanofiber morphology [79,80].

The molecular weight (M) of the polymer precursor significantly influences the electrospinning process and the properties of the resulting nanofibers. Increasing M in the precursor solution has effects similar to those of elevated polymer concentration. The increase of M of the polymer can substantially decrease the critical polymer concentration necessary in the precursor for the production of smooth nanofibers *via* electrospinning [81].

When the surface tension of the precursor solution is reduced, a lower onset voltage is sufficient to overcome the cohesive force provided by the surface tension and, consequently, start the electrospinning process [82]. Furthermore, it was discovered that when solvents with lower surface tension, such as ethanol, were used to produce precursors, the electrospinning experiment resulted in smooth, uniform fibers; however, when solvents with higher surface tension, such as dimethylformamide (DMF), were used to create precursors, the electrospun fibers exhibited significant beading [83].

In the electrospinning process, the extension of charged liquid into fibers occurs due to charge repulsion, which is why adequate charge transfer from the power supply to the polymer in solution during electrospinning is crucial. This process is intricately linked to the solvent's conductivity. A higher conductivity results in the formation of more ions on the polymer molecules, leading to thinner fibers as charge repulsion becomes a dominant effect. Introducing a small amount of polyelectrolyte (salts) to the precursor proves effective in eliminating fiber bead formation, as it enhances the number of charges and aids in elongating the jet to produce uniform fibers. It is noteworthy that electrospinning of polymer solutions encounters challenges at very high voltages, and fiber formation becomes impossible when the solution lacks conductivity. Also, extensively high conductivity can lead to the formation of multi-jets from the precursor droplet and protrusions in the fiber morphology [84,85].

The electrospun nanofibers' diameter and shape are heavily influenced by the viscosity of the polymer solution, a factor determined by various polymer properties such as M and polymer solution concentration, as mentioned above. To summarize shortly, elevating the polymer's M or concentration in the precursor solution leads to an increase in solution viscosity. It is important to note that excessively high viscosity poses challenges in the electrospinning process, making it difficult to pump the solution through the syringe pump.

2.4.2. Electrospinning process parameters

The applied voltage is a critical parameter in the electrospinning process, as it governs the number of charges carried by the jet, modulates the electrostatic repulsion among those charges, and defines the interactions between the jet and the external electric field. This voltage must be calibrated with precision; it should be elevated enough to overcome the droplet's surface tension to initiate jet formation, yet excessive voltage can destabilize the jet, potentially causing the ejection of multiple jets and leading to inconsistencies in the process [86]. Usually, when the strength of the electric field is increased, there is a corresponding rise in fluid volume ejected, producing a thicker jet and ultimately yielding fibers of greater diameter [87]. An increase in the applied voltage not only changes the morphological properties of the fibers but also affects the deposition rate of the process, causing a greater volume of product to be accumulated on the collector plate in a given length of time.

During electrospinning, the distance between the emitter, where the fibers start, and the collector, where they end up, is important for controlling the size and shape of the nanofibers produced. This distance needs to be just right so that the solvent in the fibers has enough time to evaporate, leaving dry fibers at the collector. If this distance is too short, the fibers may not dry fully, and you'll get wet fibers. Longer distances typically mean thinner fibers, but if the distance is too long or too short, the fibers might end up with unwanted beads. It is also important to note that the distance separating the emitter from the collector influences the strength of the electric field, meaning that greater distances can necessitate higher critical voltages to initiate the electrospinning process [88].

The feed rate is the speed at which the polymer solution is delivered to the emitter. This rate is dependent upon factors such as the emitter needle's internal diameter and the employed voltage that draws the solution out. Each polymer type and needle diameter present an ideal flow rate interval. Higher flow rates tend to produce thicker fibers

because more material is dispensed per unit time and could result in fiber defects, like beads, due to incomplete solvent evaporation. Excessively high flow rates can also trigger multiple jet formations. Conversely, sub-optimal flow rates can substantially prolong the production time and, in worst cases, interrupt electrospinning, causing the jet to break and potentially retract back into the needle [82].

2.4.3. Suitable polymers and solvents

Several types of polymers with different chemical structures and molecular weights are available for electrospinning as well as the type of their solvents or solvent mixtures also cover a large number. The most used polymers and their typical solvents are summarized in Table 1.

3. Surface adjustment and functionalization of electrospun nanofibers

Researchers studying membrane technology are increasingly turning to polymeric membranes because of their excellent separation selectivity, reliable membrane performance, and affordability. Diverse fabrication methods, including electrospinning [119,120], phase inversion, track-etching, sintering, and stretching, contribute to the versatility of polymeric membranes [121]. As the intricacy of pollutants in water or air continues to escalate, there is a growing demand for polymeric membranes with enhanced performance in specific applications [122]. Furthermore, the evolution of multifunctional membranes necessitates facile modification methods in membrane preparation [123, 124].

In response to these challenges, electrospun nanofiber membranes (ENMs) have garnered attention in the area of water treatment research, particularly [125–127]. Electrospinning, a cutting-edge technology, relies on the interplay of polymers with an external electric field, offering advantages such as low cost, a wide array of material options, robust versatility, and straightforward modification procedures. As the demand for high-performance membranes intensifies and the quest for easily modifiable preparations persists, electrospun nanofiber membranes have emerged as a focal point, showcasing their potential to address the evolving complexities of membrane applications in various domains.

As the application of ENMs continues to expand, the inherent limitations of single-performance nanofiber membranes have become evident in meeting the escalating demands of increasingly complex processing requirements. Consequently, heightened attention is being directed towards modification technologies aimed at imparting functional attributes to ENMs. In recent years, a noteworthy trend has emerged wherein researchers have incorporated a diverse type of functional materials into nanofibers, employing both pre-

Table 1
Polymers most commonly used for electrostatic fiber formation [89–91].

Polymer	Abbreviation	Characteristic molecular weight (kDa)	Solvent	Typical field of application	Ref.
Water soluble					
Polyvinyl alcohol	PVA	37–200	water, dimethyl sulphoxide (DMSO)	food industry, medical biology,	[92]
Polyvinylpyrrolidone	PVP	125	water, methanol (MeOH), ethanol (EtOH), DMF	tissue engineering, medical biology, pharmaceutical industry	[93]
Polyethylene oxide	PEO	100–1000	water	tissue engineering, medical biology, pharmaceutical industry	[94]
Polyethyleneimine	PEI	25	water	cross-linking auxiliary component	[95]
Polyacrylic acid	PAA	450	water	wound dressing, tissue engineering, drug delivery systems	[96]
Soluble in organic solvents					
Polylactic acid	PLA	64	DMF, chloroform ($CHCl_3$)	tissue engineering, medical biology, pharmaceutical industry	[97]
Polycaprolactone	PCL	80	DMF, DKM, $CHCl_3$	tissue engineering	[98]
Polyvinylchloride	PVC	106	DMF	filtration, sensors	[99]
Polyurethane	PUR	180	DMF, DMSO	tissue engineering, medical biology, pharmaceutical industry	[100]
Poly(lactic-*co* glycolic) acid	PLGA	120	DMF, THF, HFIP	tissue engineering, wound dressing, cancer diagnosis and monitoring	[101]
Polyacrylonitrile	PAN	85–150	DMF	drug delivery, wound dressing, carbon nanofiber precursor	[102]
Polysulfone	PSf	35–58	DMF, acetone, THF	filtration, biomedical applications	[103]
Polyimide	PI	100	DMF, DMSO, DMAc	triboelectric applications, filtration	[104]
Polyvinylidene fluoride	PVDF	100	DMF, DMSO, acetone	triboelectric applications, tissue engineering	[105]
Polystyrene	PS	100–400	DMF, THF	filtration, sensors	[106]
Polyamide	PA	10–50	DKM, acetic acid, formic acid	filtration	[107]
Polycarbonate	PC	60	Chloroform, THF, DMF	tissue engineering, bioassays, filtration	[108]
Poly(methyl methacrylate)	PMMA	150–500	Chloroform, DKM, DMF, THF	tissue engineering, filtration	[109]
Polyethylene terephthalate	PET	30–80	DKM, TFA	filtration	[110]
Natural polymers					
Cellulose	–	–	DMSO	medical biology, membrane filtration	[111]
Cellulose acetate	CA	30–50	DMF, $CHCl_3$, dimethylacetamide (DMAc), methyl ethyl ketone (MEK)	medical biology, membrane filtration	[112]
Ethyl cellulose	EC	–	EtOH, acetone	food industry, pharmaceutical industry	[113]
Collagen	–	250–300	Trifluoroethanol (TFE), hexafluoro isobutylene (HFIP)	medical biology, tissue engineering	[114]
Chitosan	Ch	50–310	Trifluoroacetic acid (TFA), HFIP	medical biology, tissue engineering	[115]
Gelatine	Ge	–	Acetic acid, Formic acid, TFE	wound dressing, drug delivery, food packaging	[116]
Silk fibroin	–	–	HFIP, TFA, Formic acid	tissue engineering, wound dressing	[117]
Zein	–	–	DMF, HFIP, EtOH, acetic acid	soft tissue engineering, wound dressing, drug delivery	[118]

electrospinning and post-electrospinning methodologies to achieve desired modifications.

The area of ENM amendment methods can be broadly classified into three principal groups: nanofiber modification technology, nanofiber surface modification, and the modification of thin film composite nanofiber membranes. This evolution in modification strategies represents a pivotal response to the imperative for tailoring ENMs to meet the intricate and multifaceted demands imposed by diverse applications, thereby ushering in a new era of enhanced functionalization and adaptability in nanofiber membrane technology.

3.1. Morphology adjustment of electrospun nanofibers - smooth nanofiber

Prior to the flourish of electrospinning technology, the formation and usage of smooth nanofiber was the most common. Such materials found applicability in water purification, including extensive use in textile wastewater filtering [128] and gas separation, particularly in air purification [129–132]. However, because of their tight stacking patterns created by thin, smooth fibers, the majority of such filters are susceptible to the unavoidable problem of excessive pressure drop. Thus, it is critical to carefully design the aggregate structure of filters made out of smooth fibers. Several methods were employed to create filters made of smooth fibers with fluffy packing patterns, including multi-jet electrospinning [133,134], free surface electrospinning [135–137], and low-temperature electrospinning [138–140].

Tuning the flow rate of the polymer solution, which significantly impacts the transfer rate of the polymer solution and the speed of the jet, is also a way to generate smooth morphology. Opting for lower feed rates is crucial to achieve optimal solvent evaporation and to ensure the production of flawless, defect-free nanofibers. This approach is essential in delivering superior quality and performance. On the other hand, extremely low flow rates may result in the solution not being readily available at the needle tip. However, excessively high flow rates could produce fibers with larger diameters and structural flaws because the solvent does not completely evaporate before reaching the collector. It is crucial to find the right balance to achieve optimal results [141,142].

The mentioned methods were also successfully implemented to produce materials for water treatment. Pervez and co-workers produced electrospun nanofiber membranes for wastewater treatment to remove dye pollution [143]. Materials synthesized from PVA were formed using a low-temperature method at 50 °C with a persulfate reagent and possessed excellent performance in catalytic degradation of methylene blue dye. The studied membranes have shown also exceptional stability after repetitive recycling steps (90 % after five cycles) [143].

Zargham et al. studied the influence of applying different flow rates to Nylon 6 solutions, ranging from 0.1 and 1.5 mL h^{-1}. Achieving remarkable results, uniform and flawless fibers with diameters of approximately 237 nm were obtained when applying a flow rate of 0.5 mL h^{-1} at a voltage of 29 kV. This was achieved with a polymer content of 20 % in the solution and a distance of 15 cm between the needle and the collector. Flow rates below 0.1 mL h^{-1} and above 1 mL h^{-1} significantly impact the quality of fiber production. These extreme flow rates lead to the development of fibers with irregular diameters and structural defects. Additionally, excessively high flow rates of 1.5 mL h^{-1} result in unstable jets, yielding larger, irregular fibers with lower density in the deposited fiber area. This is why it is crucial to calibrate flow rates for optimal fiber quality and production stability [144].

Kyselica et al. [145] conducted an innovative study on the impact of varying flow rates on a PEO solution. Their research unearthed a crucial discovery: utilizing low flow rates, precisely adequate to form the Taylor cone, resulted in the creation of nanofibers with minimal defects. Conversely, insufficient flow rates caused jet interruptions due to solution unavailability, while excessive flow rates led to dripping and the production of thicker fibers. This study highlights the pivotal role of flow rates in yielding superior nanofiber quality and underscores the significance of their precise control in the production process.

3.2. Nanofiber modification technology - ENMs with a Nanofiber Layer as the Selective Layer

ENMs with controlled fiber diameter and pore size, high and tunable porosity, low tortuosity, narrow pore size distribution, and adjusted thickness—along with a customizable structure—have piqued the interest of researchers in the industrial purification area. The conditions of the electrospinning method, e.g., the polymeric dope concentration, solvent ratio, electric voltage, and ambient temperature, have been shown to require crucial tuning. In water purification, a polymer is typically combined with inorganic fillers to form ENMs. Modifications are necessary to provide varied physicochemical features and improve performance processes. In the formation process of ENMs, the following polymers are commonly applied polyvinylidene fluoride (PVDF) [146], polysulfone (PSF) [103], polyethersulfone (PES) [147], polystyrene (PS) [148], polyacrylonitrile (PAN) [149], polyurethane (PUR) [150], polyvinyl alcohol (PVA) [151], and polydimethylsiloxane (PDMS) [152]. These membranes may be tuned under various operating circumstances to improve ENM performance. The ENM can be placed on the top of the membrane structure design and play the role of the selective layer, depending on the process. In such application, the role of ENM is essential for the entire membrane performance and process efficacy.

3.2.1. Polymer blending

It should be remembered that a choice of polymers will be a key factor during the membrane formation *via* the blending method. During the selection of polymers, the electrospinning solution's electrical conductivity, surface tension, and viscosity should be considered [153]. Selecting the right polymer solution or combination thereof plays a critical role in defining the properties of engineered nanomaterials.

Different applications require engineered nanomaterials with diverse properties, posing a challenge when using ENMs derived from a single polymer. Electrospinning offers a solution by enabling the blending of polymers with varying characteristics into a single reservoir, which is then electrospun together to enhance membrane performance [50]. Incorporating polymer blends in nanofibers can introduce novel functionalities, leveraging the unique properties of individual components. For instance, silk (SF) boasts remarkable mechanical strength and binding resistance, while PEI is a hyperbranched cationic polymer known for enhancing antibacterial activity. Ugur et al. [154] successfully combined the following polymers PEI, SF, and poly(methyl methacrylate) (PMMA) using ES technology to produce antibacterial and mechanically reinforced nanofiber membranes.

Zhang et al. [155] combined polyaniline (PANi) with a dissolved solution of styrene block copolymer polystyrene-*b*-(ethylene-*co*-butene)-*b*-styrene (SEBS) to create SBES/PANi ENMs, resulting in ENMs with enhanced strain recovery performance and thermal resistance similar to pure SEBS ENMs. Notably, the SBES/PANi ENMs exhibited exceptional resistance to corrosion when subjected to large tensile deformation on stainless steel surfaces. Similarly, in a separate study, Zhu et al. [156] developed a novel method by incorporating $NH_3{\cdot}H_2O$, trimethoxy (1 H,1 H,2 H,2H-heptadecafluorodecyl) silane (17-FAS), and PVDF powder into solutions of PVA/PAA to produce PVA/PAA ENMs, forming Janus fibrous membranes. These membranes demonstrated high water flux exceeding 27 L m^{-2} h^{-1} and nearly complete desalination effectiveness of approximately 100 % after undergoing heat treatment during the desalination process of simulated hypersaline wastewater containing sodium chloride (NaCl), sodium dodecylbenzene sulfonate (SDBS), and lubricating oil.

3.2.2. Incorporation of functional materials into nanofibers

Electrospinning is a versatile technique that allows for precise alterations at every stage of the process, enabling the fabrication of

nanofibers with tailored structures and properties. This adaptability extends to the precursor solution, where various materials can be easily incorporated to create nanofibers with unique qualities (Fig. 12). Electrospinning enables the production of fibers with enhanced functionality by dispersing these materials directly into the precursor mixture. A particularly notable class of materials for this purpose is porogen materials. These materials can be used to fabricate porous nanofibers, which have found applications in areas such as drug delivery, filtration, catalysis, and tissue engineering.

Porogen materials act as hard or soft templates that are incorporated into the electrospinning solution and subsequently removed from the resulting nanofibers. The removal of the porogen creates voids within the fiber structure, resulting in internal porosity. This porosity can enhance the mechanical properties of the fibers and improve their performance in applications requiring high surface area or permeability. The use of porogen materials represents a straightforward and effective approach to preparing porous nanofibers with advanced structural features [48].

Besides porogen materials, electrospinning also enables the incorporation of a wide range of functional materials into nanofibers. Enzymes can be embedded to create biocatalytic fibers for industrial or medical applications [157,158], while small molecules and drugs can be loaded for controlled-release systems in pharmaceutical applications. Catalysts can be integrated for use in chemical reactions [159] or energy conversion systems [160]. Antibacterial agents can be introduced to create nanofibers for filtration or wound dressing [161], and materials with specific optical or electrical properties can be embedded for use in sensors or electronic devices [162]. The ability to incorporate different functional materials into nanofibers underscores the versatility and potential of electrospinning for developing advanced materials tailored to specific application needs.

3.2.3. *Mixed matrix membranes*

Lately, there has been a growing emphasis on creating mixed matrix membranes, which involve dispersing nanoparticles throughout a continuous polymer matrix. This approach offers several advantages over both purely polymeric and inorganic membranes. The process involves the introduction of inorganic nanofillers, organic crosslinking agents, and carbon-based nanomaterials into a polymer solution to enhance the performance of engineered nanomaterials [163].

Incorporating inorganic metals involves the addition of metal nanoparticles (such as silver (Ag), and iron (Fe)) and metal oxide materials (like alumina (Al_2O_3), titania (TiO_2), metal-organic frameworks (MOFs), covalent organic frameworks (COFs), and hydrogen-bonded organic frameworks (HOFs)) [164]. This modification alters the structures as well as morphologies of composite mixed matrix ENMs, differing from their original forms. As a result, these modified ENMs exhibit enhanced water purification efficiency.

As an example of metallic nanoparticles, Ag nanoparticles, ranging in size from a few nanometers to tens of nanometers, have been used for membrane formation owing to the exceptional antibacterial properties of Ag [165]. This characteristic has sparked considerable interest in incorporating them into mixed matrix electrospun selective layers during membrane formation for water desalination particularly [166]. However, the direct addition of Ag nanoparticles to the polymer solution often leads to agglomeration, making it challenging for them to disperse onto the electrospun nanofibers. A reduction reaction between Ag^+ and Ag nanoparticles is utilized to address this issue. Yuan et al. [167] introduced Ag^+ into a PVA solution and heated it to 150 °C to render the resulting PVA ENMs composite insoluble in water. Through this process, Ag^+ is reduced by PVA, allowing for amalgamation and simultaneous modification onto the membrane mat *via* electrospinning. The resulting ENMs demonstrated optimal adsorption performance towards Hg^{2+} in water, achieving a capacity of approximately 248 mg g^{-1} at 333 K.

One of the newest class of nano-enhancers are COFs [168]. In the case of electrospun membranes [169,170], PVDF membranes served as the foundation for creating COF composite membranes, incorporating graphene oxide and oxidized carbon nanotubes (GO-OCNTs) as an intermediary layer [171]. The fabrication involved suction filtering the GO-OCNTs intermediate layer onto the electrospun substrate, followed by interfacial polymerization to form the COF layer. Integration of the intermediate layer enhanced the dye retention rate and water permeance of the composite COF membrane. Through optimization of reaction parameters during interfacial polymerization, the resulting membrane demonstrated a Coomassie brilliant blue G250 (BBG-250) rejection rate of approximately 97.1 %, with water permeability

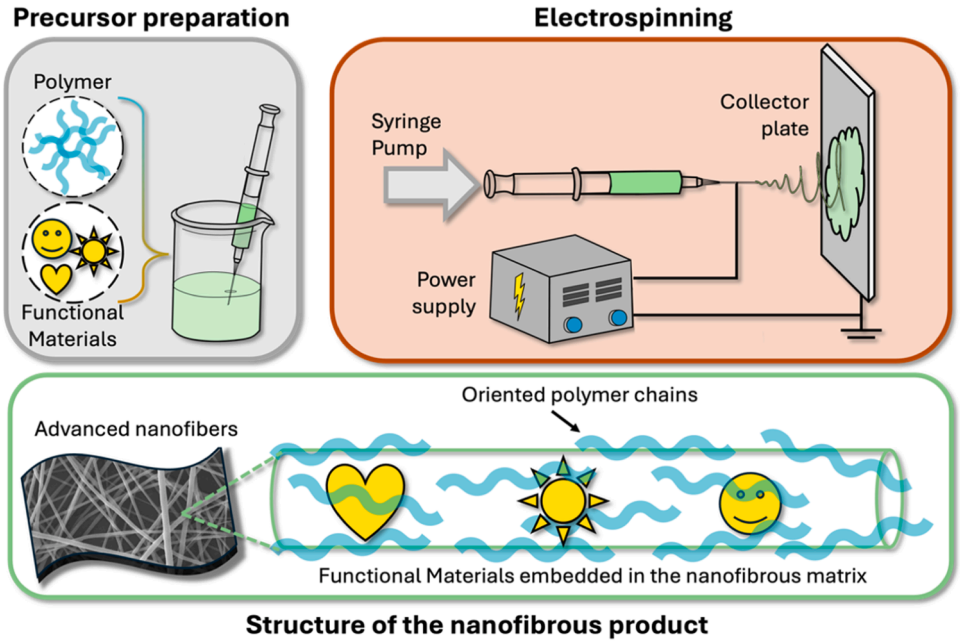

Fig. 12. Schematic representation of the incorporation of functional materials into nanofibers via electrospinning for advanced material development. The process enables the addition of functional components, such as porogens, enzymes, drugs, or catalysts, directly into the polymer precursor solution, producing nanofibers with tailored properties and enhanced functionality.

reaching 96.7 L m^{-2} h^{-1} bar^{-1}. Moreover, the COF/GO-OCNTs/PVDF composite membrane exhibited outstanding mechanical and chemical and resistance. Extended filtration experiments confirmed the membrane's sustained water permeation stability, presenting a method for fabricating dense and defect-free COF films on electrospun substrates.

The newest enhancers in the class are HOFs that were also successfully implemented onto the electrospun membranes [172]. Nanofibers with broad-spectrum antibacterial properties are produced through electrospinning, incorporating them into a photoactive HOF consisting of rod-like nanocrystals approximately 60 nm long. These HOF@polyvinylidene fluoride-co-hexafluoropropylene (PVDF-HFP) nanofibers retain outstanding tensile strength and breathability while safeguarding HOF nanocrystals from acid and alkali exposure damage. Various nanofibers containing different quantities and types of HOF nanocrystals are synthesized to enhance their efficiency in generating singlet oxygen ($^1O_2$). Among these, the nanofibers containing 0.5 wt% HOF-101-F@PVDF-HFP demonstrate the highest efficiency in $^1O_2$ generation, nearly doubling that of the HOF-101-F microcrystalline powder. Moreover, the HOF@PVDF-HFP nanofibers prove highly effective in eradicating pathogens within 30 minutes under normal light conditions (Fig. 13) [172].

Incorporating inorganic nonmetallic nanomaterials, *e.g.*, silicon dioxide (SiO_2) [173,174], carbon nanotubes (CNT) [175,176], zeolite, graphene, and graphene oxide (GO) [177–179], into polymer solutions has been a focus for enhancing functional properties. For instance, adding SiO_2 to polymer solutions improves the mechanical strength of nanofibers, raises the glass transition temperature of ENMs, and prevents bead formation during the electrospinning process [180,181].

Hou et al. [182] dissolved PVDF-HFP using a co-solvent of DMF/acetone with the addition of SiO_2 emulsion to produce PVDF-HFP/SiO_2 ENMs. Increasing the mass ratio of SiO_2 led to gradual reductions in membrane porosity but enhanced membrane thickness, resulting in improved salt rejection efficiency. The produced materials possessed the water contact angle (WCA) exceeding 150° owing to its rough hydrophobic surface. With a maximum permeate flux of 48.6 L m^{-2} h^{-1}, the membrane maintained nearly 100 % rejection of NaCl after continuous operation for 240 hours in membrane distillation.

Incorporating CNTs into polymer composites enhances the strength of polymers and tensile modulus, immobilized within nanofibers *via* ES to enhance mechanical toughness [183]. Yan et al. [184] developed a carbon nanofiber membrane by electrospinning PAN/ terephthalic acid (TPA) solution. Subsequently the materials were pre-oxidized and carbonized, achieving high desalination efficiency under sunlight and even in acidic/alkaline environments. This membrane demonstrated an evaporation rate of 1.36 kg m^{-2} h^{-1} and rejection > 99.9 % of main ions in seawater, with well-developed wettability and surface roughness.

Graphene and GO, possessing properties akin to carbon nanotubes, are attractive nanofillers owing to their outstanding thermal and chemical resistibility as well as hydrophilic moieties [185]. Woo et al. [186] introduced graphene into a PVDF-HFP solution to fabricate superhydrophobic PVDF-HFP /graphene ENMs, exhibiting high porosity and a WCA of approximately 162°. These composite ENMs demonstrated a water flux of 22.9 L m^{-2} h^{-1} and maintained a high salt rejection (*ca.* 100 %).

3.3. Nanofiber surface modification

The reason for implementing the surface modification of generated nanofiber is very often related to adjusting roughness [187], chemistry, or mitigating the wetting problem [188]. Zhao et al. developed a technique to ENM with micro-nano structures imitating beads on a string to boost transport properties and anti-wetting features in the desalination process *via* membrane distillation. The composite ENM is made up of two layers: a heat-conducting top layer made of PVDF-HFP nanofibers implanted with carbon sphere (CS) nanoparticles and a heat-insulating support layer composed of the same material. The introduced modification allows to produce materials with greater performance stability over 5000 min of direct contact membrane distillation (DCMD) operation.

Novel pre-treatment methods, such as the vapor activation method, have been established recently. Surface features were sensitive when exposed to high humidity and organic solvents. Wu et al. [189] fluorinated PVDF-HFP ENMs through vapor deposition to reduce the membrane's surface energy. Compared to traditional dip-coating, vapor deposition was found to be more useful for large-scale production. The optimized fluorinated ENMs exhibited anti-wetting features in the course of membrane distillation (MD) trials. Additionally, Liu et al. [190] applied solvent vapor to partially melt CA/PVDF ENMs, promoting contact points between nanofibers for physical crosslinking, which proved to be a simple yet efficient method for enhancing the mechanical strength of the produced separation materials.

Wu and co-workers [188] designed superhydrophobic nanofiber membranes with 3D-network strengthened pore structure for DCMD (Fig. 14). Owing to the introduction of hot-pressing to pretreat the PVDF ENMs and modifying them with a PDMS and TiO_2 nanoparticles solution, it was possible to solve the problem of lack of ENM membrane pore structure stability, poor mechanical features often faced in ENM materials as well as inadequate surface hydrophobicity. The ready samples were characterized by the contact angle for water above 160°. Such a welded structure was responsible for the excellent durability and applicability of the materials without losing integrity and performance for over 100 h. After this time, the salt rejection during the desalination *via* membrane distillation process was equal to 99.99 %. The water flux was maintained on the level ca. 40 L $m^{-2}{\cdot}h^{-1}$. The material was also effective and resistant to wetting, contacting a 3.5 wt% NaCl solution containing 0.1 mM sodium dodecyl sulfate (SDS) [188].

3.4. Membrane structure design - ENMs with nanofiber layer as supporting substrates

The nanofiber layer offers distinct advantages as a supporting substrate for ENMs, given its favorable surface-to-volume ratio and excellent porosity, which promote the formation of the selective layer [191]. Typically, the selective layer is applied onto the nanofiber support through secondary-electrospinning, polymer coating, inorganic deposition, or interfacial polymerization, all of which play pivotal roles in dictating fluid flow pathways and separation efficiency [192]. Additionally, achieving optimal performance for specific applications requires precise customization of structural aspects such as thickness and porosity for both the supporting and selective layers, necessitating independent adjustments.

The optimum composite membranes, particularly for water purification, should have a thin, perfect outer layer and a supporting layer with low tortuosity and high porosity. ENMs have significant benefits over typical ultrafiltration (UF) membranes created using phase-inversion technologies, such as a highly porous structure and completely interconnected features [193]. As a result, ENMs are generally recognized as the optimal substrates for manufacturing high-performance thin-film nanofibrous composite (TFNC) membranes. The adaptability of TFNC membranes goes beyond aqueous-based applications such as UF [194–196], nanofiltration (NF) [197–199] (Fig. 15), and forward osmosis (FO) separation [200–202], to include hemodialysis [196,203,204] and pervaporation [205–208] (Fig. 16).

3.4.1. Modification - selective layer via inorganic deposition

Engineered nanomaterials incorporating a selective layer through inorganic deposition onto the nanofiber layer typically improve the chemical and thermodynamic stability of the separation materials. The selectivity of nanomaterials significantly influences the features of such hierarchical materials. Jiang et al. [209] placed hydrophobic single-sided CNTs onto a hydrophilic PAN nanofiber layer *via* vacuum filtration to create Janus PAN/CNTs ENMs. Different PAN and CNT

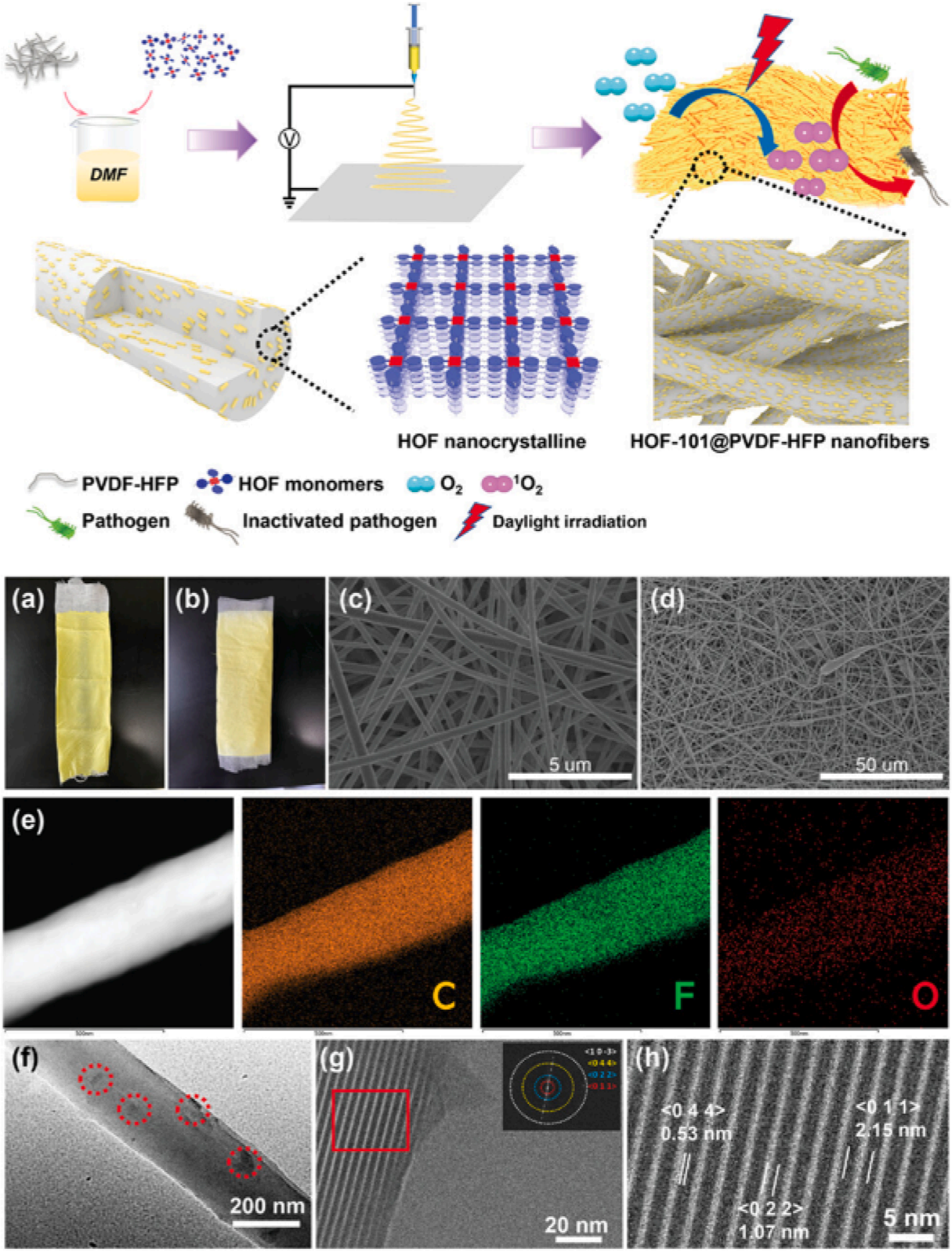

Fig. 13. A schematic showing preparation of antibacterial HOF-101-H@PVDF-HFP nanofiber (upper part). Photographs of HOF-101-H@PVDF-HFP nanofiber on a) gauze and b) non-woven fabric; SEM images of c) PVDF-HFP nanofibers and d) 10 wt% HOF-101-H@PVDF-HFP nanofibers; e) EDS images of 10 wt% HOF-101-H@PVDF-HFP nanofibers; f) TEM images of 10 wt% HOF-101-H@PVDF-HFP nanofibers; g) Structural profile of HOF-101-H on nanofiber with the FFT pattern of the chosen area (inset); h) The enlarged structure of the region of the frame in red in (g).serial HOF@PVDF-HFP nanofibers and the antibacterial mechanism (upper part). (Reproduced with permission from ref. [172], Copyright 2023 Wiley).

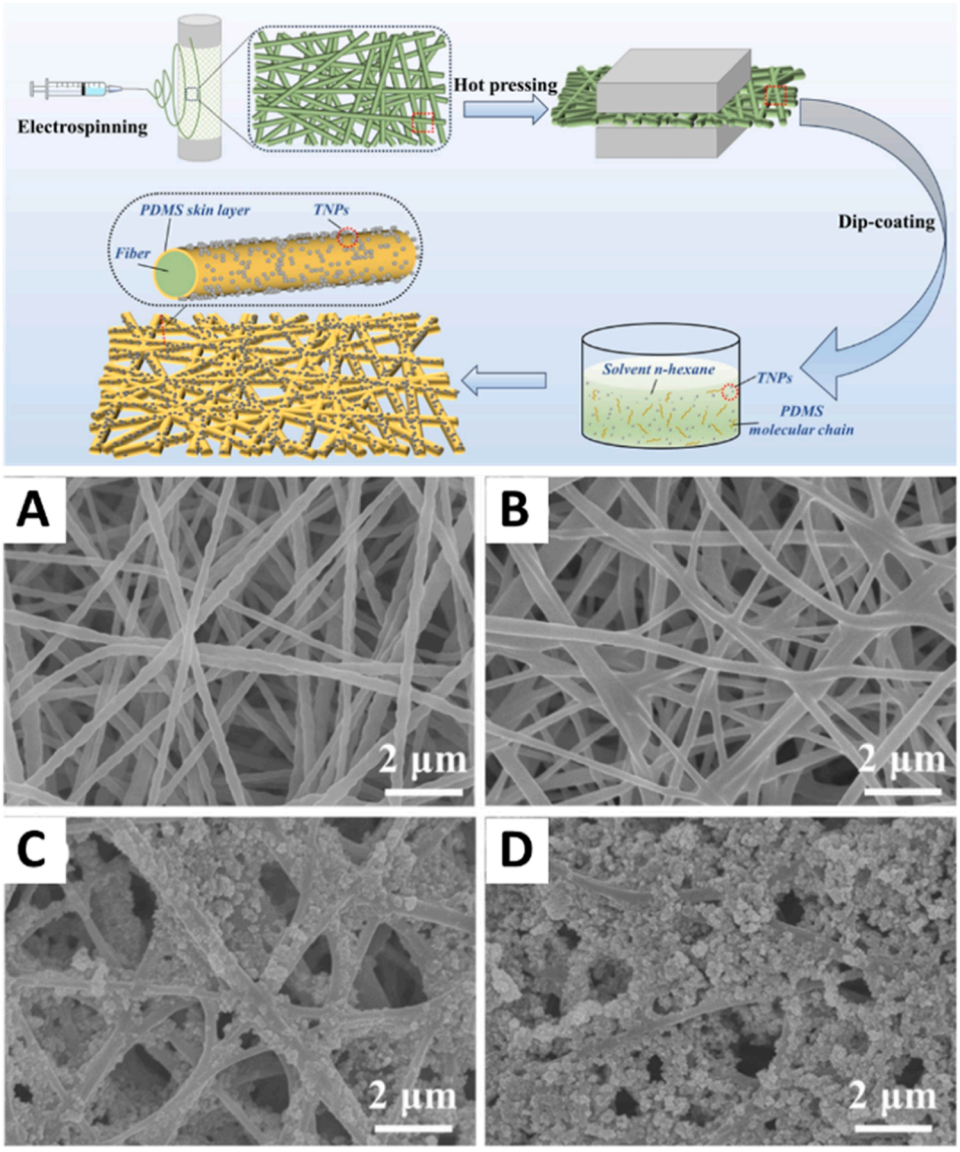

Fig. 14. Membrane formation and modification (upper figure). SEM images of pristine PVDF ENM (A), after hot pressing process and coating with 1 wt% PDMS solution (B), membrane after modification with 0.3 wt% (C) and 0.4 wt% (D) of TNPs.
Reproduced with permission from ref. [188], Copyright 2024 Elsevier.

solution concentrations yielded varying degrees of hydrophobicity/hydrophilicity on both sides of the separation material. The optimized oil rejection rate exceeded 99.5 % after incorporating CNTs, accompanied by a high flux of approximately 12,000 L m^{-2} h^{-1} MPa^{-1} (Fig. 17).

3.4.2. *Modification - selective layer via polymer coating*

Zhao and colleagues [210] applied amino-rich hydrothermal diethylenetriamine (DETA) onto the PAN nanofiber layer following an effective hydrothermal carbonization mode. An amide bond was easily formed when the amino groups of DETA interacted with the carboxyl moieties of the carbonaceous PAN nanofiber layer. The adsorption capacities for pollutants such as Cr^{6+} and 2,4-dichlorophenoxyacetic acid were approximately 290.7 mg g^{-1} and 164.5 mg g^{-1}, respectively, surpassing those of pure PAN ENMs.

Furthermore, Vanangamudi et al. [211] investigated a method of coating 18 wt% PVDF onto a hydrophilic nylon-6,6/Ch nanofiber layer to create a Janus membrane. The interaction between the membrane surface and water molecules through intermolecular hydrogen bonding enhanced hydrophilicity, resulting in the highest water permeance of approximately 5420 L m^{-2} h^{-1} MPa^{-1}. The membrane demonstrated rejection levels above 93 % for bovine serum albumin (BSA), with reduced pore sizes at approximately 3930 L m^{-2} h^{-1} MPa^{-1} liquid flux during filtration.

3.4.3. *Modification - selective Layer via Interfacial Polymerization*

In addition to deposition and coating methods, selective layers produced through interfacial polymerization (IP) can be applied onto nanofiber surfaces to create engineered nanomaterials, primarily utilized in FO and NF processes. The prevalent material for these selective layers is polyamide (PA), synthesized in the reaction of acyl chloride and polyamines.

In the case of the FO process, Tian et al. [212] applied a post-covering of a PA layer derived from *m*-phenylenediamine (MPD) and 1,3,5-trimesoylchloride (TMC) onto a polyethylene terephthalate (PET)/PVA nanofiber layer formed *via* electrospinning process. The reduced diffusive resistance primarily stemmed from the interconnected pores and low tortuosity within the nanofibrous support layer. These characteristics, including high roughness and open pores, enabled water molecule movement across the membrane. The water flux for a 0.5 M

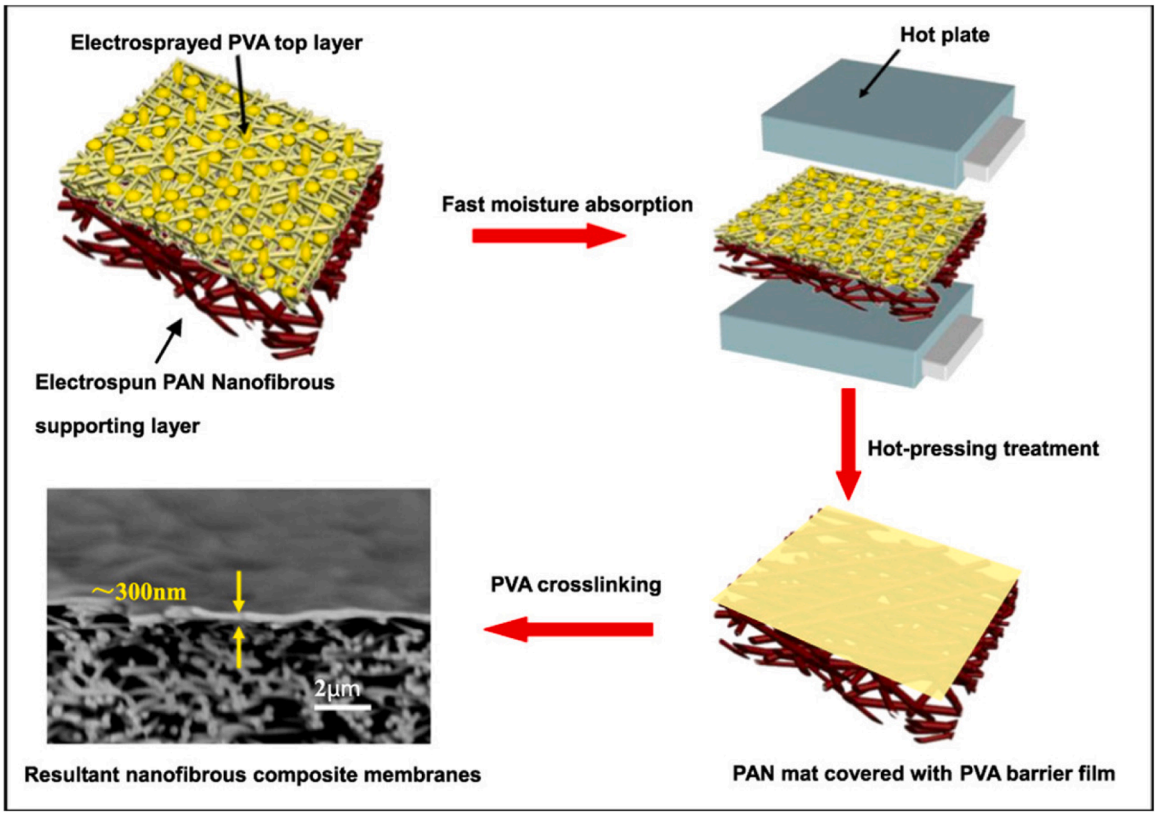

Fig. 15. Schematic illustration of the fabrication process for thin film composite membranes based on PAN nanofibrous substrate and hydrophilic PVA barrier layer. Reproduced with permission from ref. [198], Copyright 2016 Elsevier.

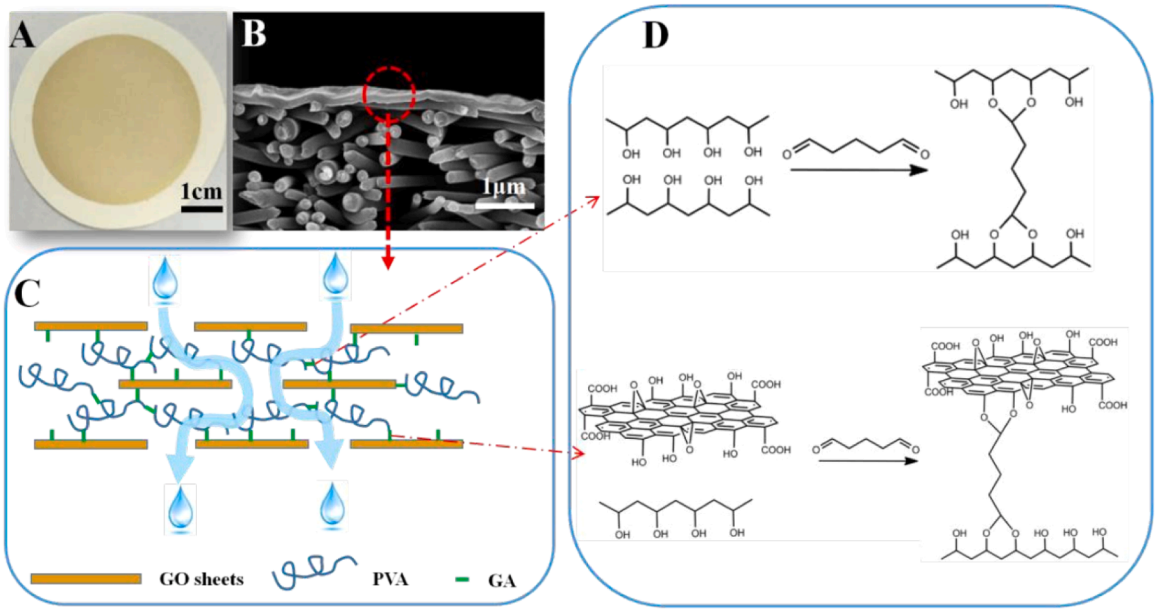

Fig. 16. Illustration of the structure design of the GO–PVA– glutaraldehyde (GA)/PAN TFNC membrane: (A) a digital photo of the GO–PVA–GA/PAN TFNC membrane, (B) cross-section SEM image of the GO–PVA–GA/PAN TFNC membrane, (C) schematic representation of the internal architecture and (D) GA chemical cross-linking in the GO–PVA barrier layer.
Reproduced with permission from ref. [208] Copyright 2017 RSC.

NaCl solution was approximately 30.6 L m^{-2} h^{-1} in the FO process. Another work focused on a construction of a PA rejection layer atop the PSF/PAN nanofiber layer through IP reaction between MPD and TMC monomers [213]. The membrane's high porosity, around 84.3 %, and numerous interconnected pores facilitated the development of a uniform PA layer, diminishing internal concentration polarization (ICP) effects and reversing salt flux during desalination. The elevated porosity encouraged mass transfer across the membrane, enabling a water flux of

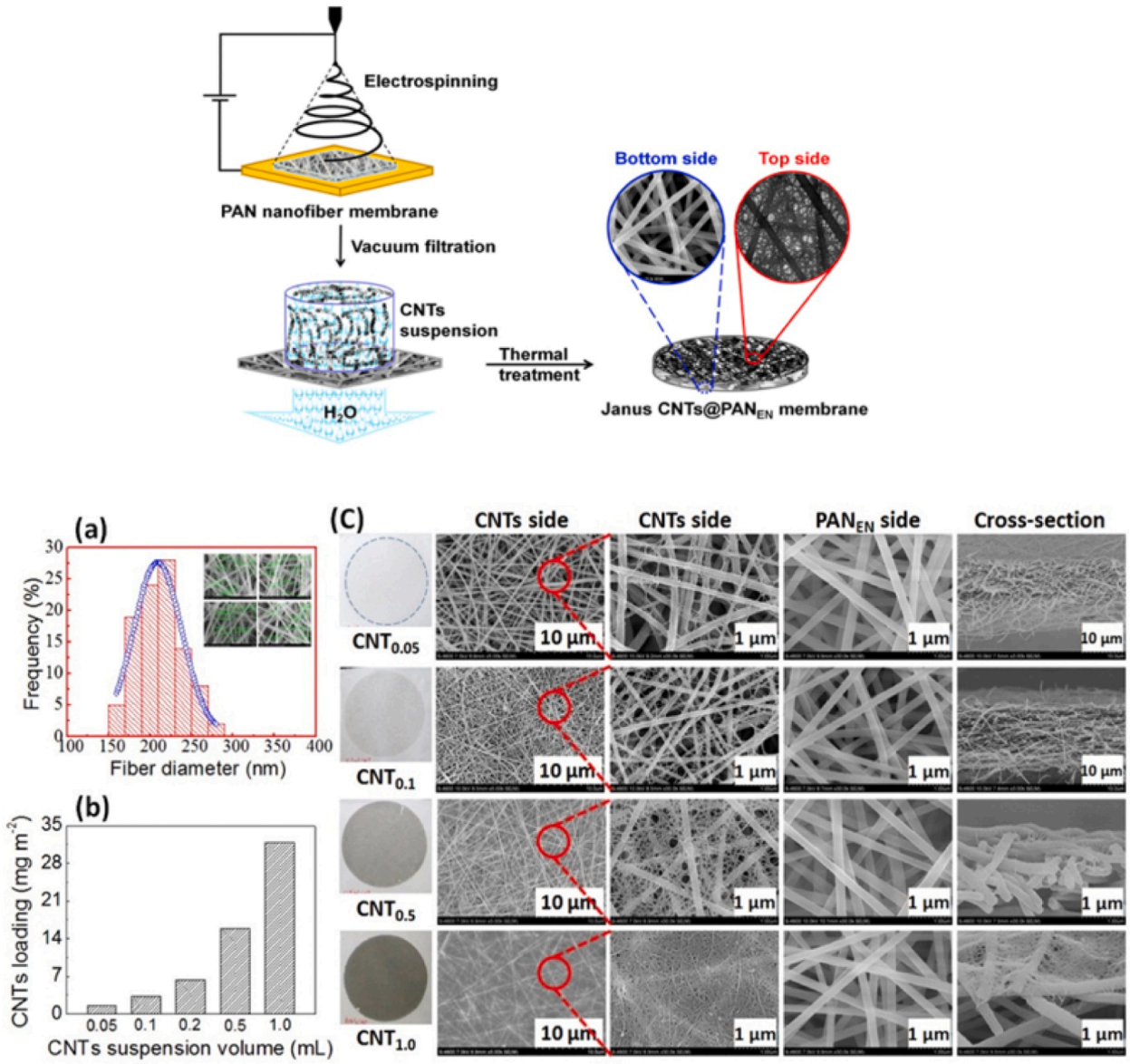

Fig. 17. Schematic illustration of the fabrication process for Janus CNTs@PAN ENMs (upper image) [209]. (a) Fiber size distribution of the CNTs@PAN ENMs. (b) CNTs loading of the CNTs@PAN ENMs with different CNTs suspension volumes. (c) Photos and SEM images of the CNTs side, PAN ENMs side and cross-section with scale bars for the CNTs@PAN ENMs with different CNTs loadings (button images).
Reproduced with permission from ref. [209]. Copyright 2017 Elsevier.

about ~38 L m^{-2} h^{-1} towards a NaCl solution in the forward osmosis process, surpassing traditional substrates fabricated through phase inversion.

4. The applications of electrospun nanofibers in separation processes

4.1. Removal of heavy metal ions from wastewater

The fast development of urbanization and industrialization has resulted in considerable water pollution, owing to the release of pollutants from industries, sewage, and agriculture [214]. Especially the contamination of heavy metals in water has created damages to the environment system and human health since they can accumulate in organisms [215]. Heavy metals such as Cu(II), Pb(II), Cr(VI), Cd(II), Ni (II), As (III), Au(III) and Ag(I) are toxic and carcinogenic [216]. Therefore, the separation of heavy metals from wastewater is crucial in wastewater treatment processes. Conventionally, electrodialysis, ion exchange, flocculation, chemical precipitation, membrane filtration, adsorption, and reverse osmosis were used to remove heavy metal ions from wastewater [24,216–219]. Among them, adsorption is the mostly studied and used method to separate heavy metals from wastewater, owing to its affordability, great efficiency, and simplicity of use, and feasible application on a large scale [24,216,220]. In the adsorption process, the preparation of high-performance adsorbents is important. The conventional adsorbents such as zeolites and activated carbons possess low adsorption capacity. Moreover, they cannot be easily regenerated [221]. Nanoparticle adsorbents possess higher adsorption capacity and fast adsorption rate. However, secondary contamination might result from their facile aggregation and challenging separation from aqueous solutions [222]. Compared with the aforementioned adsorbents, electrospun nanofiber adsorbents can effectively separate heavy metals from aqueous solutions, owing to their large surface area and desirable flexibility [24]. Electrospinning is a versatile process to fabricate nanofibers, which allows to control the diameter, microstructure, and the layout of nanofibers [25]. The electrospinning method can

be used to fabricate nanofibers from a variety of materials. Most importantly, the electrospun nanofibers can be surface functionalized to obtain high efficiency nanofiber adsorbents for the separation of heavy metals from wastewater [24,25].

PAN is utilized in the electrospinning process owing to its desirable electrospinnability and high thermal and chemical stability [223]. Mohammed et al. [217] fabricated electrospun nanofibrous composite membranes (NCMs) for Cr(VI) removal by incorporating zeolitic imidazolate framework (ZIF-8) into PAN substrate grafted with cationic PEI. Compared with pristine PAN nanofibers, the prepared PAN/PEI@ZIF-8 NCMs containing 5 wt% ZIF-8 showed the highest Cr (VI) adsorption capacity of 403.5 mg g^{-1} and enhanced thermal stability and mechanical strength. The adsorption experimental data were well described by the pseudo-second-order (PSO) kinetics model and Langmuir model, which indicated that the chemisorption occurred, and the monolayer adsorption occurred on the surface of absorbent, respectively. The adsorption mechanism consisted of the electrostatic attraction between positively charged amine groups and negatively charged Cr(VI) ions in the acidic solution, and the reduction of the adsorbed Cr (VI) to Cr(III) [217]. Miao et al. [224] synthesized Fe-MOFs and fabricated PAN/MOFs composite electrospun nanofibers by *in situ* immobilization of Fe-MOFs in PAN nanofibers for Cr(VI) adsorption. The prepared composite nanofibers can fast adsorb Cr(VI) ions in water and exhibited a high Cr(VI) adsorption capacity of 127.70 mg g^{-1} at pH 4.0. Moreover, some adsorbed Cr(VI) was reduced to less toxic Cr(III). The adsorption process was dominated by the physical adsorption process. The immobilization of MOFs on nanofibers solved the issues of aggregation and difficulty in recyclability of MOFs in the adsorption processes [224]. Chen et al. [225] prepared hyperbranched zwitterionic phosphate (ZP) groups functionalized nanofiber adsorbents (ZP-PAN nanofibers) with anti-biofouling properties for the adsorption removal of U (VI) ions from seawater. As it is shown in Fig. 18, the PAN nanofibers were first fabricated by electrospinning. Subsequently, the PAN nanofibers were grafted with hyperbranched polyethyleneimine (bPEI) and modified with phosphite *via* phosphorylation. The bPEI grafting increased the density of functional groups and improved the abundance of accessible adsorption sites for U(VI) ions. The zwitterionic phosphate groups endowed the nanofibers with anti-biofouling properties and enhanced their interaction with U(VI) ions owing to the oxygen-based donors. The prepared ZP-PAN nanofibers showed a high U(VI) adsorption capacity of 1294.0 mg g^{-1}, owing to the involvement of phosphate and amine groups in U(VI) coordination. The adsorption kinetics were well fitted with the PSO kinetics model. ZP-PAN nanofibers showed faster kinetics than bPEI-PAN nanofibers, owing to the phosphate groups with high affinity to U(VI). The ZP-PAN nanofibers showed desirable anti-protein adhesion ability since they are super hydrophilic to prevent the adhesion of microorganism.

Rosli et al. [215] fabricated Ch/ PVA electrospun nanofibers which were crosslinked with glutaraldehyde and functionalized with 1-allyl-3--methylimidazolium chloride to improve the Pb(II) adsorption capacity. In comparison to the pristine Ch/PVA nanofibers, the Pb(II) adsorption capacity of ionic liquid-modified Ch/PVA nanofibers increased to 166.34 mg g^{-1}, and the Pb(II) removal efficiency increased from 18 % to 82.5 %. The PSO kinetics and Freundlich isotherm models were used to describe the kinetic rate of the Pb(II) uptake and the adsorption equilibrium, respectively [215]. Xie et al. [24] prepared zein/PVA and collagen/PVA electrospun nanofibers for the adsorption of Cu(II). The functional groups of zein and collagen can interact with heavy metal ions to remove them from wastewater. Cu(II) adsorption capacity firstly increased and then decreased with the increase of zein or collagen content. The prepared nanofibers with 50 % collagen showed the highest Cu(II) adsorption capacity of 24.62 mg g^{-1}. The adsorption data were well fitted with a pseudo-first-order (PFO) kinetics modal, indicating that the physical adsorption occurred in the adsorption process.

CA shows desirable chemical and thermal stability, high processability and biocompatibility. However, CA lacks sufficient functional groups that can strongly electrostatically interact or chelate with heavy metal ions [226]. Therefore, it is necessary to modify CA by blending with other materials or grafting active functional groups onto the surface to endow CA with stronger interactions with heavy metal ions. Tan et al. [226] fabricate CA/TiO_2 composite nanofibers by electrospinning. Subsequently, the electrospun nanofibers were modified by polydopamine (PDA) and grafted by PEI to improve their Cr(VI) adsorption capacity (Fig. 19). The prepared CA/TiO_2@PDA@PEI composite nanofibers demonstrated the high Cr(VI) adsorption capacity of 357.1 mg g^{-1}, owing to the large number of amine groups and the positively charged CA surface at acidic solution. Langmuir adsorption model perfectly described the adsorption equilibrium, indicating the homogeneous adsorption process resulted from the strong electrostatic interaction between absorbents and Cr(VI) ions. The kinetics of Cr(VI) adsorption by the prepared nanofibers were in line with the PSO kinetics model. Most importantly, 72.1 % Cr(VI) was reduced to harmless Cr(III)

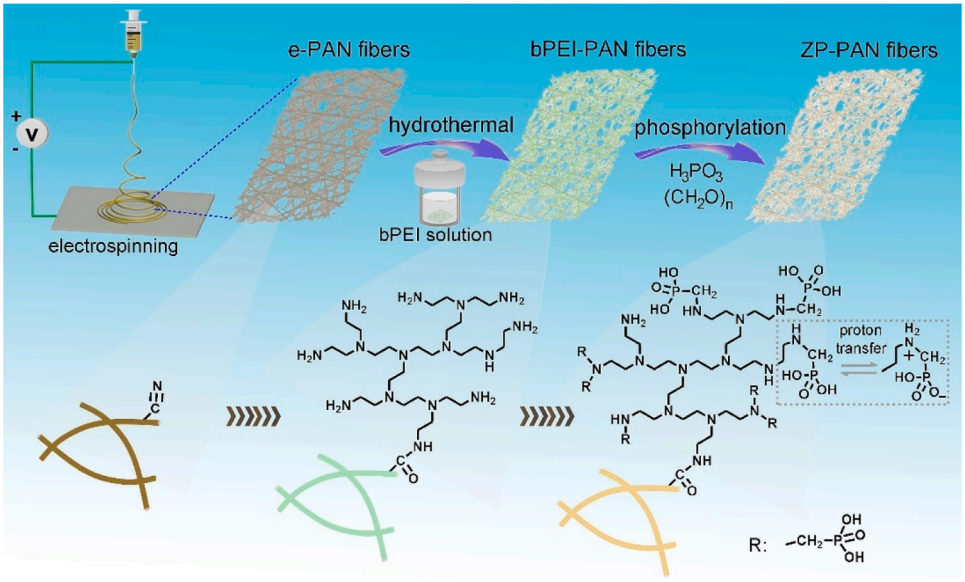

Fig. 18. The fabrication of hyperbranched zwitterionic phosphate functionalized electrospun nanofiber adsorbent (ZP-PAN nanofibers). Reproduced with permission from ref. [225]. Copyright 2023 Elsevier.

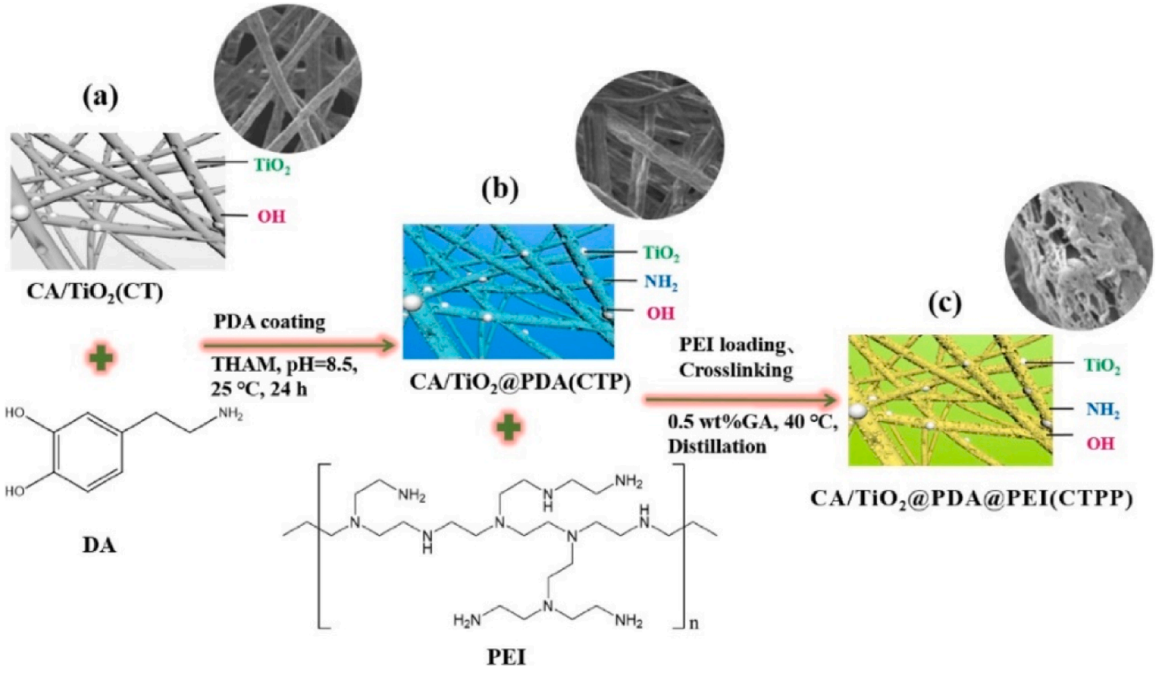

Fig. 19. The fabrication of the CA/TiO_2@PDA@PEI composite nanofibers. Reproduced with permission from ref. [226]. Copyright 2022 Elsevier.

during the adsorption process, owing to the enhanced reduction ability of CA composite nanofibers by TiO_2.

Besides the synthetic polymers, low-cost, naturally available biomaterials were also used to fabricate electrospun nanofibers. Wang et al. [219] fabricated recyclable sodium alginate (SA) electrospun nanofibers crosslinked by calcium for Cu(II) adsorption. The calcium crosslinking enhanced the mechanical strength and stability in the aqueous environment of SA nanofibers. The prepared SA-Ca nanofibers showed a high Cu(II) adsorption capacity of 285.5 mg g^{-1}, owing to the ion exchange, electrostatic attraction, and complexation between SA-Ca nanofibers and Cu(II). Moreover, the porous structure of SA-Ca nanofibers facilitated the diffusion of Cu(II) to the binding sites. The adsorption equilibrium and adsorption kinetics of SA-Ca nanofibers were fitted by the Liu model and general-order-model. Most importantly, the SA-Ca nanofibers demonstrated high Cu(II) removal efficiency equal to 99 % in the adsorption process in mineral and river water samples [219]. Zein is a biodegradable natural material that possesses plenty of functional groups, such as amino and carboxyl groups, providing rich active binding sites for heavy metal ions. Therefore, Teng et al. [214] fabricated zein electrospun nanofibers with different morphology *e.g.* rod, ribbon, and groove ribbon, for the adsorption of Pb(II) and Cd(II). The groove ribbon nanofibers provided more active adsorption sites and hydrophilic channels for heavy metals. As a result, the groove ribbon nanofibers exhibited the highest adsorption capacity for Pb(II), equal to 189 mg g^{-1} and for Cd(II), equal to 164 mg g^{-1}. The adsorption mechanism included the electrostatic interaction between the negatively charged nanofibers and the positive metal ions, the hydrogen bonding, and the complexation between metal ions and oxygen and nitrogen functional groups.

Table 2 summarizes the heavy metal adsorption performance of electrospun nanofiber materials from 2020 to 2023. As shown in Table 2, PAN was commonly used to prepare electrospun nanofibers for heavy metal adsorption. In addition to PAN, PVA, Ch, CA, SA, and zein were also used for electrospun nanofibers fabrication. Modifications such as polymer blend, the incorporation of MOFs and nanoparticles, and surface functionalization on electrospun nanofibers are necessary to improve their heavy metal adsorption capacity and recyclability in the adsorption processes. The pH value significantly affects the adsorption performance since it can affect the surface charge of nanofibers and metal ions, consequently affecting the adsorption mechanism. Langmuir isotherm model and PSO kinetic model are commonly used to describe the adsorption equilibrium and kinetics.

4.2. Removal of dyes and organic contaminants from wastewater

4.2.1. Adsorption of dyes and organic contaminants

The contamination of organic dyes in water has adversely affected the aquatic plants, ecosystem, and human health, since organic dyes are highly toxic, carcinogenic and mutagenic [261,262]. Moreover, organic dyes are difficult to remove from wastewater by using conventional methods in wastewater treatment plants, owing to their complex chemical structures [262]. Organic dye contaminants such as Methylene blue, Rhodamine B, Congo red, Reactive black 5, and Methyl orange are commonly found in the wastewater [262–266]. Therefore, developing effective methods to separate organic dyes from wastewater is crucial. Adsorption is considered the most useful technique for removal of organic dyes due to its cost-effectiveness, easy regeneration and recovery of the elected adsorbents, and high efficiency [261,262,264]. In the adsorption processes, dyes are adsorbed onto the adsorbent via various mechanisms such as the van der Waals forces, hydrogen bonding and electrostatic interactions [261]. Compared with the conventional adsorbents, such as the activated carbon, the electrospun nanofibrous adsorbents show advantages in adsorption efficiency, recyclability, cost, and applicability [262]. In addition, the open pore structure and high surface area of electrospun nanofibrous adsorbents provide abundant of adsorption sites, resulting in the high adsorption capacity of dyes and organic contaminants [261].

Li et al. [261] fabricated PCL/PVP strips with helicoidal geometries by using the immersion electrospinning method and immobilized ZIF-8 on the electrospun strips for the adsorption of Methylene blue. The helicoidal morphology and surface-area-to-volume ratios were controlled by the PCL/PVP weight ratio (Fig. 20). Owing to the high surface-area-to-volume ratios and helicoidal morphology, more ZIF-8 particles were homogeneously immobilized, providing more active adsorption sites. Owing to the synergistic effects of the nanofiber morphology and the active adsorption sites from ZIF-8, the prepared

Table 2
Summary of heavy metal ions removal performance of electrospun nanofiber materials.

Nanofiber adsorbents	Metal ions	Adsorption capacities (mg g^{-1})	Equilibrium time (min)	pH	Temperature (°C)	Initial concentration (mg L^{-1})	Isotherm kinetic	Removal (%)	Ref.
Nylon 6,6/Choline glycinate-ionic liquid	Fe(III)	379.80	120	-	Room temperature	100	-	-	[227]
CA/TiO_2@PDA@PEI	Cr(VI)	357.1	> 700	2	25	50 - 300	Langmuir, PSO	89.5	[226]
Zein	Pb(II)	189	100	-	-	1000	PSO	94.5	[214]
	Cd(II)	164						85.4	
KTS@PAN	Cs(I)	210.1	10	4–10	25	225	Langmuir-Freundlich	95	[228]
	Sr(II)	56.8				60		99	
PAN/FCS-NaY	Cu(II)	-	10	4.6	-	50	-	94.6	[229]
	Pb(II)							98.7	
PAN/PEG/MgO (magnesium oxide) nanoparticles	Cu(II)	354	180	5	25	200	Langmuir, PSO	90	[230]
PAN/PEI@ZIF−8	Cr(VI)	403.5	960	3	25	20 – 400	PSO	90	[217]
Magnetic ion-imprinted PAN	Pb(II)	130	250	7	25	10 – 400	Langmuir, PSO	97.07	[231]
Zwitterionic phosphate groups functionalized PAN	U(VI)	1294	720	7	-	20 – 500	Langmuir, PSO	99	[225]
Ch-DTPA/PEO	Cu(II)	177	120	5	Room temperature	50 – 750	Langmuir, PSO	-	[232]
	Pb(II)	142	120	5					
	Ni(II)	56	120	6					
Ch-f-PVA/SA	As (III)	540.4	90	6–7	25	200 – 400	Freundlich PSO	90	[233]
Ch/Nylon 6	Cu(II)	240	5	4	30	20 – 100	PSO	90	[234]
PEI/PVC	As(V)	115.79	180	5	25	100	Langmuir,	91	[4]
PAN/Fe-MOFs	Cr(VI)	127.7	90	4	25	10 – 2000	Redlich-Peterson, PFO	-	[224]
NiFe LDH/PAN/GO	Cr(VI)	13.1	12	6	Room temperature	10 – 20	Langmuir, PFO	98.9	[235]
MXene/PVP carbon nanofiber	Pb(II)	12.7	30	7	-	0.01 – 10	Langmuir, PSO	89	[236]
	As (III)	3.3	20					81	
Ami-PEN	Cr(VI)	279.78	50	5	25	200 – 1000	Langmuir, Avrami fractional-order	-	[237]
PAN-BT-DG	Cr(VI)	173	240	3	55	10 – 750	Freundlich PSO	-	[238]
cPAN-Ag	Pb(II)	193.8	-	-	25	0 – 400	Langmuir	90	[239]
Acrylic acid modified PET	Cu(II)	56.69 mg dm^{-2}	-	6	-	0 – 200	Langmuir	-	[240]
Acrylamide modified PET		36.64 mg dm^{-2}							
SA-Ca	Cu(II)	285.5	30	7	50	50 – 400	Liu isotherm, General-order	93	[219]
Cellulose/MWCNTs/SnO_2	Cu(II)	116.4	30	6	Room temperature	20 – 200	Freundlich	97	[241]
PAN/PEI/MWCNT-COOH	Pb(II)	346	480	6	-	30 – 400	Langmuir, PSO	98	[216]
P-PLLA/PDA/Ch	Cu(II)	270.27	40	6	Room temperature	50 – 200	Langmuir, PSO	-	[242]
PVA/ L-Cysteine	As(V)	1.3	500	7	Room temperature	0.01 – 0.3	Henry, PFO	92	[243]
PAA/PAH	Cu(II)	30.57	80	7.4	-	2	Langmuir,	92	[244]
	Cd(II)	15.85	100					98	
ZrO_2@UiO−66	As (III)	143.95	360	8	Room temperature	5 – 400	Langmuir, PSO	80	[245]
PAN/GO-HPEI	Au(III)	2893.33	960	4.7	25	50 – 600	Langmuir, PSO	89	[246]
ZIF−8@ZIF−8/PAN	Cr(VI)	39.68	90	2	25	1 – 500	Langmuir, PSO	80	[247]
TiO_2-PAN/(MWCNT/GO)-g-PCA	Cd(II)	178.57	40	8	45	50	Langmuir, PSO	97	[248]
Ch/g-C_3N_4/TiO_2	Cr(VI)	238.66	240	2	-	20 – 800	Langmuir, PSO	90	[249]
Ch/PVA/IL	Pb(II)	166.34	120	9	25	20 – 100	Freundlich, PSO	82.5	[215]
α-Fe_2O_3/PAN/$CaCO_3$/CTA	Pb(II)	181.1	60	-	Room temperature	10 – 100	Freundlich, PSO	91	[250]
	Cu(II)	268.09						77	
PEI-PAN/GO	Ag(I)	167.4	720	5.6	25	30 – 300	Langmuir, PSO	97.2	[251]
PAN/DAG	Cr(VI)	348.7	15	2	25	5 – 30	Langmuir, PSO	95.1	[252]
PAN/PEI/PPy	Cr(VI)	368.0	500	2	Room temperature	60 – 400	Langmuir, PSO	95	[253]
PAN/Polyaniline	Pb(II)	290.12	-	7	Room temperature	5 – 350	Freundlich	82	[254]
	Cr(VI)	202.53				5 – 500		90	
PAN-GO-Fe_3O_4	Cr(VI)	124.34	70	3	25	0.5 – 50	Langmuir, PSO	90	[255]
E. faecalis/CNF composite	As (III)	255.2	30	5	24	10 – 300	Langmuir, PSO	-	[256]
Ch/PVA/ Hal–NH_2	Cd(II)	454.5	120	6	25	50 – 1000	Langmuir, PSO	78	[257]
	Pb(II)	476.2		5.5				84	
Ch/PVP/PVA	Cu(II)	34.79	-	-	Room temperature	1 – 20	Langmuir, PSO	94.2	[258]
	Cu(II)	25.24						90.35	
	Cd(II)	18.07						83.33	
	Pb(II)	16.05						80.12	

(*continued on next page*)

Table 2 (*continued*)

Nanofiber adsorbents	Metal ions	Adsorption capacities (mg g^{-1})	Equilibrium time (min)	pH	Temperature (°C)	Initial concentration (mg L^{-1})	Isotherm kinetic	Removal (%)	Ref.
PVA/IONP	As(V)	30.0	1200	5	25	0.1 – 2	PFO	> 80	[220]
PAN/$Fe(NO_3)_3$	Cr(VI)	445.3	-	1	25	300	-	98.9	[259]
Thiol-functionalized CA	Cu(II)	49.0	240	4	25	20 – 400	Langmuir, PSO	-	[260]
	Cd(II	45.9							
	Pb(II)	22.0							

Abbreviations appeared for the first time: KTS – potassium tin sulfide, FCS – Freeze-dried Chitosan, DTPA – diethylenetriaminepentaacetic acid, LDH – layered double hydroxides, PEN – polyarylene ether nitrile, BT-DG – guanidinium-based ionic covalent organic framework, PAH – polyallylamine hydrochloride, PCA – poly citric acid, CTA – cellulose triacetate, DAG – diaminoglyoxime, PPy – polypyrrole, Hal-HH2 – amine-grafted halloysite nanotube, IONP – ultra-small nanoparticles.

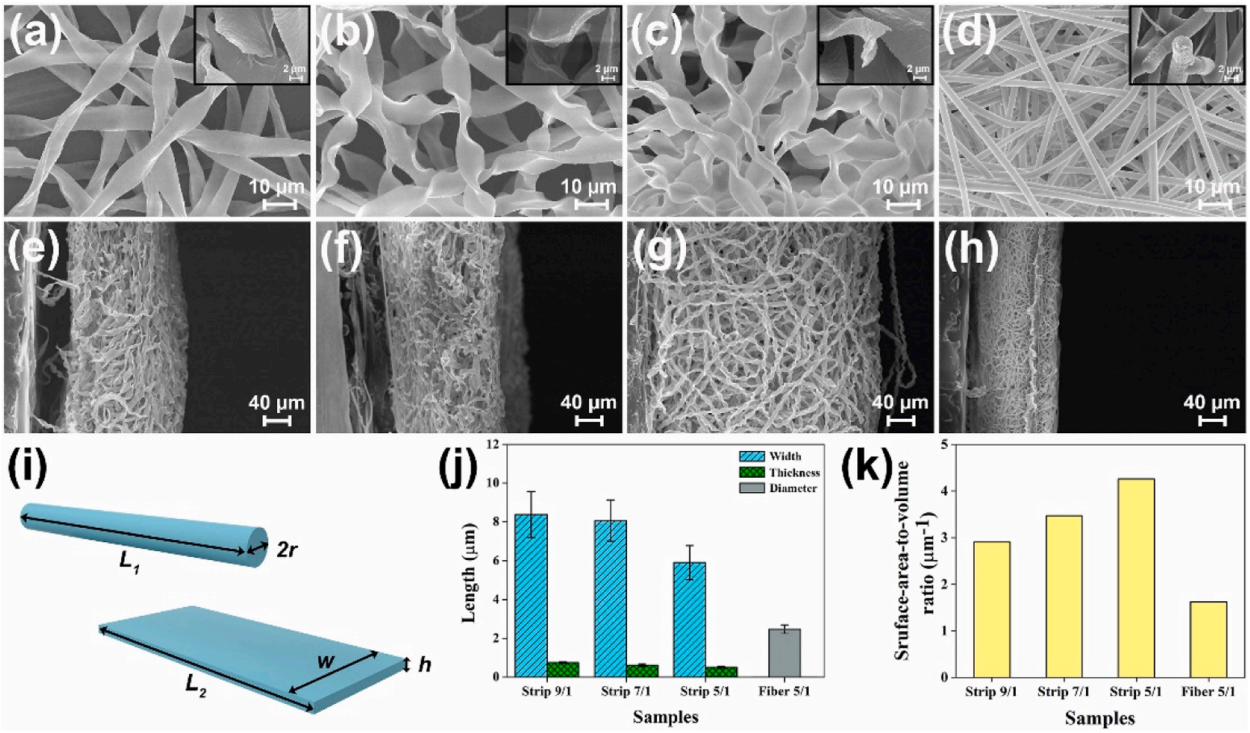

Fig. 20. SEM images of the electrospun architectures (a, e) strip 9/1, (b, f) strip 7/1, (c, g) strip 5/1, and (d, h) fiber 5/1. (i) Schematic of the simplified geometry for surface-area-to-volume ratio calculation. (j) Geometric properties of samples, and (k) the calculated surface-area-to-volume ratio.
Reproduced with permission from ref. [261]. Copyright 2023 Elsevier.

PCL/PVP/ZIF-8 strip showed a high Methylene blue adsorption capacity of 151.6 mg g^{-1}, which is 4 times higher than the PCL/PVP/ZIF-8 conventional straight nanofibers. Electrostatic and π-π stacking interactions were the main adsorption mechanism for Methylene blue adsorption. The control of nanofiber geometry and the incorporation of MOFs could provide electrospun nanofibers with higher adsorption kinetics and efficiency [261]. The bio-adsorbent *Moringa oleifera* (MO) has a high affinity to Congo red. To improve its reusability and adsorption capacity, Narayan et al. [262] fabricated MO incorporated PAN electrospun nanofibers for the adsorption of Congo red. The prepared PAN/MO nanofibers exhibited high Congo red adsorption capacity equal to 55.56 mg g^{-1}, and achieved 90 % removal efficiency in 2.5 h. The adsorption kinetics and equilibrium were well described by the PSO model and Freundlich model, respectively. The multilayer heterogeneous adsorption occurred on the prepared nanofibers. The prepared PAN/MO nanofibers showed high regenerative ability in several cycles of adsorption-desorption, indicating the applicability of nanofiber supported bio-adsorbents on an industrial scale.

Wang et al. [263] fabricated PVDF/PDA/β-Cyclodextrin (β-CD) electrospun nanofibers with core-shell structure for the bidirectional adsorption of cationic dyes (Methylene blue) and anionic dyes (Phenolphthalein). As shown in Fig. 21**A**, PVDF electrospun nanofibers were used as a supporting matrix. The PVDF fibers show a smooth surface and uniform morphology with an average diameter of about 400 nm. Subsequently, the PDA layer was formed on the surface of PVDF electrospun nanofibers, and the β-CD molecules were incorporated on the PDA modified nanofibers *via* hydrogen bonding between hydroxyl groups of β-CD and amine groups of PDA. After modification, the average diameter of the nanofiber increased to 660 nm, the surface became rougher, and some loosely stacked particles appeared. The modified nanofibers possess a rougher and thicker shell layer, which can benefit the diffusion and penetration of organic dyes. The prepared PVDF/PDA/β-CD nanofibers exhibited super-hydrophilic properties, owing to the amino groups of PDA and hydroxyl groups of β-CD. The adsorption kinetic and equilibrium of PVDF/PDA/β-CD nanofibers were well described by the PSO model and Langmuir model, respectively. The PVDF/PDA/β-CD nanofibers showed high adsorption capacity for Methylene blue, resulting from morphology and core-shell structure of electrospun nanofibers, the electrostatic attraction and π-π stacking (Fig. 21**B**), and high adsorption capacity for Phenolphthalein, resulting from hydrogen bonding and the host-guest inclusion complexation (Fig. 21**B**) [263].

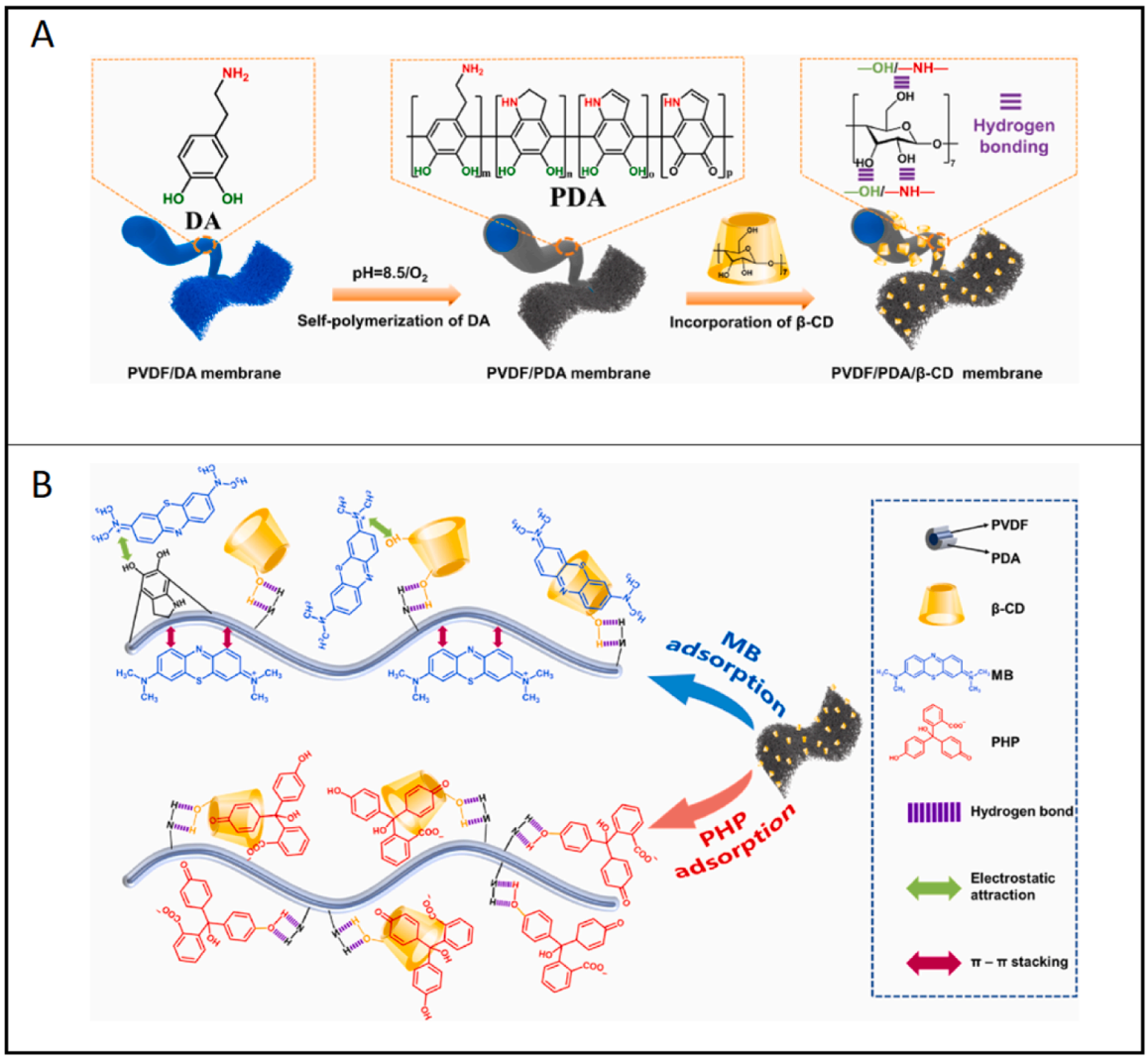

Fig. 21. The scheme of the fabrication process (A), and the dye adsorption mechanism (B) of PVDF/PDA/β-CD composite electrospun nanofibers. Reproduced with permission from ref. [263]. Copyright 2022 Elsevier.

Owing to the persistence and toxicity of per- and polyfluoroalkyl substances (PFAS), the presence of PFAS in aquatic environments has posed threats to human health [267]. Especially, it is challenging to remove short-chain PFAS from water by using conventional adsorbents due to the weaker hydrophobic interaction. Kang et al. [267] fabricated PEI-PVC electrospun nanofiber adsorbents for the adsorption of both short [perfluorobutanoic acid (PFBA) and perfluorobutanesulfonic acid (PFBS)] and long-chain [perfluorooctanoic acid (PFOA) and perfluorooctanesulfonic acid (PFOS)] PFAS. At pH 7, PEI-PVC nanofibers showed high adsorption capacities of 84.26 mg g^{-1} for PFBA, 214.37 mg g^{-1} for PFBS (short-chain PFAS), and 213.76 mg g^{-1} for PFOA and 326.39 mg g^{-1} for PFOS (long-chain PFAS). The high adsorption capacities of PEI-PVC NF were resulted from the strong electrostatic attraction with PEI and the pore-mediated adsorption driven by nanopore structure.

Table 3 summarizes the adsorption performance of electrospun nanofibers for dyes and organic contaminants from 2020 to 2023. As shown in Table 3, PAN, PVDF, PVA, PVC, PCL, polyether block amide (PEBA 2533), and zein were used for electrospun nanofibers fabrication. Modifications such as surface modification, polymer blend, and the incorporation of MOFs and nanoparticles, are used to improve their adsorption capacity for dyes and organic contaminants and recyclability in the adsorption processes. Langmuir isotherm model and PSO kinetic model are commonly used to describe the adsorption equilibrium and kinetics.

4.2.2. *Filtration of dyes*

In addition to the utilization of electrospun nanofibers as adsorbents, nanofibrous membranes were also prepared and used in the dynamic adsorption or adsorptive filtration processes. Lim et al. [280] fabricated MIL-101(Cr) (Matérial Institut Lavoisier) incorporated PAN electrospun nanofibrous membranes with a layer-by-layer hierarchical structure for the removal of Methyl orange and Rose Bengal. The prepared MIL-101 (Cr)/PAN electrospun nanofibrous membranes demonstrated the high removal efficiency for Methyl orange (95 %) and Rose Bengal (99 %) in isopropanol, owing to the electrostatic attraction and high isopropanol flux equal to 60 L m^{-2} h^{-1} at low pressure 0.04 bar, owing to the porous nanofibrous morphology and layer-by-layer structure. Most importantly, the prepared membranes showed a desirable regeneration and recyclability, which is beneficial in industrial-scale solvent recovery [280]. Wang et al. [281] prepared PEI/PVC adsorptive electrospun nanofibrous membranes for the removal of Cibacron brilliant yellow from wastewater. The prepared PEI/PVC showed hydrophilic properties and a positive charge in the pH 4–9, owing to the presence of PEI. The

Table 3
Summary of adsorption performance of electrospun nanofiber materials for the removal of dyes and organic contaminants.

Nanofiber adsorbents	Dyes or organic contaminants	Adsorption capacities (mg g^{-1})	Equilibrium time (min)	pH	Temperature (°C)	Initial concentration (mg L^{-1})	Isotherm kinetic	Removal (%)	Ref.
PVDF/PDA/β-CD	Methylene blue	188.3	30	-	-	10	Langmuir, PSO	70	[263]
	Phenolphthalein	203.7						50	
(3-Aminopropyl) triethoxysilane (APTES) crosslinked Ch/ PPLLA	Rhodamine B	86.43	180	6	Room temperature	300	Langmuir, PSO	95	[264]
	Methylene blue	82.37	120						
PAN/MO	Congo red	55.56	400	7	-	15 – 85	Freundlich, PSO	88	[262]
PEBA 2533	Histamine	13	20	-	25	0.5 – 30	Langmuir, PSO	66	[268]
	Putrescine	11						91	
	Cadaverine	10						83	
	Tyramine	14						96	
PCL/PVP/ZIF−8	Methylene blue	151.6	120	-	20	15 – 180	Langmuir, PSO	98	[261]
Al_2O_3/PAN	Methylene blue	0.96	-	9	Room temperature	10 – 30	Langmuir, PFO	88	[269]
SSAS/PAN	Crystal violet	439.85	1000	7	25	50 – 1000	Dubbinin–Radushkevich, PFO	-	[270]
Clay/PVA	Crystal violet	121.73	120	10.4	25	25 – 400	Redlich-Peterson, PFO	99.34	[271]
$La(OH)_3$@cellulose	Congo red	624	-	7	25	10 – 400	-	98.8	[5]
ZIF-L/PAN	Malachite green (MG)	5216	120	3 – 7	20	200 – 1600	Langmuir, PSO	95.0	[272]
Silk nanofibers	Reactive black 5	62.2	5	5	25	25 – 400	Langmuir, PSO	98.0	[265]
polydopamine-coated PVA	Methylene blue	20.1	120	11	25	20 – 200	Langmuir, PSO	90.0	[273]
EDA-ECNFs	Methylene blue	119.8	100	9	25	25 – 200	Dubinin–Radushkevich, PSO	-	[274]
melam-ECNFs		116.7							
NiFe LDH/PAN/GO	Rose Bengal	6.19	12	6	Room temperature	3 – 13	Langmuir, PFO	80.6	[235]
	Brilliant blue	7.74						92.1	
PAN-COOH-CEW	Toluidine blue O	546.24	30	10	25	0.1 – 5	Langmuir, PSO	97.32	[275]
PVP-SiO_2	Methylene blue	30.4	60	10	25	10 – 60	Langmuir, PSO	95.0	[276]
PEI-PVC	PFBA	98.7	300	7	25	5 – 250	Langmuir, PSO	28.0	[267]
	PFBS	222.36						48.2	
	PFOA	234.85						51.2	
	PFOS	319.82						62.2	
Zein	Congo red	168.00	50	2	25	20 – 2000	PSO	-	[214]
Ch-PVA	Methylene blue	99.9	300	12	Room temperature	10 – 300	Langmuir, PSO	88.8	[277]
Ch/PVA/GA/PEI	Methyl orange	70.8	1200	4	25	20 – 200	Langmuir	43.6	[266]
PEN	Methylene blue	796.25	100	7	Room temperature	0 – 150	Langmuir, PSO	99.0	[278]
ZIF−8@Ch/PVA	Malachite green	1000.00	150	6	25	10 – 40	Langmuir, PSO	90.0	[279]

Abbreviations appeared for the first time: PPLLA – porous poly (L-lactic acid), SSAS – poly(sodium styrene sulfonate–*co*–acrylonitrile–*co*–styrene), ECNFs – electrospun carbon nanofibers, CEW – chicken egg white.

prepared reusable membranes showed a high water flux of 3031 L m^{-2} h^{-1} at 1 bar and dye removal efficiency of 95 % [281]. Kadirvelu and Fathima [282] used keratin to modify the PEI/PAN electrospun nanofibrous membranes for the improvement of the Alizarin Red S removal efficiency since keratin possesses amino acids and amphoteric functional groups for the sorption of organic dyes. The keratin modified PEI/PAN membranes demonstrated an enhanced rejection capacity of 93.25 %, which is 33 % higher than the pristine membranes, owing to the decreased surface roughness and the electrostatic repulsion mechanism. The keratin modification also endowed the membrane with easy regeneration since the dye deposition on the membrane surface and pore clogging were inhibited, owing to the formation of electrostatic repulsion layer from keratin [282].

Table 4 summarizes the dye removal performance by using electrospun nanofibrous membranes. It can be seen that various polymers, such as PAN, PCL, PVC, and sulfonated polyethersulfone (SPES) were used for the fabrication of nanofibrous membranes. The pressure used for the dynamic adsorption or adsorptive filtration process was usually no more than 1 bar and the water permeability was generally high, owing to the high porous structure of electrospun nanofibrous membranes. To enhance the removal efficiency of organic dyes, the incorporation of polymers, MOFs and nanoparticles and the surface modification of membranes were used.

4.2.3. *Catalytic degradation of dyes*

The utilization of photocatalysis is cost-effective for the degradation of organic dyes and contaminants in the wastewater [289]. As shown in Table 5, electrospun nanofibers were used as supporting materials for the immobilization of catalysts to fabricate nanofiber composite materials for the degradation of organic dyes and contaminants. The combination of catalysts with electrospun nanofibers could enhance the degradation efficiency of organic dyes since the electrospun nanofibers possess high surface area and porosity, providing more contact sites for the interaction between catalysts and dyes [289,290]. Moreover, the catalyst/nanofiber composites can be easily recycled from the aqueous solution after the catalytic reaction. Hassan et al. [289] fabricated TiO_2-GO/PAN-CA nanofiber composite for the photocatalytic degradation of Methylene blue. The incorporation of TiO_2-GO increased the nanofiber diameter and enhanced the mechanical properties of nanofibers. The prepared TiO_2-GO/PAN-CA nanofiber composite showed a high degradation efficiency of 97 % for Methylene blue under visible light after 2 hours [289]. Lv et al. [290] prepared porous

Table 4
Summary of separation performance of nanofibrous membranes for dye removal.

Membranes	Dyes	Dye concentration (mg L^{-1})	Pressure (bar)	Water permeability (L m^{-2} h^{-1} bar^{-1})	Removal rate (%)	Ref.
MIL−101(Cr)/PAN	Acid fuchsin	10	0.14	5066	99	[283]
	Methyl orange			8808	99	
	Rose Bengal			7574	99	
PS	Basic red 46	50	-	530	99	[284]
	Methylene blue			530	99	
PAN-ZnO	Methylene blue	20	1	1016	99	[285]
	Rhodamine B	20		1016	97	
	Congo red	50		1016	99	
	Sunset yellow	20		1016	98	
	Methyl orange	20		1016	96	
Keratin-PEI/PAN	Alizarin red S	40	0.1	30	93.25	[282]
PCL-FeTA-APTES	Methylene blue	40	-	11.3 mL m^{-2} h^{-1}	98	[286]
G-C_3N_4/RGO/TiO_2/PVDF	Methyl orange	-	1	1261	94.2	[287]
PAN/MIL−101(Cr)	Methyl orange	50	0.04	60 L m^{-2} h^{-1}	95	[280]
	Rose Bengal				99	
poly(m-phenylene isophthalamide) (PMIA)/β-FeOOH−12	Methylene blue	10	0.2	3000 L m^{-2} h^{-1}	99.99	[288]
SPES	Methylene blue	6	-	320 L m^{-2} h^{-1}	99.9	[164]
PEI/PVC	Cibacron brilliant yellow	10	1	3031	95.0	[281]

Table 5
Summary of the electrospun nanofiber materials used as catalysts for the degradation of dyes and organic contaminants.

Nanofibers	Dyes or organic contaminants	Initial concentration (mg L^{-1})	Exposure time (min)	Power source	Degradation (%)	Ref.
CdSe@CA	Methylene blue	1	40	Visible light	74.65	[292]
Ag-CdSe@CA					70.78	
CdSe/GO@CA					88.34	
Ag-CdSe/GO@CA					89.63	
$Bi_2ZnB_2O_7$/PAN	Methylene blue	5	180	Visible light	82.00	[293]
GO/SnO_2/PAN	Sulfamethoxazole	5	480	Electrochemical	85.00	[294]
ZnO/Poly-cyclodextrin	Methylene blue	15	120	Stimulated visible irradiation	94.30	[6]
TiO_2-GO/PAN-CA	Methylene blue	15	120	Visible light	97.00	[289]
DMG/TiO_2/PAN	Methylene blue	10	60	UV lamp	97.00	[290]
CuS@CS	Tetracycline	10	120	Solar light	81.30	[291]
TiO_2-CuO	Tetracycline	100	75	UV lamp	86.00	[295]
CdS@void@TiO_2@PPy nanofibers	Tetracycline	5	300	Visible light	77.00	[296]
Sr-doped $Bi_4O_5Br_2$/Bi_2MoO_6/PAN	4-chlorophenol	10	60	Visible light	100.00	[297]
CuCo@CNF	Acid Red 1	50	20	-	99.00	[298]

dimethylglyoxime (DMG)/TiO_2/PAN electrospun nanofiber mats for the removal of Methylene blue and Ni^{2+} from wastewater. The prepared nanofiber mats showed a high Ni^{2+} adsorption capacity equal to 48.69 mg g^{-1}, owing to the ability of DMG to sense and adsorb Ni^{2+}. The DMG/TiO_2/PAN showed a desirable photocatalytic degradation efficiency of 97 % for Methylene blue within 60 minutes, owing to the construction of heterojunctions between Ni(DMG)$_2$ and TiO_2 nanoparticles and the decrease of electrons and holes transport pathways [290]. Huang et al. [291] fabricated copper sulfide (CuS)/Ch electrospun nanofiber composites with photo-Fenton catalytic and photothermal activities to enhance the degradation of tetracycline. The prepared CuS/Ch nanofiber composites possessed high porosity and surface area and showed fast degradation reaction under near infrared laser irradiation, owing to the formation of electron-hole pairs and local hyperthermia. What is more, the prepared nanofiber composites could be easily separated from the reaction mixture and reused after the regeneration of adsorption sites [291].

4.3. Oil-water separation

Nanofiber webs have gained interest from both academia and industry since they have a high specific surface area, tight pore size, highly porous structure, tunable wettability, and remarkable functionality. The fast advancement of nanofiber production techniques has led to the efficient and cost-effective mass production of nanofiber webs. Consequently, there has been an increasing focus on utilizing electrospun nanofibers in diverse fields.

Nanofiber webs have proven to be particularly useful in the cleaning

of oily wastewater. The commercially used oil-water cleaning technologies like separation with gravity, sedimentation, oil skimming, adsorption, filtration, dissolved air-flotation, coagulation, centrifugation, and biological treatment are ended with drawbacks in terms of fouling, facile secondary pollution, low filtration efficiency, low removal efficiency, high price and high operation cost, corrosion and high energy demands [299,300]. Among them, the membrane technology offers a great opportunity for the separation of oily wastewater owning to low cost, low energy demand, excellent separation performance, and less impact on the environment. Nevertheless, the primary issue afflicting membrane separation techniques is membrane fouling. Membrane fouling continues to be a significant technical obstacle in the separation industry. Nanofibers are an excellent choice for infor membrane technology due to their highly porous structure, enabling high permeability and tight pore size. This results in increased filtration and separation efficiency and helps to solve vital energy environment issues [301,302]. Additionally, nanofibers possess a high specific surface area, which allows for the functionalization of the surface with active compounds or groups to enhance filtration performance [303]. Moreover, in the event that the pores become blocked with foulants, the interconnected pore structure of nanofibers allows liquids to flow through alternative paths [304].

The previous studies showed nanofiber membranes had a flow rate that was several times greater than that of phase-inversion membranes [305,306]. The main reasons are high surface pore density and the higher pore opening size, which results in high permeability and better fouling resistance. Choong et al. [307] demonstrated that the membrane fouling with emulsified oil depends on the fiber diameter, which is related to the membrane pore size. Based on their research, the density of the fouling layer is influenced by the available space within the membrane as it develops. As the droplet diameter to fiber diameter ratio (dp/df=2.5) increases, the likelihood of oil droplets entering the membrane decreases. Thus, a more permeable layer of fouling material forms outside the membrane. When dp/df is equal to 0.57, droplets accumulate in the pores of the membrane, leading to a decrease in rejection rate compared to a higher dp/df ratio. Also, a majority of the oil droplets cross the membrane without contacting the fibers.

Despite the significant advantages of utilizing nanofibers in membrane technology, there are several challenges that need to be addressed to enhance their suitability for selectively removing oil-water mixtures. These challenges include sorption selectivity between oil and water, mechanical strength, fouling issues, and membrane cleaning. Recent studies have demonstrated promising results in enhancing the characteristics of nanofiber membranes, overcoming these obstacles, and making them more effective for oil-water separation.

4.3.1. *Sorption selectivity of membrane between oil and water*

The sorption selectivity of nanofiber membranes depends on their composition, structure, and surface properties. The material can be polymeric, natural, or inorganic based. The interaction between the membrane and component (oil or water), the molecular size, polarity, and chemical characteristics of the components also influence sorption selectivity. By altering the membrane material, the sorption selectivity can be increased for target pollutant. One good example is porous superhydrophobic cellulose acetate butyrate (CAB) nanofiber. The hydrophobic and oleophilic properties of CAB, together with the porous structure of the nanofibers, are believed to result in a larger surface area, which makes them well-suited for sorption applications [308].

However, there is not a wide range of nanofiber membrane material, which may cause not effective sorption. For this reason, sorbents can be used as additives for the nanofiber membrane. For instance, Chen et al. [309] produced UiO-66-NH_2 and PAN using electrospinning. Subsequently, they applied hydrophobic modification to gain selectivity for oil. Adding UiO-66-NH_2 to fibers results in enhanced surface roughness of the composite membrane, resulting in a considerable enhancement in oil affinity. The composite membrane was used to adsorb different chemicals, including kerosene, colleseed oil, methyl silicone oil, methylbenzene, and dichloromethane. The highest adsorption capacities for these substances were 21.9, 31.5, 39.9, 19.9, and 39.7 g g^{-1}, respectively. The results were 32–96 % higher than those of the pure PAN adsorbent.

4.3.2. *Membrane's mechanical strength*

The mechanical characteristics of the nanofiber membrane limited their use in pressure-driven liquid filtration. For this reason, a composite structure is preferred. Using the lamination technique, nanofibers were combined on a support material, and the tensile properties of the polyamide 6 (PA6) and PAN membranes has been improved up to 22 and 9-fold, respectively [310]. The lamination process is simple to handle and allows for the use of different adhesives in the form of powder, liquid, or web. The adhesion can be achieved by heat-pressing, welding, or curing [311–315]. Due to the transition of the lamination process to a roll-to-roll method, it will be more convenient to overcome this challenge for the application [316]. Fig. 22 shows an illustration of nanofiber membrane process for oily wastewater process.

4.3.3. *Membrane fouling and surface modification*

Membrane fouling is a significant drawback of using nanofibers in membrane technology. To eliminate membrane fouling, researchers focus on changing the structure of the nanofiber membrane, feed solution properties, or membrane cleaning process. The most straightforward approach to mitigate membrane fouling involves improving hydrophilicity and oleophobicity or vice versa. Surface modification of nanofiber membranes has attracted significant interest in recent years to enhance process development and reduce limitations. Table 6 displays the latest research on modifying nanofiber membranes to separate oily wastewater. Based on the literature review and Table 6, PVDF is a frequently utilized polymeric fiber for separating oily wastewater. PVDF is highly hydrophobic, chemically and thermally stable, has high resistance to oxidation, and has outstanding mechanical properties [317]. Due to these features, PVDF has become an attractive material for membrane technology. Another widely utilized polymer in oil-water separation is cellulose. In contrast to PVDF, cellulose is known for being hydrophilic, biodegradable, sustainable, and containing three free hydroxyl groups per monomer unit [318]. The arrangement of hydroxyl groups allows for the creation of strong hydrogen bonds, making it easier to modify and attach additional functional groups or nanoparticles. A crucial aspect of the modification process is ensuring the secure bonding of the modifier to the membrane surface. Inadequate attachment may lead to secondary pollution issues during the filtration process.

The membrane can be designed for water-in-oil or oil-in-water separation. Water-in-oil separation indicates the separating water droplets dispersed in an oil phase. Similarly, oil-in-water configuration signifies the dispersion of oil droplets within a water phase. For this reason, membranes with different selectivity are needed.

4.3.3.1. Water-in-oil separation. Membranes utilized for the separation of water and oil must possess hydrophobic properties in order to effectively reject water and enable the smooth flow of oil. This characteristic exhibits hydrophobicity, which results in the membrane being impermeable to water, successfully repelling water droplets and preventing their passage through the membrane. Enhancing the hydrophobicity of the surface through surface structure modification can facilitate the separation of water-in-oil. For instance, Liang et al. [328] developed a lotus leaf-like structure by applying a sprayable premodified SiO_2 nanofiber coating onto a PVDF nanofiber membrane. This approach enhances water-in-oil emulsion separation efficiency and provides antifouling properties. When subjected to various oils, the modified membrane demonstrated superhydrophobic properties, achieving an average water rejection rate of 99.49 % for water-in-isooctane

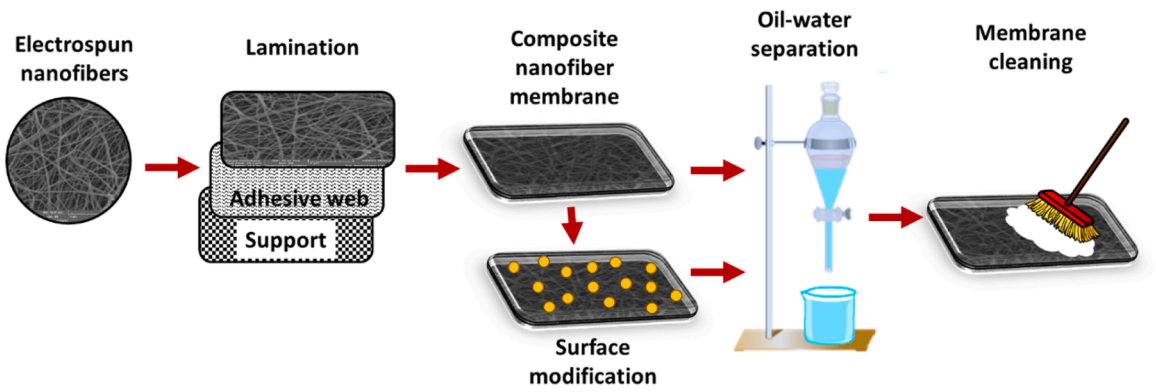

Fig. 22. The schematic illustration of nanofiber membrane preparation and oily wastewater separation.

Table 6
Recently published studies on modified nanofiber membranes for the filtration of oily wastewater.

Nanofiber membrane	Surface modification	Filtration performance	Reference
PVDF	Application of Tannic acid (TA) and APTES on the membrane, the strong oxidizing with sodium periodate (SP) to optimize the wettability of the membrane to form superhydrophilic/underwater superoleophobic membrane.	High flux of 1871 L m^{-2} h^{-1} and exceptional separation efficiency of 99.83 % for oil–water emulsions, solely driven by gravity, with outstanding recyclability demonstrated after 10 cycles.	[319]
PVDF	Self-polymerized PDA, silver nanoparticles (AgNPs) immobilization and self-assembly of thiol on PVDF nanofiber membrane	pH-responsive nanofibrous membrane, pH> 10 superhydrophilic, pH< 10 superhydrophobic, separation efficiency > 99.2 % for light oil(toluene, isooctane and *n*-hexane)/water mixture and 96.5 % for heavy oil(dichloromethane)/water mixture with a consistant flux of around 2500 L m^{-2} h^{-1} for water and 11000 L m^{-2} h^{-1} for oil during the 10-cycle separation process.	[320]
PVDF	Adding Diethylenetriaminepentaacetic acid (DTPA)-functionalized multi-walled carbon nanotube (MWCNT)/TiO_2 into PVDF electrospinning solution to develop a hydrophilic and underwater oleophobic membrane for separating cooking-in-water, engine-in-water, and hexane-in-water emulsions	Separation efficiency> 97.4 ± 1 %, stable flux over than 930 L m^{-2} h^{-1} during 10-cycle process of separation.	[321]
PUR	Modification of CNTs and PDA onto PUR nanofibers for separation of emulsions (created by blending different oils such as cyclohexane, heptane, and toluene).	With a separation efficiency of up to 99.9 %, the water permeate flux reaches up to 4195 L m^{-2} h^{-1}) after undergoing numerous cycle separation tests.	[322]
PLA	By using coaxial electrospinning method, creating nanoscale clusters of fluorine-modified SiO_2 (F-SiO_2) and applying PDMS coatings.	Remove 100 % water droplets in oil droplets which is larger than 150 nm in the emulsion created with Span 80, n-oil (such as n-octane, olive oil, and soybean oil), and deionized water, permeability up to 13818.8 L m^{-2} h^{-1}·bar^{-1}), permeance recovery rate up to 98.4 %.	[323]
Cellulose	Magnetic nickel (Ni) layer and hydrophobic PDMS coating with electroless deposition (ELD).	The oil adsorption capacity is greater than 60 % of the volumetric absorption capacity. The cyclic stability is above 80 % of the adsorption capacity after 200 cycles. The oil-retention ability is over 80 % at 200 rpm for oils such as n-hexane and dichloromethane.	[324]
Cellulose	Deacetylation of cellulose acetate based cellulose nanofibers binding with the zwitterionic copolymer poly(sulfobetaine methacrylate-*r*-glycidyl methacrylate) with the epoxy groups in it.	Hydrophilic/oleophobic surface with average separation efficiency > 98 % for the toluene/water, n-hexane/water, and cyclohexane/water emulsions. High recycling and stability for a minimum of 20 cycles.	[325]
Cellulose	The synthesis of hydrophilic-oleophobic composite aerogels involves polycondensation of cellulose nanofiber and three silane coupling agents.	With an absorption capacity reaching up to 11.5 g g^{-1} and remarkable reusability, the composite aerogels demonstrate sustained absorption efficiency even after five absorption-regeneration cycles for hexadecane-water mixtures.	[326]
Carbon	Superhydrophobic and superoleophilic carbon nanofiber membrane with rod-shaped ZnO nanostructure is created through the in-situ growth of ZnO nanorods and fluoridated modification combination.	Oil flux achieves approximately 3531 L m^{-2} h^{-1}, with a separation efficiency exceeding 99 % even after multiple cycles of separation for a diverse oil-water mixture comprising carbon tetrachloride, dichloromethane, petroleum ether, ethyl acetate, and n-hexane oils along with water	[327]

emulsions, 99.85 % for water-in-cyclohexane emulsions, and 99.30 % for water-in-diesel emulsions. Xu et al. [329] engineered hydrophobic membranes tailored for separating water-in-oil emulsions. These membranes feature a tubular nanofiber structure comprising hybrid PVC, which is precisely interwoven with 2D nanofibers and 3D microspheres. By incorporating an inorganic additive, hydrophobic nano silica (SiO_2,) and employing a PET hollow braided tube as a supporting base, the group successfully constructed a novel 3D structure. The design utilizes continuous interfaces of water, oil, and solid materials by combining 2D PVC nanofibers with 3D microspheres. This combination effectively slows down the water-wetting process and enhances the hydrophobic stability of the 3D nanofiber membrane. A SiO_2 additive was used to enhance the hydrophobicity of the electrospun nanofibers membrane, increasing lipophilicity and achieving superhydrophobicity in the presence of oil. The membrane achieved a permeation flux of up to 358.60 L m^{-2} h^{-1} and a separation efficiency of over 95 % only from the force of gravity. Following a prolonged separation experiment, the membrane's separation efficiency remained consistently high. Similarly, the incorporation of SiO_2 nanoparticles into the PVDF spinning solution facilitated the one-step fabrication of a nanofiber membrane with

superhydrophobic and superoleophilic properties[330]. By adjusting the quantity of SiO_2 nanoparticles, the surface roughness of the nanofibers is modulated, leading to a transition in the wettability of the nanofiber membrane from hydrophobic (contact angle $< 140°$) to superhydrophobic (contact angle $> 150°$). This modification results in outstanding separation efficiency (99 ± 0.1 %), accompanied by a high separation flux (1857 ± 101 L m^{-2} h^{-1}), excellent multi-cycle performance, and stable chemical resistance. In a separate study [331], researchers integrated carbon nanofibers (CNFs) with a hollow structure onto the framework of PDMS foam. This integration demonstrated a robust interfacial adhesion, contributing to the uniform decoration of CNFs throughout the structure. By purposefully increasing surface roughness in this manner, the membrane hydrophobicity was substantially increased, which resulted in improved efficacy for oil adsorption up to 2.56-fold and facilitated simple procedures for separating highly viscous oil (crude oil) and water.

Recently, a remarkable membrane with asymmetric wetting properties has been developed for effectively separating both oil-in-water and water-in-oil emulsions across diverse and challenging environments [332]. The electrospun nanofiber membrane, composed of SiNPs/ZnNPs-SiO_2/TiO_2 (SZST), demonstrates remarkable versatility in swiftly modulating its wettability across diverse environments (*e.g.*, strongly acidic and alkaline, high or low temperature and even salty environment). This feature enables the membrane to achieve controllable separation of both oil-in-water and water-in-oil emulsions. The superhydrophobic SiNPs/ZnNPs surface efficiently separates water-in-oil emulsions, while the SiO_2/TiO_2 surface of the nanofiber membrane effectively separates oil-in-water emulsions, with separation efficiencies exceeding 99 % for both types of emulsions. This research indicated that, membranes can alter their separation behavior under various environment condition.

4.3.3.2. Oil-in-water separation. Membranes utilized for separating oil from water must be hydrophilic to attract and enable the flow of water while resisting oil. This characteristic inhibits the membrane from being wetted by oil and eases the separation of oil droplets from the aqueous phase. One example can be provided where PUR nanofiber is coated with acidified CNTs on the surface and then treated with polydopamine to provide superhydrophilic and underwater superoleophobic properties in a nanofiber composite [322]. The PUR nanofibrous membrane's hydrophilicity significantly increased with the addition of acidified CNTs and PDA, attributed to the many polar groups in PDA molecules and the water adsorption capability of the acidified CNTs. Heptane, cyclohexane, and toluene oils stabilized with SDS in emulsion are used for testing. The membranes achieved high separation efficiency, and water permeate flux, with oil rejection rates exceeding 99.7 % and permeating flux values of 4108, 5293, and 7240 L m^{-2} h^{-1} for separating heptane-in-water, toluene-in-water, and cyclohexane-in-water emulsions, respectively. These performance metrics were consistently maintained even after undergoing multiple cyclic separation tests.

By using hydrophilic SiO_2 NPs, membrane hydrophilicity can be improved. As an example, Gao and colleagues [333] developed a superhydrophilic membrane through a straightforward one-step electrospinning process, incorporating PVP and hydrophilic SiO_2 nanoparticles into PVDF for successful oil-water separation. The modified membrane exhibits superhydrophilicity (with a WCA of 0°) and pronounced oleophobicity in water (with an oil contact angle surpassing 145°). It demonstrates excellent separation efficiency, surpassing 99.5 % for various oil-water mixtures (xylene, n-hexane, dichloromethane, linseed, motor oil, and petroleum ether) and exceeding 97 % for various oil-in-water emulsions. Moreover, even after undergoing 30 test cycles, the membrane displays commendable separation performance and reusability. In another research, Geng et al. [334] created a nanofiber composite membrane made of poly(m-phenylene isophthalamide) (PMIA)/PAN/SiO_2 specifically for separating oil and water under challenging conditions. Nanofibers were created by electrospinning a PMIA, PAN, and SiO_2 solution. The composite membrane's super amphiphilicity and rough surface structure resulted in super-oleophobicity in water and super-hydrophobicity in oil, leading to a separation efficiency of over 99.6 % even in acidic, alkaline, and saline environments.

The key factor in improving the membrane performance for water-in-oil or oil-in-water processes is the regulation of membrane hydrophobicity/hydrophilicity and oleophilicity/oleophobicity in the presence of an oil-water mixture/emulsion. Surface alteration is a highly successful method. To enhance the hydrophilicity and oleophobicity of the nanofiber membrane, it must possess at least one of the following features: a) Incorporation of functional groups like -OH, COOH, polar functional groups such as -NH_2, or polyelectrolytes like sulfonic acid and quaternary ammonium groups; b) Addition of hydrophilic polymers like PVA, polyethylene glycol (PEG), or PVP; c) Integration of hydrophilic additives such as hydrophilic nanoparticles or surfactants; d) Use of zwitterionic materials containing both positive and negative charge groups.

On the other side, to enhance the hydrophobic and oleophilic properties of a nanofiber membrane, it must include at least one of the following characteristics: a) Presence of functional groups including fluorine-containing groups (-CF_3), perfluorosulfonic acid groups, siloxane groups (Si-O), aromatic hydrophobic groups (e.g. phenyl rings), long hydrophobic alkyl chains (e.g., -CH_3, -CH_2-), carboxylic acid derivatives (e.g. esters and fatty acids); b) Utilization of hydrophobic polymers such as polypropylene (PP) or PVDF; c) Incorporation of hydrophobic additives such as hydrophobic nanoparticles or surfactants; d) Existence of nanoscale surface roughness.

4.3.4. Membrane cleaning

Electrospun membranes, known for their extensive porosity, provide exceptional efficacy in filtering and separating processes, resulting in notable efficiency in oily wastewater separation. Yet, a challenge emerges when handling oils that possess a low surface tension, as they have a tendency to disperse and infiltrate the surfaces of membranes, hindering their immediate use in separating oil and water. In order to exploit the benefits of electrospinning membranes, researchers have focused on creating nanofibrous membranes that can effectively eliminate different types of oils. These membranes have demonstrated outstanding efficacy in removing contaminants. However, membrane fouling is an unavoidable issue where pollutants adhere to the membrane's surfaces and pores, leading to a notable decrease in separation efficiency and membrane lifespan. Moreover, the current superwetting membranes that exhibit only one sort of wettability have restrictions, limiting their effectiveness to particular oil/water mixes. The classification of these membranes as either "oil-removing" or "water-removing" hinders their practical application in complex wastewater treatment situations. Therefore, it is crucial to focus on reducing membrane fouling and creating adaptable membranes as key areas of study. Researchers enhance the self-cleaning properties of the membrane to decrease membrane fouling [335–337]. However, despite possessing a self-cleaning surface, as the number of cleaning cycles increases, membrane fouling becomes inevitable. The recurring issue of membrane fouling, caused by repetitive usage, leads to problems such as reduced permeation flow and restricted recyclability, highlighting the necessity for inventive solutions in membrane technology. In the course of the process, membranes often undergo both physical and chemical cleaning procedures to eliminate contaminants [338]. Various physical cleaning techniques such as forward flush, reverse flush, and air flush, are used. Membranes are submerged in a solution with chlorine bleach, hydrochloric acid, or hydrogen peroxide for chemical cleaning. The fluid diffuses across the membranes for a set period, then a flush is done either forward or backward to remove pollutants efficiently. Typically, commercial membranes come with established cleaning protocols tailored for end users. In contrast, nanofiber membranes currently lack

standardized cleaning procedures. Existing literature research shows limited attention to the cleaning of nanofiber membranes, with only a few studies addressing this aspect.

As an example, Gul et al. [339] fabricated nanofiber membranes using PVDF, PAN, and PA6. Subsequently, the membranes were subjected to contamination by utilizing wastewater derived from a 50/50 v/v mixture of engine oil and water. Various chemical cleaners such as alkaline NaOH, acidic citric acid (CA), and surfactants like SDS and Triton were tested at different concentrations. Furthermore, combinations of these cleansers were tested to enhance the cleaning procedure. Alkaline washing of the fouled membrane with Triton X-100 surfactant led to a flux recovery that was two to five times greater than cleaning without a surfactant. The binary solution of 5 % sodium hydroxide + Triton showed the highest flux recovery rate during alkaline cleaning, whereas the individual solution of 1 % citric acid had the highest flux recovery rate during acidic cleaning. In another work, Xu et al. [329] used sodium hypochlorite (NaClO) and CA solutions as chemical cleaners for the PVC hybrid nanofiber membranes. Following chemical cleaning, the WCAs of the PVC membrane remained consistently above 140°, and the separation efficiency exhibited minimal change, surpassing 95 %. The research findings highlight the need for distinct cleaning protocols tailored to each membrane type, considering their material composition and the pollutants present in the feed. Further research and examination into cleaning procedures, specially developed for nanofiber membranes, are necessary to determine the future direction.

4.4. Membrane distillation

MD is a membrane process where the driving force is the difference in chemical potential between the feed and the permeate side of the membrane, characterized as a thermally induced vapor pressure difference [340,341]. It is considered potential method for purifying water, and compared to other frequently employed membrane separation techniques, it offers several advantages. These include the absence of a need for external pressure (*i.e.* reverse osmosis (RO)), reduced vapor spaces when compared with conventional distillation methods such as multi-effect distillation (MED) and multi-flash distillation (MFD), a theoretical 100 % salt rejection, and lower requirement for high mechanical property standards [342,343]. Moreover, it incorporates lower operational temperatures, eliminating the necessity for elevated heat levels. The critical factor here is the temperature difference (ΔT), as illustrated in Fig. 23, where the dependence of the ΔT on the operating temperature is counter-proportional [340].

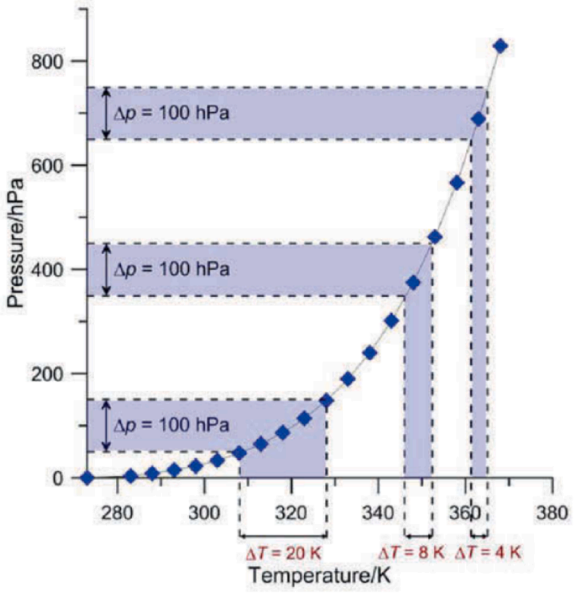

Fig. 23. Relation between temperature and vapor pressure of water. Reproduced from ref. [340] – Creative Commons CC BY 4.0 license.

The membrane stands out as a crucial element in all membrane processes. In MD, specific criteria must be met to qualify a membrane as a suitable candidate for the process. Firstly, the membrane must exhibit porosity. Inadequate porosity can hinder water vapor transport due to pores being too small, or it can lead to membrane wetting if the pores are too large. Secondly, it needs to be hydrophobic to prevent undesired wetting during the process. Lastly, although some heat loss is inevitable, optimizing the heat and energy efficiency of the process by limiting heat transfer through the membrane is important [342]. The membrane can be produced with numerous methods, including stretching, phase inversion, and electrospinning. Notably, ENMs are increasingly becoming a focus in membrane distillation. This rising interest is linked to the distinctive properties of these membranes, which exhibit high porosity, resulting in a large surface area, robust mechanical strength, and a significant degree of interconnection. Moreover, membranes created through electrospinning can be easily customized by adjusting process parameters, allowing control over attributes such as porosity, fiber diameter distribution, and membrane thickness [16,344]. However, some issues still have to be addressed in order to prepare an appropriate membrane for MD.

4.4.1. Antiwetting

The fundamental issue in MD is membrane wetting, which stops the entire process and prevents efficient separation. This critical issue underscores the urgency of exploring and implementing enhanced solutions. One prevalent strategy to address this challenge involves the application of surface modifications, which prove to be a popular and effective means of improving membrane properties. Diverse methodologies can be employed to deal with the issue of membrane wetting and optimize the performance of MD systems. These treatments include a variety of surface modifications designed to reduce or eliminate the negative effects of wetting, resulting in continuous and effective separation processes.

Meng et al. [345] prepared membranes by PDA/PEI co-deposition and subsequent silicification and fluorosilanization of the nanofibers. The modification increased water, glycerol, and diiodomethane contact angle values and a drastic increase in mineral oil contact angle (from 20° to 125°), imparting omniphobic properties to the surface. The DCMD desalination results revealed increased wetting resistance for the mixture of NaCl and SDS in the feed solution (Fig. 24) [345].

Wu et al. [189] used a vapor deposition (VD) method for the fluorination of the membrane surface. An omniphobic membrane with WCA over 150°, and ethanol contact angle over 120° was acquired. In the desalination MD procedure, membranes exhibited higher salt rejection in comparison with unmodified membranes and stable flux for an 8-hour experiment using 3.5 % NaCl/0.4 mM SDS feed mixture[189].

A multi-layer re-entrant structure was successfully fabricated by Xu et al. [346] via subsequent immersion of PVDF-HFP/APTES electrospun membrane into Si NPs solution in an ammonia-ethanol mixture (9/1, v/v), and tetraethoxysilane (TEOS): deionized water (DI): Ethanol (1/2/20, v/v/v), respectively. The obtained membrane was characterized by contact angle values for water – 151.49°, mineral oil – 140.64°, 4 mM SDS – 119.59°, and ethanol – 107.50°. (Fig. 25). Membrane distillation experiments confirmed high antiwetting properties of the membranes. The salt rejection was maintained at nearly 100 % for the whole duration of the experiment with 0.4 mM SDS in the feed, while the pristine PVDF-HFP membrane exhibited wetting after the first 0.1 mM SDS portion [346].

4.4.2. Antifouling

Although membrane distillation is more resistant to fouling than pressure-driven processes, it is still a significant problem that must be

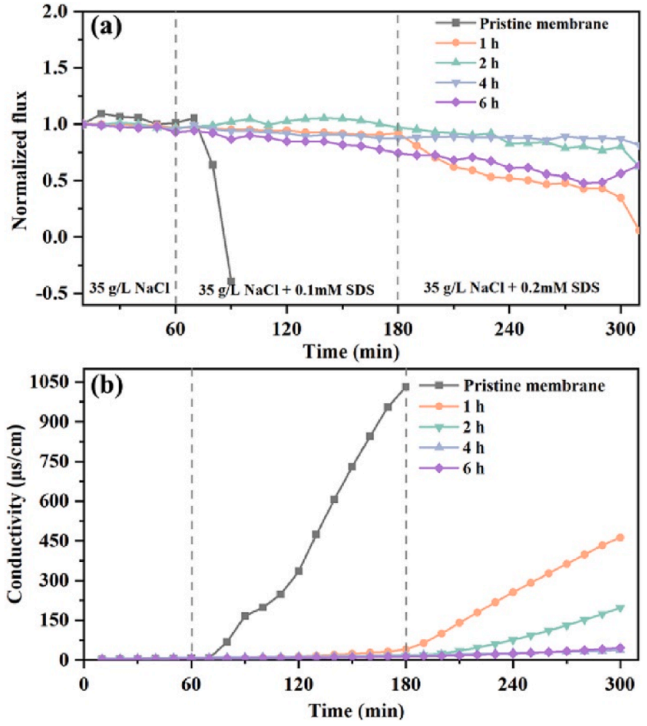

Fig. 24. MD performance of the pristine membrane and omniphobic membranes determined with different PDA/PEI co-deposition time using synthetic hypersaline water as feed solution, (a) normalized flux and (b) conductivity of permeate solution.
Reproduced with permission from ref. [345]. Copyright 2023 Elsevier.

carefully addressed. This risk is especially acute in wastewater and real seawater treatment, where a variety of organic compounds are present. Although necessary for efficacy, the important necessity for robust hydrophobization in membrane distillation tends to increase fouling-related concerns, underlining the significance of targeted research and new solutions to solve these issues.

Xu et al. [347] prepared an electrospun nanofibrous membrane with three different precursors (Polytetrafluoroethylene (PTFE)/PVA/PAN). The membranes needed additional modification with silica nanoparticles and 17-FAS to acquire a micro-nano-structured surface with amphiphobic properties. They demonstrated membranes' stable water flux (6.48 kg m^{-2} h^{-1}) within 24 h experiment with 1000 ppm diesel oil in the feed. Furthermore, the flux remained stable even after cleaning in a 3-cycle experiment (Fig. 26) [347].

Janus membranes gain interest in membrane separation fields for their dual character. Xu et al. [348] prepared a dual-layer ENM (C-PAN/PH) with additional catalytic properties for shale gas wastewater treatment. Hydrophilic PAN (C-PAN) and hydrophobic PVDF-co-HFP, (PH) were used to fabricate nanofibrous layers, and Co-TPML was used as the catalyst. The obtained membranes were evaluated in a DCMD setup. The C-PAN/PH membrane exhibited higher fluxes in comparison with pristine PH membrane in all tested feed solutions (*i.e.* 13.8 and 10.0 kg m^{-2} h^{-1}, respectively, with NaCl feed solution). The C-PAN/PH was resistant to fouling during a 10 h experiment with kerosene as feed and maintained around 90 % of initial flux (13.6 and 13.1 kg m^{-2} h^{-1} for 1000 and 3000 ppm of kerosene, respectively) while the PH membrane drastically decreased flux to 0 kg m^{-2} h^{-1} in 4 h [348].

Frequently, promising new materials are employed as modifiers to improve the characteristics of membranes. Kebria et al. [349] have synthesized hydrophobic hyper-branched dendritic (HB-Den) structures containing aluminum to incorporate in the PVDF nanofibrous membrane matrix. The WCA has risen from 128° to approximately 140°. Real seawater was used as a feed solution in the air-gap membrane distillation (AGMD) experiment to evaluate antifouling properties. According to the results, the modified membrane (HB-Den3) exhibited a lower flux decline in comparison with the native PVDF membrane (7 % and 26 %, respectively). Moreover, the HB-Den3 membrane had better flux

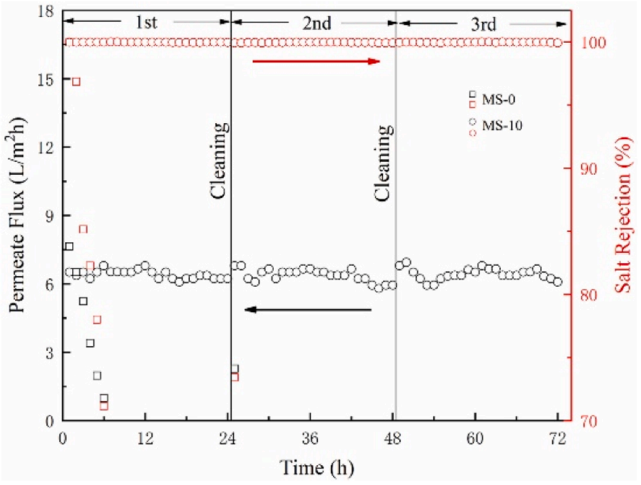

Fig. 26. Permeate flux and salt rejection of the MS-0 and MS-10 in MD process during the three cycles test.
Reproduced with permission from ref. [347]. Copyright 2022 Elsevier.

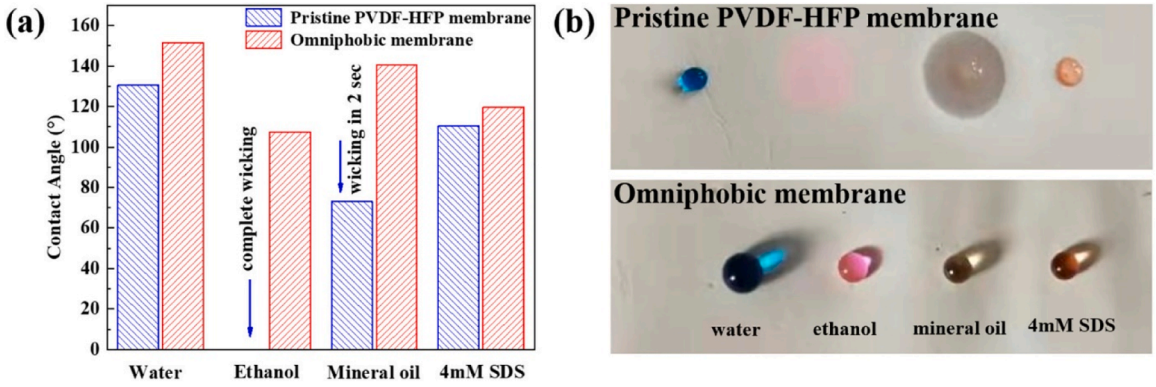

Fig. 25. Membrane wettability results of (a) contact angles of the control PVDF-HFP membrane, omniphobic membrane; (b) photos of several different testing liquids.
Reproduced with permission from ref. [346]. Copyright 2021 Elsevier.

recovery (94.5 %) compared with native PVDF (75.5 %) (Fig. 27). The results proved better antifouling properties and suitability of modified membranes for MD application [349]. While most papers focus on antiwetting and antifouling properties, some intriguing niche solutions have emerged, particularly in membranes with photothermal conversion properties. This phenomenon finds utility in solar-driven membrane distillation (SDMD), where solar energy is absorbed and converted into heat within the hydrophilic layer of the membrane. This additional heat raises the temperature of the feed, affecting the water vapor flux through the membrane. Ding et al. [350] formulated a dual-layer composite nanofibrous membrane with an integrated layer of PAN-Ag nanoparticles. The proposed membrane achieved an energy conversion efficiency of over 75 %. Despite the relatively low water vapor flux of 1.2 kg m^{-2} h^{-1}, it is remarkable that this was accomplished without a temperature differential between the feed and permeate sides in the MD process. Similarly, Chen et al. [351] demonstrated a comparable approach, achieving a water flux of 44.4 kg m^{-2} h^{-1} with a temperature difference (ΔT) of 60°C. They utilized polypyrrole (PPy) as the photothermal layer, resulting in an excellent flux and energy conversion efficiency of 92.2 %. These findings signify a promising direction for the development of low-energy consumption membrane distillation processes.

Table 7 provides a comprehensive overview of the performance of modern ENM's, with a focus on the impact of surface modifications and electrospinning process parameters. These adjustments are strategically employed to enhance membrane performance and introduce additional benefits. Notably, the modified membranes demonstrate heightened resistance to both organic and inorganic fouling, signifying improved fouling mitigation capabilities. Furthermore, surface modifications contribute to enhanced antiwetting behavior, showcasing the diverse improvements achieved through tailored enhancements.

As indicated in Table 7, the majority of research in the field of electrospun membranes centers on desalination applications in membrane distillation, with key properties being antiwetting and antifouling. Nevertheless, other applications such as oil-water separation and the treatment of dye wastewater are also gaining prominence. The main base materials used include PVDF and PVDF-co-HFP, with fluorinated substances being the most frequently employed modifiers. This choice is rationalized by the advantageous properties conferred by these materials, including excellent mechanical properties, chemical and thermal resistance. However, it is crucial to highlight that many of these substances are not environmentally friendly, indicating a need for future research to focus on more sustainable alternatives.

4.5. The application of nanofibers in air filtration

Currently, nanofibers are mostly linked to their application in the filtration industry. This is mostly due to the proven reliability of nanofibers in the filtration industry, leading to their commercialization in many applications [388]. The development of nanofibers, particularly in their application of air filtration, has rapidly advanced during the past two decades, thanks to the advent of the initial large-scale electrospinning machinery [389].

Attaining a position alongside cellulose papers, glass fibers, spunbond and meltblown fabrics, or cellulose/synthetic fiber mixes, which are widely recognized as the primary materials for air filtration, is a challenging task. However, nanofiber-coated filters surpass conventional filters in terms of their forceful characteristics. Nanofiber filter media provide superior cost-effectiveness and efficiency compared to traditional filters. They possess reduced energy demands and exhibit greater longevity [390].

4.5.1. Importance of air filtration

Air pollution is a major worldwide problem that presents significant risks to both human health and the environment, and the sustenance of our existence relies on a continuous provision of fresh and clean air for respiration, whether in our residences, urban areas, rural environments, or workplaces [391]. Therefore, air filters have become essential components of our modern world. Air filter media is employed in various dimensions and configurations in power plants engaged in electrical energy generation [392], heavy industries involved in metalworking processes, including metal grinding, cutting, and welding [393], vehicles used for transportation [394], the air conditioning systems of large commercial buildings or shopping centers [395], and in reducing flue gas pollution from factories and coal power plants.

Air filter types using fabric filter media can be grouped together as follows;

- Cartridge filters
- Bag or Pocket filters
- Pad filters
- Particulate air filter
- Roll filters
- Activated carbon filters

4.5.2. Particle capture mechanism in air filtration

The capture mechanism relies upon the material type, as well as the physical and chemical structure of the filter media employed. Occasionally, multiple mechanisms can coexist within a single filter media.

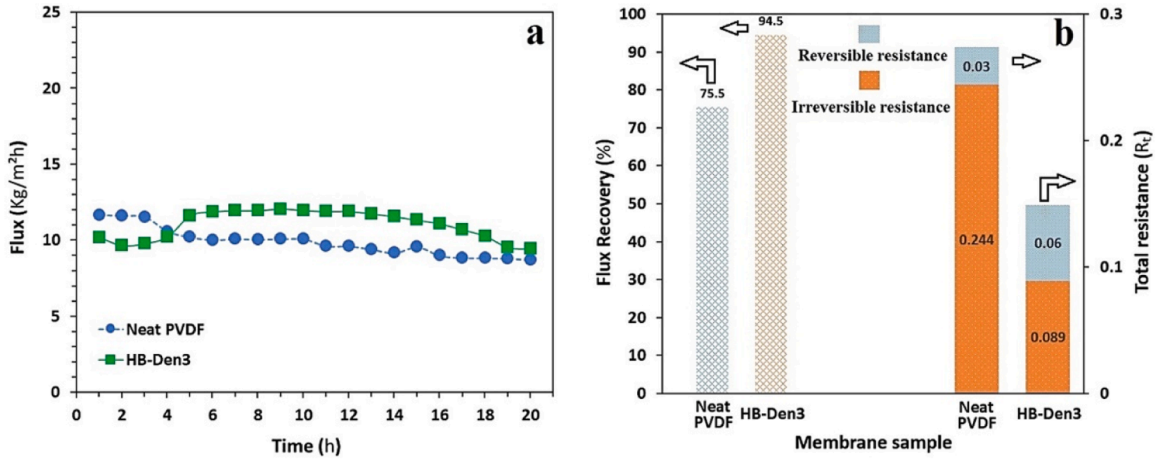

Fig. 27. Real seawater filtration results (a), and anti-fouling properties of ENMs (b). Reproduced with permission from ref. [349]. Copyright 2020 Elsevier.

Table 7
Summary of publications using electrospun membranes in membrane distillation application.

Membrane Base Material	Modifiers	Application	Properties	WCA [°]	Water vapor flux [kg m^{-2} h^{-1}]	Electrospinning parameters							Ref.
						Polymer solution concentration [%]	Voltage [kV]	Precursor flow rate [mL h^{-1}]	Tip-collector distance [cm]	Rotation speed [rpm]	T [°C]	RH%	
PVDF-co-HFP	PDA, PEI, PDTS, TMOS	Desalination	Antiwetting	~160	39.31	15, 20, 25	20	60	15	300	25	50	[345]
PVDF-co-HFP	FDTS	Desalination	Antiwetting	154.1	10.5	15	17.5	1	15	-	21–22	40–50	[189]
PVDF-co-HFP	SiNP, APTES, FDTS, TEOS	Desalination	Antiwetting	151.49	19.11	15	17	1	13	-	-	-	[346]
PTFE/PVA/PAN	TEOS	Desalination, Oil-water separation	Antiwetting, Antifouling, Antiscaling	~160	17.09	10	25	0.48	10	500	27	20	[347]
PAN, PVDF-co-HFP	Co-TPML	Deaslination, Oil-water separation, Micropolutant removal	Antifouling, Catalitic	36.6/130.3 (Janus membrane)	13.8	~7/20	10.4/20	1	15	300	20–25	40–50	[348]
PVDF	Hydrophobic hyper-branched dendritic (HB-Den)	Desalination	Antifouling	138.3	10.7	16	-	0.5	-	550	24	60	[349]
PVDF-co-HFP	MCF−5, FAS	Desalination, Wastewater treatment	Antiwetting, Antifouling	143	8	15	20	1.7	15	1300	35	80	[352]
PET	FAS	Desalination	Antiwetting	up to 140	20–22	30	22	0.9	11	-	25	5	[353]
PVDF	PDMS, SiO_2NP	Desalination, Wastewater treatment	Anriwetting, Antifouling	156.9	28.5	12	30	2	20	-	23	45	[354]
PVDF/ZnO	PDTS	Desalination	Antiwetting, Antiscaling	162.3	11.5	8	16	0.5	15	140	RT	50	[355]
PVDF	SiNP, FAS17	Desalination	Antiwetting	154.6	11.5	13.5	25	1.5	15	250	25	40	[356]
PVDF	BisF-Bz	Desalination	Antiwetting	132.7	19.28	15	24	1.2	15	-	-	-	[357]
PA6	F-POSS, PVDF NP.	Desalination	Antiwetting, Antifouling	149	8.7	13–16	20	-	18	-	25	45	[358]
PTFE/PVA	vinyl-POSS	Desalination	Antiwetting	151	40	43 (PTFE)	28	1	18	-	25	35	[359]
PUR	PTFE NP	Desalination	Antiwetting	133.9	44	8	30	3	24	-	25	45	[360]
PVDF-co-HFP	pGS, CTAB, FAS, SiNP	Desalination, Oil-water separation	Antiwetting, Antifouling	150/20	19.5/24.6	16	14	1	15	140	23	55	[361]
PAN, PVP	-	Desalination	Antiwetting	up to 160	up to 20.4	from 5.5 to 19	12, 16	1.2	15	40	-	20	[362]
PVDF-co-HFP	HKUST−1, AlFu, UiO−66-NH_2, Activated carbon	Amonia removal	Amonia removal performance	-	9.5 (Amonia transfer flux)	15	20	1	15	-	23–25	30–40	[363]
PES/CNTs	PVDF-co-HFP/CNTs	Desalination	Antiwetting	144	22.2	23/15 (PES/PcH)	20/22	1/1.2	15	50 (mm/s)	-	-	[364]
PVDF-co-HFP	F-POSS	Desalination	Antiwetting	152.4	~8	20	13.5	1.2	-	1200	-	-	[365]
PVDF	PDMS	Desalination	Antiwetting	148.7	35	5	14	2	15	-	29–31	40–50	[366]
PS	-	Desalination	Antiwetting	139.9	11.68	20 (wt/v%)	20	6	17	560	22–25	50–60	[367]
PVDF	PDMS, PAN, AgNP	Desalination	Photothermal conversion	-	1.2	15	28	0.3	15	500	30–35	30	[350]
PVDF-co-HFP	ZIF−71	Desalination, Dye wastewater treatment	Antiwetting	135	19.2	20	20	1	15	300	25	30	[368]

(*continued on next page*)

Table 7 (*continued*)

Membrane Base Material	Modifiers	Application	Properties	WCA [°]	Water vapor flux [kg m^{-2} h^{-1}]	Electrospinning parameters							Ref.
						Polymer solution concentration [%]	Voltage [kV]	Precursor flow rate [mL h^{-1}]	Tip-collector distance [cm]	Rotation speed [rpm]	T [°C]	RH%	
PVDF-co-HFP	PPy, SiO_2, PAN	Desalination	Antiwetting, Photothermal conversion	148	44.4	~15/~9(dual-layer)	18/14	0.12 (mm/min)	20	-	24	55/40	[351]
PAN	APTES, SiNP, PFDTS	Desalination	Antiwetting	145	16	11	22	1	15	-	22	50	[369]
PVDF	ATO, PAN	Desalination	Antiwetting, Antifouling, Photothermal conversion	~130	-	15 wt%/1.5(wt/v%) PAN/PVDF	20	1	15	-	-	-	[370]
PAN/SAN	-	Desalination, Oil-water separation	Antiwetting, Antifouling	37.5/141.7	34.89	8/17	22/18	5.4	30	-	-	-	[371]
PVDF	-	Desalination	Antiwetting	up to 148	up to ~12	17/25	15	1/0.4	15	-	18	30	[372]
PVDF	PTFE	Desalination	Antiwetting	122.4	27.7	5–20	24	1.2	15	-	-	-	[373]
PVDF,	P(MMA-*r*-MPS)-g-PDMS, TiO_2 NPs	Desalination	Antiwetting, Antiscaling	150.4	34.5	-	13	0.5	15	200	25	30	[374]
PVDF-co-HFP	CNTs	Desalination	Antiwetting	140.7	18.5	20	20	1	15	300	25	30	[175]
PVDF-co-HFP	-	Desalination	Antiwetting	156.6	38.8	15	15	-	15	-	20	50	[375]
PVDF-co-HFP	AlFu MOF	Desalination	Antiwetting	135	22.7	17.5	18/15/13	1	15	-	21–22	40–50	[376]
PMMA	-	Desalination	Antiwetting	164.2	41.04	20	18	9.6	30	-	-	-	[377]
PVDF	ZnO nanowires, POTS	Desalination	Antiwetting, Antiscaling	150	15.7	17	10	0.5	16	-	-	-	[378]
PTFE	PNIPAM/PS	Desalination	Antifouling, Thermoresponsive wettability	100.3	35.78	-/15 (PTFE/PNIPAM-PS)	20/18	1	15/10	-	-	-	[379]
PVDF-co-HFP	TFS	Desalination	Antiwetting, Antifouling	> 150	17	8	18	1	15	145	-	-	[380]
PVDF-co-HFP	CB, F-POSS	Desalination, Gypsum removal	Antiwetting, Antiscaling	162	40	15	30	0.1 (mm/min)	18	-	25	60	[381]
PVDF, PVDF-co-HFP	FG	Desalination	Antiwetting,	157	up to 15.9	19/15	18	0.5	18	500	25	45	[382]
PET	PVDF-co-HFP	Juice concentration	Antifouling	143.7	8.62	-	11–18/22 (PET/PH)	1.5/1	12	-	25	35	[383]
PVDF	Lycopodium particles	Desalination	Antiwetting	161.6	52.4	25	24	1.25	27.5	-	22	28.9	[384]
PVDF	iPP	Dye wastewater treatment	Antifouling	157.2	53.9	15	28	0.3	15	-	37	31	[385]
PVDF	PFTS	Desalination, Oil-water separation	Antiwetting, Antifouling	173.2	17–20	25	24	0.88	15	80	-	-	[386]
PVDF-co-HFP	ODA- rGO	Desalination	Antiwetting	146	21.2	19	10–20	1	18	-	-	-	[387]

Abbreviations appeared for the first time: PDTS – 1 H,1 H,2 H,2H-perfluorodecyl-triethoxysilane, TMOS – Tetramethyl orthosilicate, FDTS – 1 H, 1 H, 2 H, 2H-perfluorodecyltrichlorosilane, Co-TPML – nano-catalysts, MCF-5 – mesocellular silica foam, BisF-Bz – bis-(4-fluorophenyl-bisphenol-benzoxazine), POSS – polyoctahedral silsesquioxanes, pGS – poly(glycidyl methacrylate-sulfobetaine methacrylate), CTAB – cetyl-trimethylammonium bromide, AlFu – aluminum fumarate, PFDTS – 1 H,1 H,2 H, 2H-Perfluorooctyltriethoxysilane, ATO – antimony tin oxide, MMA – methyl methacrylate, MPS – 3-methacryloxypropyltrimethoxysilane, PNIPAM – poly (N-isopropylacrylamide), TFS – Trichloro(1 H,1 H,2 H,2H-heptadecafluorodecyl)silane, CB – carbon black, FG – fluorinated graphite, iPP – isotactic polypropylene ODA – octadecylamine.

The capture mechanisms in a fiber system, where a single particle is transported through a pore in a filter medium, can be described below (Fig. 28).

- Sedimentation or gravity settling refers to the process where larger and denser particles can settle within a filtration system [396].
- Straining or sieving refers to the process where particles are retained if they are bigger than the pores in the filter media and lack sufficient inertia to cause harm.
- Internal impaction refers to the phenomenon when a particle deviates from the fluid's streamline and instead continues along its current trajectory until it collides with the filter media. The most effective configuration consists of large particles with high density, high velocity, and very small fibers [397].
- Interception occurs when a particle, as it moves along a streamline, makes contact with the filter media and is captured. The effectiveness of this procedure depends on the relationship between the particles' size and the pores' size, as well as the strength of the bond between the particles and the filter material [398].
- The effectiveness of the diffusion mechanism is dependent on the size of the particles and the densities of the fluid and particles. A particle's movement is affected by the fluid's general flow and the random motion resulting from collisions with smaller molecules in the fluid, referred to as Brownian motion. This can direct the particle toward the filter material, potentially causing it to get caught [399].
- In the context of electrostatic deposition, the particle's surface charge may be different from that of a fiber or pore in the filter media, resulting in its redirection toward the medium and subsequent retention [400].

Air filter media collects particles by depth filtration and surface filtration [401]. Depth filtration is the process in when a particle moves through a pore until it reaches a point where the pore is too small to pass through. The particle is solely retained due to its dimensions. Once the pore is obstructed, it remains blocked until the filter media gets too clogged, rendering it no longer usable for further processing. At this juncture, it is necessary to discard and replace the medium or alternatively, clean it. Surface filtration refers to the process that happens in close proximity to the initial surface of a filter material. In this scenario, particles within a system can interact solely with a pore, offering the sole opportunity for entrapment (Fig. 29). With time, the pores in the medium may become obstructed by solid particles. To address this issue, surface filtration media can be cleaned or revitalized by directing a pulse or steam of clean fluid in the opposite direction.

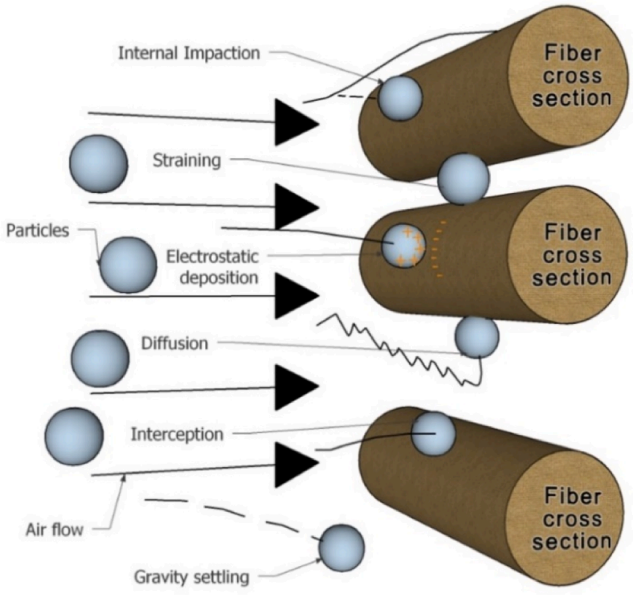

Fig. 28. Particle capture mechanism.

Traditional fiber-based filters, including meltblown, spunbonded, and glass fiber use depth filtration but have limited capacity to filter small particles because of structural issues like thick fiber diameter, big pore size, and low porosity. Decreasing the diameter of the fibers can greatly improve the filtration effectiveness of the fiber filter. Nanofibers have significant potential as a surface filtering medium due to their tight pore size, small diameter, open pore structure, and high porosity.

4.5.3. *Polymeric electrospun nanofiber-based air filters*

Since the early 1990s, electrospun nanofiber air filters have served as highly efficient air filtration media due to their exceptional capacity to capture PM particles from the air [402]. This is attributed to their extensive surface area, extremely small fiber diameters, highly porous structure with consistent and uniform pore size, and lightweight nature. Electrospun nanofibers have found applications across a broad spectrum of filtration needs, including car cabin filters, personal protection equipment, indoor air cleaners, window screens, respiratory facemasks, industrial dust collectors, and gas turbine filters. A variety of natural and synthetic polymers, including but not limited to PA [403], PUR [404], PVDF [405], CA [406], PVA, Ch [407], PSF [408], and PAN [409], have demonstrated efficacy in producing nanofiber filters with remarkable performance. PA has gained significant prominence as a preferred synthetic polymer for air filter production owing to its robust and enduring physical and chemical properties.

During the early 2020 s, the global demand for respiratory face masks surged as a result of the Covid pandemic. Nanofiber filter media emerged as the primary air filters, playing a crucial role in ensuring essential protection. Transparent nanofibers made of PA 11 were created for usage in facemasks. These nanofibers have excellent filtering capabilities, achieving filtration effectiveness of 89 % against PM1.0 particles. Additionally, they have a low-pressure drop of 6.5 Pa cm^{-2} [410]. In order to achieve a minimal decrease in pressure, a self-powered nanofiber membrane made of PA 6 was created. This membrane utilizes electrostatic adsorption to enhance its filtration effectiveness. The combination of PA 6 nanofibers with PVC nanofibers leads to a phenomenon known as the triboelectric effect, where electrostatic charges are generated due to air vibration between the adjacent nanofiber membranes. This, in turn, led to an increase in electrostatic adsorption with an equivalent decrease in pressure. At a flow velocity of 0.1 m/s, the self-powered nanofiber membrane demonstrated an electrostatic voltage of 257.1 mV. Additionally, the self-powered composite nanofiber membrane exhibited a high removal efficiency of 98.75 % and a low pressure drop of 67.5 Pa for NaCl aerosol particles with a diameter of 0.3 μm (Fig. 30). This indicates that the membrane, which incorporates electrostatic charges, has a superior quality factor compared to the membrane without such charges [411].

A separate investigation involved the use of PA 6 nanofibers that were electrospun onto two cellulose-based filter media. The objective was to enhance the filtering efficiency of engine air intake filters. The experimental results demonstrated that the collection efficiencies for all particle size ranges were improved by approximately 10 % and 25 % when using filter media that had been coated. The nano-coated filter media's improved capacity to capture tiny dust particles is attributed to its increased surface-to-volume ratio and decreased pore size, which enhance interception and impaction mechanisms. Therefore, air filters coated with electrospun nylon-66 nanofibers can be a suitable alternative to conventional cellulose media. The dust retention capacity of the filter media was measured to be within the range of 43 ± 1 g m^{-2} g^{-1}. Remarkably, the dust retention capacity of the cellulose filter medium remained nearly unaffected even after the application of the nanocoating [412].

PAN is frequently employed as a polymer material for air filtration due to its exceptional physical and chemical characteristics. A study was

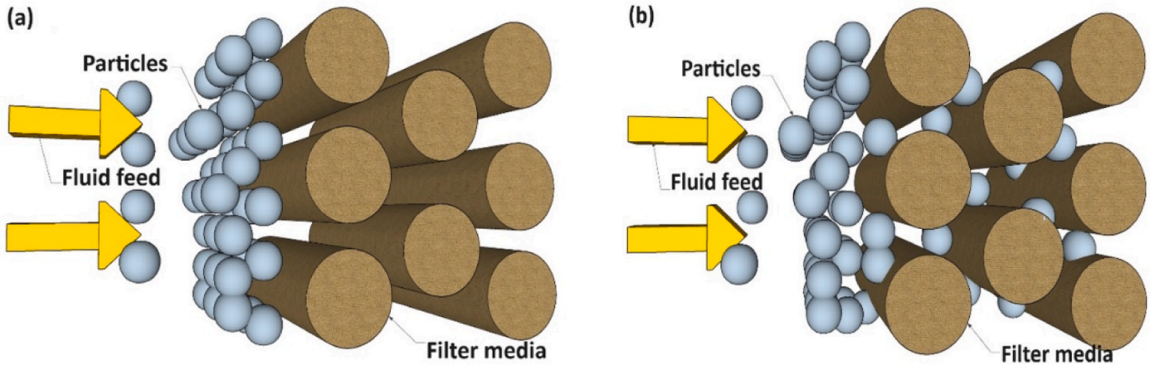

Fig. 29. Surface filtration (a) and Depth filtration (b).

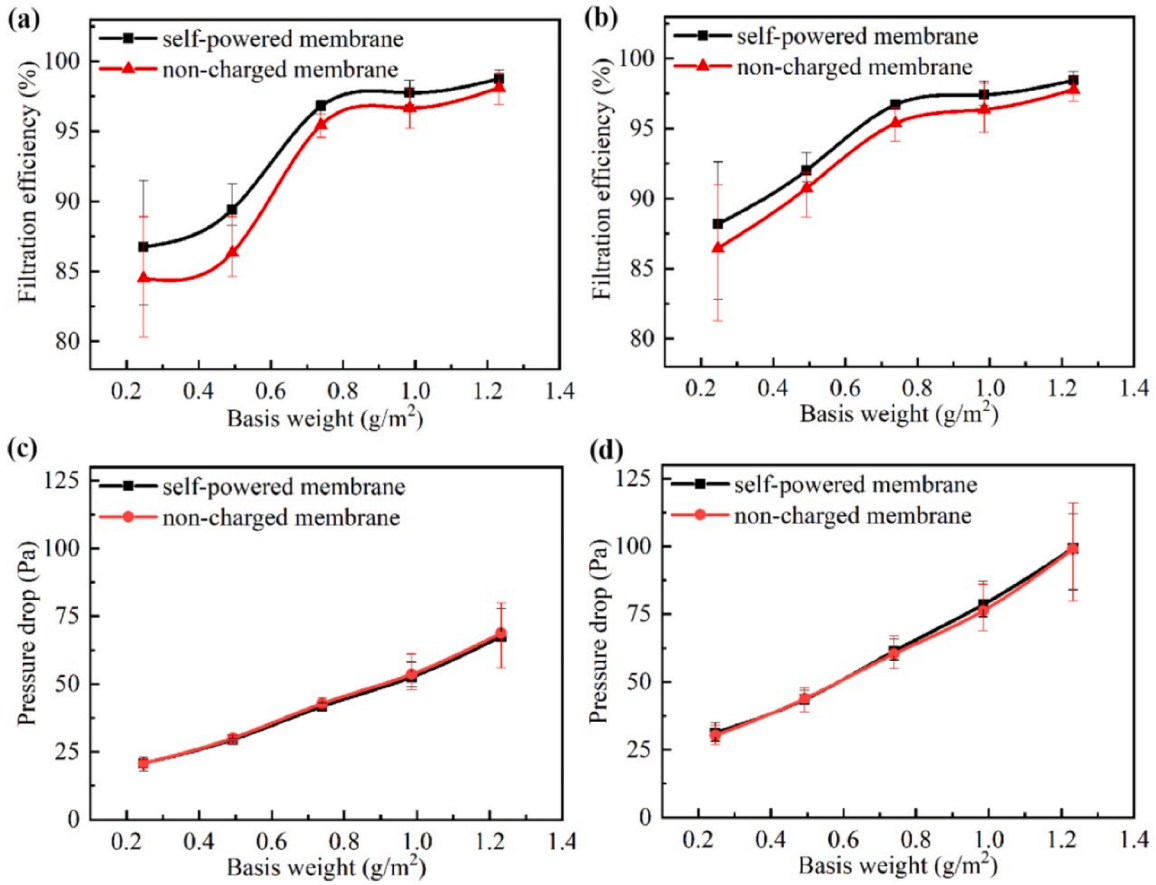

Fig. 30. The filtration efficiency (FE) of the composite membranes under different airflow velocities:(a) 0.1 m/s and (b) 0.15 m/s. The pressure drop in the composite membranes under different airflow velocities: (c) 0.1 m/s and (d) 0.15 m/s. [411] – Creative Commons CC BY 4.0 license.

done to create PAN nanofiber membranes using electrospinning with thicknesses varying from 20 to 100 μm. The membranes were made using polymer concentrations of 10, 12, and 14 % (w/v) in DMF. The densities of membranes are rather low, ranging from 0.11 to 0.21 g cm^{-3}, but their porosities typically fall within the range of 80–92 %. The membranes, which were 20 μm thick, had a filtering efficiency greater than 99.7 % in removing particles measuring 0.3 μm [409].

Cheng et al. introduced a compelling method employing meticulously arranged PAN nanofibers. Researchers assert that well-organized fibers offer significant benefits compared to randomly placed conventional fiber filtration materials. The PAN nanofibers produced exhibit a well-ordered structure, featuring fiber diameters ranging from 240 to 404 nm and pore widths ranging from 1.91 to 6.45 μm. These nanofiber membranes showcase outstanding air filtration efficacy, achieving efficiencies ranging from 94.83 % to 99.60 % for aerosol particles approximately 300 nm in diameter. This filtration performance is accompanied by a pressure decrease ranging from 33 to 98 Pa [413].

In addition to PA and PAN, PVDF exhibits exceptional chemical and weathering resistance. Additionally, they exhibit unique electroactive properties such as piezoelectric and pyroelectric features due to their inherent charged nature, resulting in enhanced filtering efficacy. Xiao et conducted a study on the electrospinning process of PVDF nanofibers in a DMF environment, using concentrations of 6 %, 8 %, 10 %, 12 %, and 14 % (Fig. 31). An optimal filtering efficiency of over 99 % has been achieved with a moderate pressure drop of 52 Pa by utilizing a 10 %

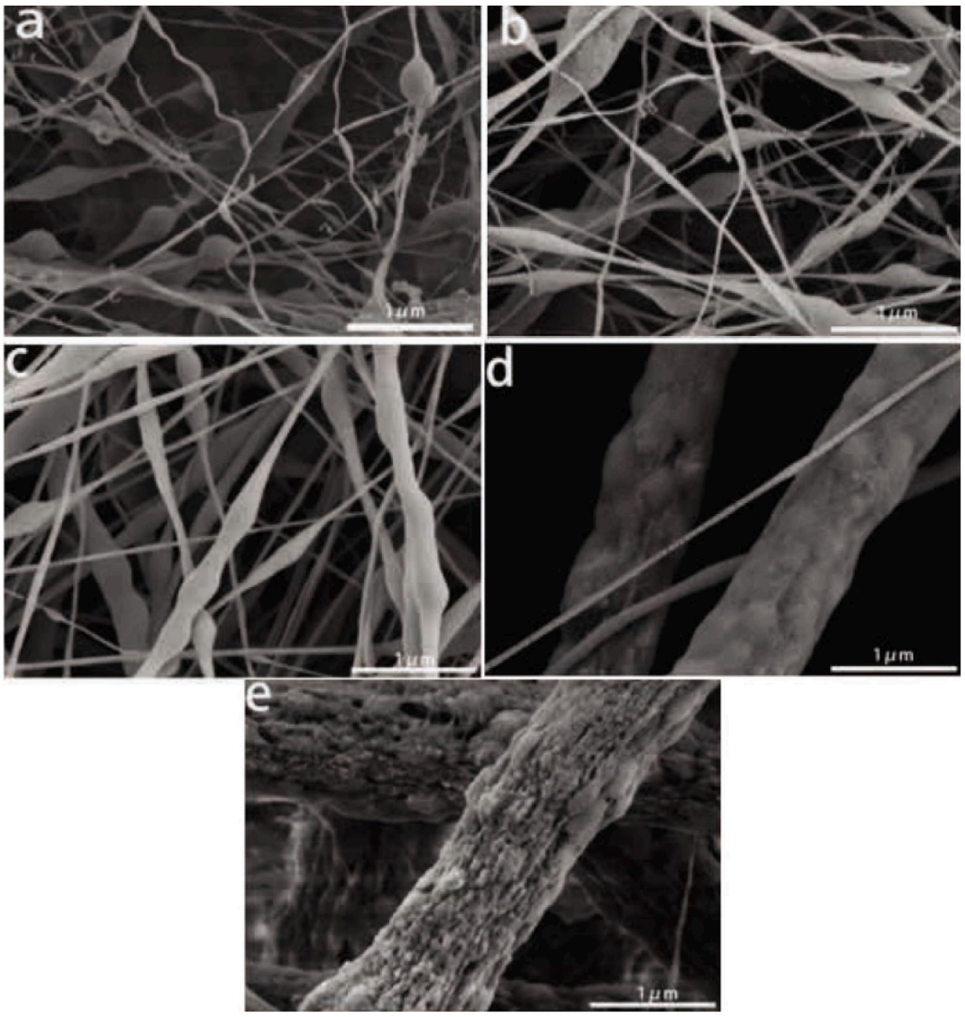

Fig. 31. Fiber morphology and its diameter distribution. (A) 6 % solution concentration, (B 8 % solution concentration, (C) 10 % solution concentration, (D) 12 % solution concentration, and (E) 14 % solution concentration [414] – Creative Commons CC BY 4.0 license.

concentration. The nanofibrous membrane derived from a solution concentration of 10 % is considered the optimal sample for air filtration [414].

Xiong et al. [415] carried out a promising study where they manufactured superfine nanofibers of PVDF with a size range of 20–35 nm. These nanofibers were used to create window screen air filters that efficiently capture PM from outdoor air when natural ventilation is used. The study findings indicate that PVDF nanofibers possess a small pore size of 0.72 μm and a high porosity of 92.22 %. As a result, the filters made from these nanofibers show outstanding performance, with a 99.92 % interception efficiency for PM0.3 particles, 69 Pa air resistance, over 80 % transparency, and consistent filtration even after 100 hours of UV exposure. This work introduces an innovative method for creating nanofibers with diameters at the nanoscale level and designing air filters with exceptional performance [415].

PUR nanofibers are the sole nominees in the field of nanofibers in terms of possessing exceptional mechanical strength, elasticity, and impact resistance. A study paper outlines a manufacturing process employing the electrospinning method coupled with the phase separation of charged droplets to produce air filters comprised of thermoplastic PUR nanofiber/net membranes. By integrating various Li^+ ion concentrations, it becomes possible to adjust the average pore areas of TPU nanofiber/net membranes, ranging from 0.6504 μm^2 to 0.0083 μm^2. The resulting air filter, constructed from optimized TPU nanofiber/net membranes, indicates exceptional characteristics. These include an outstanding PM0.1 removal efficiency of up to 97.08 %, a pressure drop of approximately 58 Pa, a quality factor of 0.061 Pa^{-1}, and exceptional optical transparency. Moreover, this innovative filter weighs merely 6 $g{\cdot}m^{-2}$ [404].

4.5.4. *Hybrid electrospun nanofiber-based Filters*

While homogeneous nanofibers demonstrate exceptional properties in air filtration applications, the demands of our technologically advanced and comfortable modern world come at a price. Air pollution poses significant challenges, and hybrid nanofibers offer a solution to enhance existing nanofibrous filters and address these problems.

The combination of polymeric nanofibers with metal nanoparticles (TiO_2 [416], $AgNO_3$ [417], CuO [418], ZnO [419], MgO [420], GO [421] and CNTs [422]), MOFs [423–425], conductive polymers [426], and hyperbranched polymers [427] provides advantageous additive characteristics, including antibacterial [428], self-cleaning [429], adsorption [430] and electroconductive capabilities [431]. Kwon et al. researched the photocatalytic efficiency of CA nanofibers when paired with TiO_2 nanoparticles. Hybrid nanofibers fabricated by emulsion-based electrospinning method. The TiO_2-CA nanofibers demonstrated exceptional filtering performance, achieving a remarkable 99.5 % efficiency for PM0.5, along with a photocatalytic efficiency of 78.6 % for the removal of nitrogen oxide (NO) [416]. Airborne PM is not the only difficult component in the air that has to be cleansed by filter media. There is also the presence of high temperature flue gas

emitted by industries, particularly thermal power plants, which typically release gas at temperatures ranging from 260 to 300 °C [432]. Xie et al. fabricated polyimide nanofibers embedded with ZIF-8 nanocrystals for the purpose of high temperature air purification (Fig. 32). The polyimide (PI)- propylsilsesquioxane (POSS)@ZIF hybrid filter showed remarkable thermal stability, favourable mechanical properties, and a significant BET specific surface area of 794.21 $m^2 g^{-1}$. The filter showed a notable PM0.3 filtration efficiency of 99.28 % and a decreased pressure drop of 49.21 Pa at a high temperature of 280 °C [433].

Another research study investigated the utilization of dual needle electrospinning to fabricate hybrid nanofibrous membranes comprising Ch, silver nanoparticles, polyvinyl alcohol, and CA. Additionally, the study explored the influence of varying ratios of Ch/AgNPs to fabricate air filtration membranes with high efficiency and exceptional antibacterial properties. Findings revealed that the produced hybrid nanofibers achieved a filtering efficiency of 99.78 % for PM2.5, a low-pressure drop of 61.15 Pa, and an augmented inhibition zone ranging from 100 % to 141 % [417]. Zhao et al. [427] conducted research on air filter media designed to possess superior filtration capabilities along with antibacterial properties. The media was composed of a combination of PVDF nanofibers and hyperbranched polymer. The 2-hydroxypropyl trimethyl ammonium chloride terminated hyperbranched polymer (HBP-HTC) is employed as an additive in PVDF electrospinning. The PVDF/HBP-HTC membrane, with a branching nanofibers network, exhibits enhanced mechanical qualities and improved filtration efficiency. The membrane achieves an outstanding filtration efficiency of 99.995 % for 0.26 μm NaCl particles. Additionally, it demonstrates a decreased pressure drop of 122.4 Pa on a 40 μm-thick sample. Furthermore, the PVDF membranes have outstanding antibacterial properties because they include many quaternary ammonium salt groups in HBP-HTC. The membrane with 3.0 wt% HBP-HTC showed a bacterial inhibitory rate of 99.9 % against both *S. aureus* and *E. coli* [427].

4.6. Filtration and separation of biological compounds

Nanofibrous materials have potential for environmental purposes such as water treatment or the filtration of air pollution due to their extremely high surface area and porosity. Pathogenic agents in wastewater, including bacteria, viruses, *etc.,* pose several threats to human health. Electrospun membranes could offer a very high permeability and selectivity. However, the application of nanofibrous membranes in the treatment and analysis of biological media, such as human blood or body secretions, is also of growing interest [434]. Regarding the biological molecules or agents such as bacteria, viruses, antibodies, proteins, or nucleic acids, nanofibrous systems can be applied to capture or retain the biologicals (Fig. 33). The application of nanofibrous mats for the

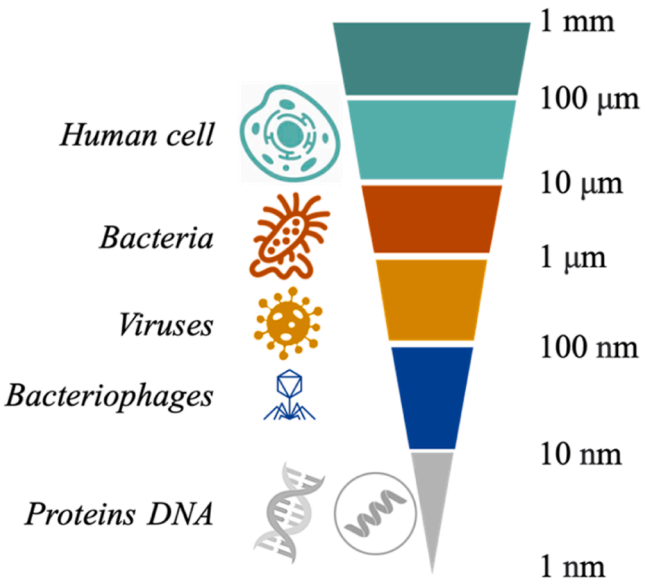

Fig. 33. Illustration of the typical size of biological compounds (cells, bacteria, viruses, bacteriophages, DNA and Proteins) which are commonly targeted in the filtration of air and water.

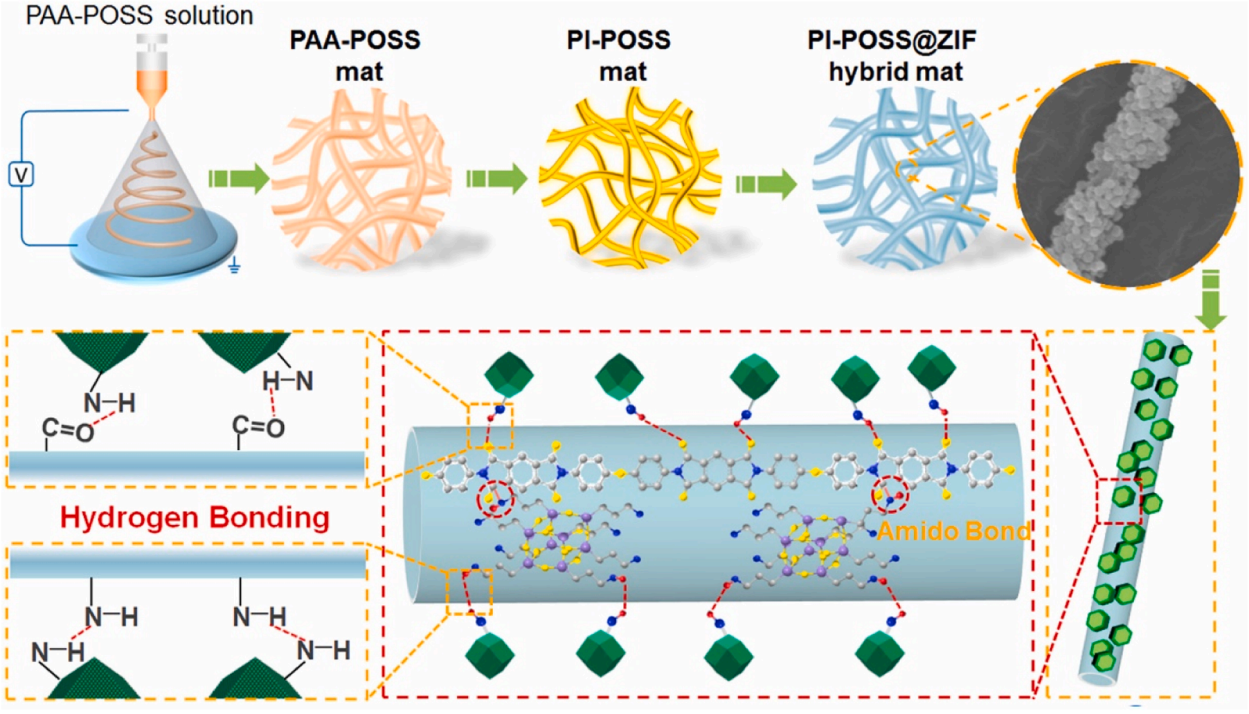

Fig. 32. Schematic illustration for fabrication process of PI-POSS@ZIF hybrid mat [433].
Reproduced with permission from ref [433]. Copyright 2021, Elsevier.

filtration or separation of biological compounds can be divided into two classic cases depending on the medium, which could be gas or liquid [435].

4.6.1. Removal of biological compound from air

In the case of air filtration, the main mechanisms could be capturing, deposition, or absorption. The filtration process of biological particles similar to other particles, depends on physical parameters, such as fiber diameter, particle size, pore size, and spatial distribution of fibers and air flow [436].

Among antimicrobial air filters, three different approaches are used, (i) polymers with antimicrobial properties; (ii) nanoparticles with antimicrobial effect loaded nanofibers; (iii) coated nanofibrous mats with antibacterial molecules. The antimicrobial effect of nanofibrous filters is commonly based on the bactericidal effect, which means the disruption of the cell membrane. Ag, Au, and Cu and metal oxides such as TiO_2, ZnO, and MgO are popular and generally applied, while metal ions and reactive oxygen could be released from the metal oxidation, causing cell death by damaging the membrane proteins [437].

Some recent studies showed that polymer nanofibers loaded with metal-oxide nanoparticles (*e.g.* ZnO, TiO_2 or Ag nanoparticles) could offer improved mechanical stability and better filtration effectivity on bacterial removal from air. Especially Ag particle/polyacrylic nitryl nanofibrous composites showed a high antibacterial effect, good efficiency, and low pressure drop [434]. Metal nanoparticles such as silver, gold, copper or zinc embedded in or supported on nanofibers also have antiviral effects [438]. Regarding the polymeric scaffold of nanofibrous filters PAN, PLA, PVDF, and PCL are the most commonly used in indoor air filtration or protecting materials such as facemasks, biological cabinets or surgical respiratory systems [439–441]. As a novel approach, the development of biodegradable nanofibrous membranes has started to get more environmental benefits.

Coronavirus disease indicated several innovations in the field of healthcare, thus special facemasks against the viruses have been also researched. In general, a face mask helps prevent airborne, droplet, and aerosol transmission, and the primary control mechanism is based on the reduction of exposure. The mask helps in filtering out particles of different sizes through various (*i*) inertial impaction, (*ii*) interception, (*iii*) diffusion, and (*iv*) electrostatic attraction between oppositely charged particles and filter media. Diffusion could be observed in the case of particles smaller than 0.1 μm, combination of diffusion and interception works for particles between 0.1 to 0.5 μm size [442]. Interception and inertial impaction are valid for particles larger than 0.5 μm. Viruses usually are in the ranges of 0.01 to 0.20 μm. The evolution of face masks has always been driven by different health issues, and commonly worldwide infections indicate the most effective inventions. From the first face mask which was made from cloths-like tissues in the 13th century, mainly paper-based or sponge-like filters had been developed, then the masks from gaze layers were the most similar to the nowadays well-known surgical mask. Modern face mask works with polymer fibers with antimicrobial and antiviral effects. These smart masks could be produced by different methods such as dip coating, spray coating, melt-blowing, and electrospinning. A unique advantage of electrospun nanofibrous face mask, the homogeneity of antimicrobial and/or antiviral agents is much better than dip coating or melt-blowing based masks [443].

4.6.2. Removal of biological compound from water

The removal of biological contamination from baths and drinking water is a key issue. The application of nanofibrous filters meets challenges. For example, the mechanical properties of the electrospun membranes are a critical parameter since water treatment means high mechanical stresses, which could lead to the deformation and compaction of the membrane. This unfavorable process could significantly decrease the porosity and the permeability [444].

The additional limitation could be the too hydrophobic character of the polymer nanofibers (e.g., PLA, PAN, PVDF), which cause aggregation and clogging in the pores. The finetuning of the pore size and pore size distribution of the electrospun fiber mats also could bring difficulties. Typically, the diameter of bacteria located in water is larger than 0.2 μm. Therefore, the pore size of the electrospun membrane should be smaller than 0.2 μm with a narrow distribution value, since the presence of larger pores reduces the purity, the too small pores cause hard pressure drop and decreased efficiency [445].

TFNC, consisting of 3 layers, is a novel application of electrospun nanofibrous mats in the removal of bacterial. The first is an ultrathin selective barrier, the second layer is the nanofibrous layer (typically PAN or PVDF nanofibers) and the third layer is a nonwoven PET film. The first two layers affect the filtration, and the third layer is a substructure layer to provide the proper mechanical strength of the membrane. The effectivity of TFNC membranes could be seen in the experiments with ultra-fine cellulose and PAN, which provided an extremely high retention rate (more than 99.9999 %) for *E. coli* filtering and MS2 virus, with 30 nm sizes [76].

Nanofibrous composite materials such GO loaded PUR nanofibrous membranes can be also effectively used against Gram-positive and Gram-negative bacteria. PUR/GO composite nanofibrous membranes have better thermal and mechanical stability than single materials, in addition, they show higher water flux and low clogging due to their hydrophilic nature [446].

Electrospun nanofibers could be used for water analysis as well, for example, micro-scale techniques such as microextraction supported by nanofibers are a promising alternative for the selective enrichment of analytes from samples with high complexity, such as living water. Solid phase microextraction (SPME) has been introduced as a sample preparation tool. Since SPME is able to integrate sampling, isolation and enrichment of analytes, it is an applicable method for the field of food industry, environmental analysis, and clinical and pharmaceutical investigation [447]. For example, poly(*N*-isopropylacrylamide) (PNIPAAm) was electrospun on PS support, and the produced PNIPAAM/PS-based system could be used for the extraction of drugs from plasma [448].

4.6.3. Analysis of biological samples based on electrospun materials

In the precise and rapid investigation of biological samples (such as blood, urine, or other body secretions), the sample treatment and preparation are key issues, thus, it requires selective and effective separation techniques. Time and accuracy are key factors in the flow of clinical information and diagnosis, and innovative methods are needed to ensure that they have great potential. Electrospun nanofibers as membrane materials can be used for the separation of biological compounds from the host biological matrix.

Nowadays several couple meet with fertilization difficulties. Among several reason for infertility, the quality of sperm cells is one of the major problems. To measure sperm cell viability, motility is one of the primary factors, and isolating sperm cells based on motility is an important step. Currently, centrifugation techniques are widely used, but the biochemical and DNA integrity of the spermatozoa could be damaged. Nanofibrous membranes could mean a promising alternative since the permeation properties of the membrane can be well-fitted to the sperm cells and ensure a mild condition during the separation process. For example, PCL nanofibers were successfully used for the separation of sperm cells, and results showed the purity achieved was similar to the commercially standardized centrifugal method, however, the processing time was significantly shortened (it decreased 98 % compared to the centrifugal method). Thus, nanofibrous tools could support fertilization protocols or the work of judicial offices [449].

Exosomes are vesicular bodies released by different types of cells and contain organic specific compounds, like mRNAs and proteins. Exosomes can induce a regulating signal in recipient cells, thus, they have a key role in the sporulation of cancerous cells. It can be harvested from different human fluids such as blood, urine, and saliva, thus, exosomes

could be promising markers for a non-invasive investigation. However useful they are, the isolation of exosomes meets difficulties, ultracentrifugation, filtration with commercial kits, and microfluidics are not real effective. In addition, these methods are not able to separate exosomes from another splitting piece of membranes or lipid structures. To avoid these limitations, a core-shell nanofibrous membrane from gelatin (shell) and PCL (core) was developed using an electrospinning technique and specific antibodies. Specific antibodies were immobilized on the nanofibers to ensure the selectivity to the exosome. Results showed that prepared core-shell nanofibers could catch exosomes from fluid samples then their recovery was also achievable [450].

Among blood-based analyses, and blood plasma separation is usually required with a purity superior to 99 %. In addition, hemolysis and leukolysis should be avoided for accurate clinical investigations. *Lab-On-Chip* devices based on microfluidic process became popular, since they work with small samples in an extremely short time. PLA-based nanofibrous membranes had been successfully integrated to Chip-device, and results proved nanofibrous membranes decreased the degree of hemolysis compared to the commercially available tools [434].

5. Emerging problems and future perspectives in the scale-up application of electrospun nanofibers in industry

The transition from laboratory-scale electrospinning to industrial-scale production poses significant challenges, particularly in achieving consistent quality and high production rates. Critical areas requiring focused optimization include mass production processes, downstream collection methods, and parameter adjustments, which are prone to issues such as fiber morphology inconsistencies and equipment inefficiencies.

One notable challenge in industrial electrospinning is the impact of increased flow rates on fiber quality. Higher flow rates can lead to inadequate solvent evaporation, resulting in bead formation, increased pore sizes, and larger fiber diameters. Additionally, the type and configuration of the collector significantly influence the structural and mechanical characteristics of the resultant nanofibers. The reliance on organic solvents introduces further complexity due to safety and environmental concerns during scale-up.

Multi-needle electrospinning and free surface electrospinning are commonly explored to address these challenges. Multi-needle systems enhance production capacity by generating multiple jets simultaneously. However, the interaction of electrostatic fields can lead to jet repulsion, and needle clogging is a frequent issue, both of which adversely affect fiber quality. Free surface electrospinning offers an alternative by forming multiple jets from an open surface, eliminating the clogging issue. Stationary and rotating spinnerets are utilized in this process, though the higher voltage requirement and solvent evaporation dynamics complicate process control and fiber uniformity.

To improve mass production, innovative designs and secondary forces have been introduced. For example, geometric variations in multi-needle setups (e.g., linear, circular, or hexagonal configurations) have been developed to mitigate electrostatic interference and increase production efficiency. Modifications to free surface electrospinning, such as alternating current applications and centrifugal force integration, have shown a potential to enhance output and fiber quality. Secondary forces, including magnetic and centrifugal forces, have also been employed to stabilize jet formation and improve scalability.

Despite promising advances, most studies in this area are rooted in academic research, with limited translation to industrial practices. Significant progress in commercialization will require additional technological innovations, rigorous process validation, and sustained corporate investment.

In summary, while scalable electrospinning techniques have made strides in addressing production challenges, further development and industry collaboration are essential to realize their full potential in large-scale nanofiber manufacturing.

6. Critical analysis of electrospinning techniques: pros, cons, and implementation challenges

Electrospinning is a highly versatile and efficient technique for producing nanofibers, offering exceptional control over fiber morphology and properties. However, its industrial scale-up remains challenging due to technical and operational limitations. A balanced evaluation of its advantages, limitations, and potential for further implementation is outlined below.

Advantages of electrospinning techniques

1. **Versatility in material use**:
   - o Accommodates a wide range of polymers, including synthetic and natural materials.
   - o Supports material blending and incorporation of inorganic particles to enhance functionality.
2. **Fine control over nanofiber properties**:
   - o Precise adjustment of fiber morphology (size, structure) by tuning solution and process parameters.
   - o Surface modifications enable tailoring for specific applications, such as hydrophobicity, conductivity, or adsorption capacity.
3. **Application versatility**:
   - o Useful in separation processes (e.g., wastewater treatment, air filtration, and oil-water separation).
   - o Demonstrates high efficiency in environmental and biological compound removal.
   - o Cost-effective compared to traditional methods in filtration and adsorption processes.
4. **Innovations in scale-up techniques**:
   - o Multi-needle and free surface electrospinning offer pathways for increased production rates.
   - o Advances in spinneret design and secondary force integration (e.g., centrifugal, magnetic) show promise in enhancing scalability.

Limitations of electrospinning techniques

1. **Challenges in industrial scale-up**:
   - o **Process consistency**: Variations in fiber morphology during large-scale production due to factors like flow rate and solvent evaporation.
   - o **Production rate**: Traditional single-needle setups are inefficient for mass production.
   - o **Parameter sensitivity**: Complex interdependencies between voltage, feed rate, and solution properties make process optimization difficult.
2. **Technical barriers in scale-up methods**:
   - o **Multi-needle electrospinning**:
     - ■ Interaction of electrostatic fields between jets can cause instability.
     - ■ Needle clogging leads to inconsistent fiber quality and operational downtime.
   - o **Free surface electrospinning**:
     - ■ High voltage requirements increase operational complexity and energy consumption.
     - ■ Solvent evaporation dynamics hinder the control of solution concentration and viscosity.
3. **Environmental and safety concerns**:
   - o Widespread use of organic solvents introduces risks of toxicity, flammability, and environmental pollution.
   - o Safe handling and disposal of solvent waste require additional infrastructure and compliance with regulations.
4. **Dependence on academic studies**:
   - o Limited translation of research advancements into industrial applications.
   - o Lack of robust, scalable prototypes for commercial deployment.

7. Concluding remarks and recommendations

This review provided an explicit and comprehensive summary of the preparation, modification and applications (Fig. 34) of electrospun nanofibers from 2020 to 2023. The examples discussed in this review demonstrate the versatility and adaptability of electrospun nanomaterials in addressing complex separation processes. This review provides a thorough discussion on how several electrospinning methodologies such as melt, bubble, and 3D electrospinning, facilitate the fabrication of nanofibers with customized properties dependent on the specific application. Melt electrospinning is free of solvents and advantageous for ecologically sensitive applications, whereas free-surface and bubble electrospinning has potential for large-scale production but faces difficulties in preserving consistent fiber quality and web evenness. Herein, this review discussed that adjusting electrospinning solution properties (including viscosity and conductivity) and electrospinning settings (such as voltage and feed rate) is essential for regulating nanofiber diameter and surface morphology. It is challenging to optimize the properties of electrospun nanofibers to meet specific requirements, owing to the complexity and many spinning parameters to be controlled by the electrospinning process. The traditional trial-and-error approaches to parameter optimization have been time-consuming and costly, and they lack the precision necessary to address these challenges effectively. Therefore, the utilization of machine learning and artificial intelligence will allow researchers to navigate the intricate parameter space of electrospinning more efficiently, bypassing the need for extensive trial-and-error experimentation. This transformative approach holds the potential to significantly reduce the time and resources invested in producing electrospun nanofibers with specific properties for a wide range of applications [451]. A more detailed analysis of the utilization of machine learning in the fabrication of electrospun nanofibers can be found in Subeshan et al. [451]. Incorporating metal dioxides to nanofiber material for photocatalytic degradation in wastewater treatment or hydrophilic coatings for anti-fouling membranes shows how strategic modifications can improve the performance of the membrane. It is important to emphasize the necessity of combining such advantageous with practical considerations, such as cost and scalability, while also recognizing that predictive models and sophisticated and advanced characterization techniques to improve manufacturing stability.

The review examines not only the electrospinning technique, important parameters and production methods, but also key applications and commonly used polymeric materials. The application of electrospun nanofibers for the purification of water and air, emphasizes PAN-based nanofibers for metal ion adsorption and PVDF nanofibers for efficient air filtration. In this review, it is emphasized that efficacy of electrospin nanofiber membranes in separation procedures, indicating that surface functionalization (e.g. plasma treatment, metal oxide modification) improves characteristics like hydrophilicity and fouling resistance. Another example such as chitosan-modified nanofibers, demonstrate the incorporation of biocompatibility for microbial elimination, however, scalability remains a significant concern. This review also proposed further exploration of composite materials to balance mechanical robustness with separation efficiency and highlight the limits that include biofouling and the environmental consequences of cleaning procedures.

The following future directions and potential solutions were recommended:

1. **Enhanced design and innovation:**
   - o Develop advanced needle configurations (e.g., hexagonal, circular) to optimize jet formation and minimize clogging.
   - o Incorporate secondary forces, such as magnetic or centrifugal forces, to stabilize and increase production efficiency.
2. **Improved process control:**
   - o Integration of real-time monitoring systems for dynamic adjustment of parameters during operation.
   - o Exploration of alternative spinning mechanisms, such as alternating current or hybrid electrospinning setups.
3. **Environmental sustainability:**
   - o Shift toward green solvents and solvent-free electrospinning techniques.
   - o Implement closed-loop solvent recovery systems to minimize waste and environmental impact.
4. **Industry-academia collaboration:**
   - o Foster partnerships to bridge the gap between laboratory findings and industrial application.
   - o Incentivize corporate investment in scaling up electrospinning technologies through funding and policy support.
5. **Diversified applications:**
   - o Leverage electrospun nanofibers in emerging fields, such as biomedical devices, energy storage, and advanced filtration systems.
   - o Expand the functionalization of nanofibers to meet evolving market demands.

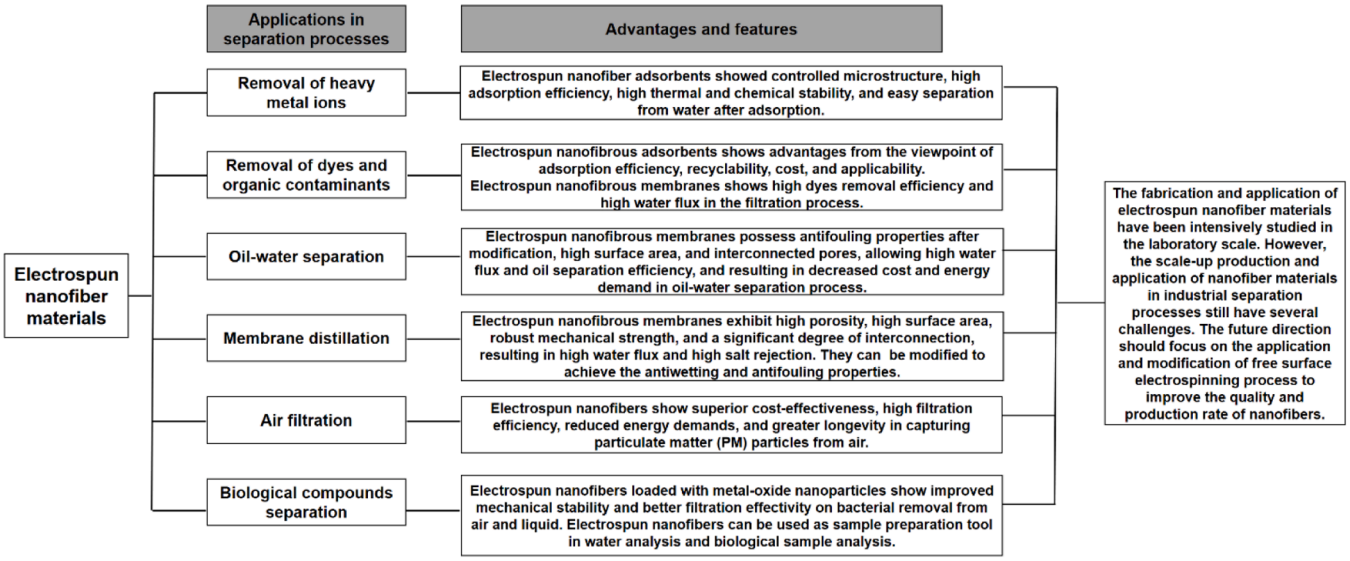

Fig. 34. The summary diagram of the separation applications of electrospun nanofiber materials.

CRediT authorship contribution statement

Guoqiang Li: Writing – review & editing, Writing – original draft, Visualization, Methodology, Formal analysis, Data curation, Conceptualization. **Waldemar Jankowski:** Writing – original draft, Methodology, Data curation. **Wojciech M. Kujawski:** Writing – review & editing, Project administration, Funding acquisition, Formal analysis, Conceptualization. **Gergő Tóth:** Writing – review & editing, Writing – original draft, Validation, Methodology, Formal analysis. **Ferenc Ender:** Writing – review & editing, Supervision, Project administration, Funding acquisition, Conceptualization. **Norman Sepsik:** Writing – review & editing. **Joanna Kujawa:** Writing – original draft, Visualization, Validation, Supervision, Methodology, Conceptualization. **Baturalp Yalcinkaya:** Writing – original draft, Methodology, Formal analysis, Data curation. **Fatma Yalcinkaya:** Writing – review & editing, Writing – original draft, Supervision, Project administration, Funding acquisition, Conceptualization. **Diána Balogh-Weiser:** Writing – original draft, Methodology, Formal analysis.

Declaration of Competing Interest

The authors declare that they have no known competing financial interests or personal relationships that could have appeared to influence the work reported in this paper.

Acknowledgement

The support from International Visegrad Fund (Visegrad Grant No. 22310110 – "Central European network for wider application of electrospun nanofibers") is kindly acknowledged. Authors acknowledges also the János Bolyai Research Scholarship of the Hungarian Academy of Sciences BO/00175/21 (grantholder Diána Balogh-Weiser) and Servier-Beregi PhD Fellowship (grantholder Gergő Tóth).

Data Availability

No data was used for the research described in the article.

References

[1] D. Lv, M. Zhu, Z. Jiang, S. Jiang, Q. Zhang, R. Xiong, C. Huang, Green electrospun nanofibers and their application in air filtration, Macromol. Mater. Eng. 303 (2018) 1800336.
[2] N.A.A.M. Amin, M.A. Mokhter, N. Salamun, M.Fb Mohamad, W.M.A. W. Mahmood, Anti-fouling electrospun organic and inorganic nanofiber membranes for wastewater treatment, South Afr. J. Chem. Eng. 44 (2023) 302–317.
[3] M.O. Aijaz, M.R. Karim, M.H.D. Othman, U.A. Samad, Anti-fouling/wetting electrospun nanofibrous membranes for membrane distillation desalination: a comprehensive review, Desalination 553 (2023) 116475.
[4] Z. Wang, S.B. Kang, H.J. Yun, S.W. Won, Efficient removal of arsenate from water using electrospun polyethylenimine/polyvinyl chloride nanofiber sheets, React. Funct. Polym. 184 (2023) 105514.
[5] C. Ao, J. Zhao, T. Xia, B. Huang, Q. Wang, J. Gai, Z. Chen, W. Zhang, C. Lu, Multifunctional La(OH)3@cellulose nanofibrous membranes for efficient oil/water separation and selective removal of dyes, Sep. Purif. Technol. 254 (2021) 117603.
[6] K.S. Ranjith, Z.I. Yildiz, M.A. Khalily, Y.S. Huh, Y.-K. Han, T. Uyar, Membrane-based electrospun poly-cyclodextrin nanofibers coated with ZnO nanograins by ALD: ultrafiltration blended photocatalysis for degradation of organic micropollutants, J. Membr. Sci. 686 (2023) 122002.
[7] M.K. Shahid, B. Mainali, P.R. Rout, J.W. Lim, M. Aslam, A.E. Al-Rawajfeh, Y. Choi, A review of membrane-based desalination systems powered by renewable energy sources, Water 15 (2023) 534.
[8] H. Sanaeepur, A. Ebadi Amooghin, M.M.A. Shirazi, M. Pishnamazi, S. Shirazian, Water desalination and ion removal using mixed matrix electrospun nanofibrous membranes: a critical review, Desalination 521 (2022) 115350.
[9] E. Czyż, F. Švec, D. Šatínský, Recent advances in application of nanofibers as extraction sorbents in environmental analysis, TrAC Trends Anal. Chem. 180 (2024) 117970.
[10] Z. Shao, H. Chen, Q. Wang, G. Kang, X. Wang, W. Li, Y. Liu, G. Zheng, High-performance multifunctional electrospun fibrous air filter for personal protection: a review, Sep. Purif. Technol. 302 (2022) 122175.
[11] A.H. Behroozi, M. Al-Shaeli, V. Vatanpour, Fabrication and modification of nanofiltration membranes by solution electrospinning technique: a review of influential factors and applications in water treatment, Desalination 558 (2023) 116638.
[12] K. Lang, T. Liu, D.J. Padilla, M. Nelson, C.W. Landorf, R.J. Patel, M.L. Ballentine, A.J. Kennedy, W.-S. Shih, A. Scotch, J. Zhu, Nanofibers enabled advanced gas sensors: a review, Adv. Sens. Energy Mater. 3 (2024) 100093.
[13] J. Zhu, H. Cheng, P. Zhu, Y. Li, Q. Gao, X. Zhang, Electrospun nanofibers enabled advanced lithium–sulfur batteries, Acc. Mater. Res. 3 (2022) 149–160.
[14] Y. Li, J. Zhu, H. Cheng, G. Li, H. Cho, M. Jiang, Q. Gao, X. Zhang, Developments of advanced electrospinning techniques: a critical review, Adv. Mater. Technol. 6 (2021) 2100410.
[15] A.S. Niknejad, S. Bazgir, A. Kargari, M. Barani, E. Ranjbari, M. Rasouli, A high-flux polystyrene-reinforced styrene-acrylonitrile/polyacrylonitrile nanofibrous membrane for desalination using direct contact membrane distillation, J. Membr. Sci. 638 (2021) 119744.
[16] L. Francis, F.E. Ahmed, N. Hilal, Electrospun membranes for membrane distillation: the state of play and recent advances, Desalination 526 (2022) 115511.
[17] G. Yan, Z. Yang, X. Zhang, H. Li, L. Wang, Z. Li, J. Chen, Y. Wu, Antibacterial biodegradable nanofibrous membranes by hybrid needleless electrospinning for high-efficiency particulate matter removal, Chem. Eng. J. 461 (2023) 142137.
[18] Z. Ru, X. Zhang, M. Zhang, J. Mi, C. Cao, Z. Yan, M. Ge, H. Liu, J. Wang, W. Zhang, W. Cai, Y. Lai, Y. Feng, Bimetallic-MOF-Derived ZnxCo3–xO4/carbon nanofiber composited sorbents for high-temperature coal gas desulfurization, Environ. Sci. Technol. 56 (2022) 17288–17297.
[19] Y. Feng, M. Zhang, Y. Sun, C. Cao, J. Wang, M. Ge, W. Cai, J. Mi, Y. Lai, Porous carbon nanofibers supported Zn@MnOx sorbents with high dispersion and loading content for hot coal gas desulfurization, Chem. Eng. J. 464 (2023) 142590.
[20] Y. Sun, X. Zhang, M. Zhang, M. Ge, J. Wang, Y. Tang, Y. Zhang, J. Mi, W. Cai, Y. Lai, Y. Feng, Rational design of electrospun nanofibers for gas purification: principles, opportunities, and challenges, Chem. Eng. J. 446 (2022) 137099.
[21] W. Feng, M. Zhang, X. Zhang, J. Mi, C. Yang, J. Wang, Y. Feng, Carbon nanofibers supported sorbents with enhanced performance via microwave-assisted in-situ structural modifications for H2S removal, Sep. Purif. Technol. 350 (2024) 127883.
[22] X. Zhang, Z. Ru, Y. Sun, M. Zhang, J. Wang, M. Ge, H. Liu, S. Wu, C. Cao, X. Ren, J. Mi, Y. Feng, Recent advances in applications for air pollutants purification and perspectives of electrospun nanofibers, J. Clean. Prod. 378 (2022) 134567.
[23] X. Zhang, Z. Ru, T. Wang, W. Feng, M. Zhang, J. Wang, J. Mi, M. Ge, Y. Feng, Insights to the microwave effect in formation and performance promotion of iron-based carbon nanofibrous composites for H2S removal, Compos. Commun. 37 (2023) 101468.
[24] S. Xie, J. Hu, K. Li, Y. Zhao, N. Ma, Y. Wang, Y. Jin, G. Guo, R. Kumar, J. Li, J. Huang, H. Tian, Substantial and efficient adsorption of heavy metal ions based on protein and polyvinyl alcohol nanofibers by electrospinning, Int. J. Biol. Macromol. 253 (2023) 126536.
[25] R. Beiranvand, N. Sarlak, Electrospun nanofiber mat of graphene/mesoporous silica composite for wastewater treatment, Mater. Chem. Phys. 309 (2023) 128311.
[26] A.M. Al-Dhahebi, J. Ling, S.G. Krishnan, M. Yousefzadeh, N.K. Elumalai, M.S. M. Saheed, S. Ramakrishna, R. Jose, Electrospinning research and products: the road and the way forward, Appl. Phys. Rev. 9 (2022).
[27] S. Jiang, H. Schmalz, S. Agarwal, A. Greiner, Electrospinning of ABS nanofibers and their high filtration performance, Adv. Fiber Mater. 2 (2020) 34–43.
[28] M. Rahmati, D.K. Mills, A.M. Urbanska, M.R. Saeb, J.R. Venugopal, S. Ramakrishna, M. Mozafari, Electrospinning for tissue engineering applications, Prog. Mater. Sci. 117 (2021) 100721.
[29] Y. Yan, X. Liu, J. Yan, C. Guan, J. Wang, Electrospun nanofibers for new generation flexible energy storage, ENERGY Environ. Mater. 4 (2021) 502–521.
[30] M.M. Abdul Hameed, S.A.P. Mohamed Khan, B.M. Thamer, N. Rajkumar, H. El-Hamshary, M. El-Newehy, Electrospun nanofibers for drug delivery applications: methods and mechanism, Polym. Adv. Technol. 34 (2023) 6–23.
[31] Y. Xing, J. Cheng, H. Li, D. Lin, Y. Wang, H. Wu, W. Pan, Electrospun ceramic nanofibers for photocatalysis, Nanomaterials 11 (2021) 3221.
[32] M. Hashmi, S. Ullah, A. Ullah, Y. Saito, M.K. Haider, X. Bie, K. Wada, I.S. Kim, Carboxymethyl cellulose (CMC) based electrospun composite nanofiber mats for food packaging, Polymers 13 (2021) 302.
[33] P. Vass, E. Szabó, A. Domokos, E. Hirsch, D. Galata, B. Farkas, B. Démuth, S. K. Andersen, T. Vigh, G. Verreck, G. Marosi, Z.K. Nagy, Scale-up of electrospinning technology: applications in the pharmaceutical industry, WIREs Nanomed. Nanobiotechnology 12 (2020) e1611.
[34] G.I. Taylor, Disintegration of water drops in an electric field, Proc. R. Soc. Lond. Ser. A. Math. Phys. Sci. 280 (1964) 383–397.
[35] G.I. Taylor, Electrically driven jets, Proc. R. Soc. Lond. A. Math. Phys. Sci. 313 (1969) 453–475.
[36] D.W. Hutmacher, P.D. Dalton, Melt electrospinning, Chem. Asian J. 6 (2011) 44–56.
[37] M. Zakaria, K. Shibahara, A.H. Bhuiyan, K. Nakane, Effects of varying melt flow rates on laser melt-electrospinning of low-density polyethylene nanofibers, J. Appl. Polym. Sci. 138 (2021) 50282.
[38] K. Morikawa, A. Vashisth, T. Bansala, P. Verma, M.J. Green, M. Naraghi, Melt electrospinning polyethylene fibers in inert atmosphere, Macromol. Mater. Eng. 305 (2020) 2000106.

[39] Q.-S. Li, H.-W. He, Z.-Z. Fan, R.-H. Zhao, F.-X. Chen, R. Zhou, X. Ning, Preparation and performance of ultra-fine polypropylene antibacterial fibers via melt electrospinning, Polymers 12 (2020) 606.
[40] A. Bachs-Herrera, O. Yousefzade, L.J. del Valle, J. Puiggali, Melt electrospinning of polymers: blends, nanocomposites, additives and applications, Appl. Sci. 11 (2021) 1808.
[41] T.D. Brown, P.D. Dalton, D.W. Hutmacher, Melt electrospinning today: an opportune time for an emerging polymer process, Prog. Polym. Sci. 56 (2016) 116–166.
[42] Y. Liu, J.-H. He, Bubble electrospinning for mass production of nanofibers, Int. J. Nonlinear Sci. Numer. Simul. 8 (2007) 393–396.
[43] Y. Li, A. Dong, J. He, Innovation of critical bubble electrospinning and its mechanism, Polymers 12 (2020) 304.
[44] R. Yang, J. He, L. Xu, J. Yu, Bubble-electrospinning for fabricating nanofibers, Polymer 50 (2009) 5846–5850.
[45] N. Bakhtiary, M. Pezeshki-Modaress, N. Najmoddin, Wet-electrospinning of nanofibrous magnetic composite 3-D scaffolds for enhanced stem cells neural differentiation, Chem. Eng. Sci. 264 (2022) 118144.
[46] D. Puppi, F. Chiellini, Wet-spinning of biomedical polymers: from single-fibre production to additive manufacturing of three-dimensional scaffolds, Polym. Int. 66 (2017) 1690–1696.
[47] S.P. Miguel, C.S.D. Cabral, A.F. Moreira, I.J. Correia, Production and characterization of a novel asymmetric 3D printed construct aimed for skin tissue regeneration, Colloids Surf. B: Biointerfaces 181 (2019) 994–1003.
[48] S. Yarova, D. Jones, F. Jaouen, S. Cavaliere, Strategies to hierarchical porosity in carbon nanofiber webs for electrochemical applications, Surfaces 2 (2019) 159–176.
[49] M. Ragab, N.A. Elgindy, Recent advances in nanofibers fabrication and their potential applications in wound healing and regenerative medicine, Adv. Mater. Lett. 9 (2018) 665–676.
[50] J. Xue, T. Wu, Y. Dai, Y. Xia, Electrospinning and electrospun nanofibers: methods, materials, and applications, Chem. Rev. 119 (2019) 5298–5415.
[51] M.L. Mejía Suaza, Y. Hurtado Henao, M.E.Moncada Acevedo, Wet electrospinning and its applications: a review, TecnoL. ógicas (2022) 25.
[52] Y. Zheng, J. Miao, N. Maeda, D. Frey, R.J. Linhardt, T.J. Simmons, Uniform nanoparticle coating of cellulose fibers during wet electrospinning, J. Mater. Chem. A 2 (2014) 15029–15034.
[53] Y. Wu, Z. Dong, S. Wilson, R.L. Clark, Template-assisted assembly of electrospun fibers, Polymer 51 (2010) 3244–3248.
[54] S. Sterk, M.E.T. Silva, A.A. Fernandes, A. Huß, A. Wittek, Development of new surgical mesh geometries with different mechanical properties using the design freedom of 3D printing, J. Appl. Polym. Sci. 140 (2023) e54687.
[55] M. Rafiq, R.S. Khan, T.U. Wani, A.H. Rather, T. Amna, M.S. Hassan, S.-u. Rather, F.A. Sheikh, Improvisations to electrospinning techniques and ultrasonication process to nanofibers for high porosity: ideal for cell infiltration and tissue integration, Materials Today, Communications 35 (2023) 105695.
[56] B. Ksapabutr, T. Chalermkiti, M. Panapoy, Effect of nozzle shapes on the formation of taylor cone and the oscillation of fibers during electrospinning process, CMU. J. Nat. Sci. 4 (2005) 115–119.
[57] H. Qu, S. Wei, Z. Guo, Coaxial electrospun nanostructures and their applications, J. Mater. Chem. A 1 (2013) 11513–11528.
[58] A. Khalf, K. Singarapu, S.V. Madihally, Cellulose acetate core–shell structured electrospun fiber: fabrication and characterization, Cellulose 22 (2015) 1389–1400.
[59] Y. Lin, Y.-y Yao, X.-z Yang, L.-m Shen, R.-x Li, D.-c Wu, Effect of gas flow rate on crystal structures of electrospun and gas-jet/electrospun poly(Vinylidene fluoride) fibers, Chin. J. Polym. Sci. 27 (2009) 511–516.
[60] G. Xu, X. Chen, Z. Zhu, P. Wu, H. Wang, X. Chen, W. Gao, Z. Liu, Pulse gas-assisted multi-needle electrospinning of nanofibers, Adv. Compos. Hybrid. Mater. 3 (2020) 98–113.
[61] H.S. SalehHudin, E.N. Mohamad, W.N.L. Mahadi, A. Muhammad Afifi, Multiple-jet electrospinning methods for nanofiber processing: a review, Mater. Manuf. Process. 33 (2018) 479–498.
[62] G. Zheng, J. Jiang, X. Wang, W. Li, J. Liu, G. Fu, L. Lin, Nanofiber membranes by multi-jet electrospinning arranged as arc-array with sheath gas for electrodialysis applications, Mater. Des. 189 (2020) 108504.
[63] G. Jiang, S. Zhang, Y. Wang, X. Qin, An improved free surface electrospinning with micro-bubble solution system for massive production of nanofibers, Mater. Lett. 144 (2015) 22–25.
[64] O.O. Dosunmu, G.G. Chase, W. Kataphinan, D.H. Reneker, Electrospinning of polymer nanofibres from multiple jets on a porous tubular surface, Nanotechnology 17 (2006) 1123.
[65] L. Wei, R. Sun, C. Liu, J. Xiong, X. Qin, Mass production of nanofibers from needleless electrospinning by a novel annular spinneret, Mater. Des. 179 (2019) 107885.
[66] H. Niu, T. Lin, Fiber generators in needleless electrospinning, J. Nanomater. 2012 (2012) 725950.
[67] A. Kotzianova, J. Klemes, O. Zidek, Z. Mlynar, M. Pokorny, V. Velebny, Effect of different emitter types on the production of nanofibrous tubular structures: thickness uniformity and productivity, AIP Adv 9 (2019) 025036.
[68] J.P. Canejo, M.H. Godinho, Cellulose Perversions, Materials 6 (2013) 1377–1390.
[69] D. Li, Y. Wang, Y. Xia, Electrospinning nanofibers as uniaxially aligned arrays and layer-by-layer stacked films, Adv. Mater. 16 (2004) 361–366.
[70] W. Teo, S. Ramakrishna, Electrospun fibre bundle made of aligned nanofibres over two fixed points, Nanotechnology 16 (2005) 1878.
[71] L. Kong, G.R. Ziegler, Rheological aspects in fabricating pullulan fibers by electro-wet-spinning, Food Hydrocoll. 38 (2014) 220–226.
[72] L. Zhu, B. Zaarour, X. Jin, Direct generation of electrospun interconnected macroporous nanofibers using a water bath as a collector, Mater. Res. Express 7 (2020) 015082.
[73] Y. Xu, P. Guo, A.-T. Akono, Novel wet electrospinning inside a reactive pre-ceramic gel to yield advanced nanofiber-reinforced geopolymer composites, Polymers 14 (2022) 3943.
[74] S. Li, B.-K. Lee, Electrospinning of circumferentially aligned polymer nanofibers floating on rotating water collector, J. Appl. Polym. Sci. 137 (2020) 48759.
[75] K.S. Ogueri, C.T. Laurencin, Nanofiber technology for regenerative engineering, ACS Nano 14 (2020) 9347–9363.
[76] S. T. M, A.B. Arshad, P.T. Lin, J. Widakdo, M. H. K, H.F.M. Austria, C.-C. Hu, J.-Y. Lai, W.-S. Hung, A review of recent progress in polymeric electrospun nanofiber membranes in addressing safe water global issues, RSC Adv. 11 (2021) 9638–9663.
[77] A. Al-Abduljabbar, I. Farooq, Electrospun polymer nanofibers: processing, properties, and applications, Polymers 15 (2023) 65.
[78] R. Abdulhussain, A. Adebisi, B.R. Conway, K. Asare-Addo, Electrospun nanofibers: exploring process parameters, polymer selection, and recent applications in pharmaceuticals and drug delivery, J. Drug Deliv. Sci. Technol. 90 (2023) 105156.
[79] U. Abdillah, H. Yazid, S. Ahmad, N. Makhtar, S. Zaubidah, R. Shan Chen, N. Hadifah Syifa, The effect of various electrospinning parameter and sol-gel concentration on morphology of silica and titania nanofibers, IOP Conf. Ser. Mater. Sci. Eng. 1231 (2022) 012012.
[80] J.E. Ruiz Rocha, K.R. Moreno Tovar, R.Navarro Mendoza, S. Gutiérrez Granados, S. Cavaliere, D. Giaume, P. Barboux, J.S.Jaime Ferrer, Critical electrospinning parameters for synthesis control of stabilized polyacrylonitrile nanofibers, Nanomaterials 13 (2023) 2648.
[81] G. Eda, S. Shivkumar, Bead-to-fiber transition in electrospun polystyrene, J. Appl. Polym. Sci. 106 (2007) 475–487.
[82] G.R. Williams, B.T. Raimi-Abraham, C.J. Luo, Electrospinning fundamentals. in: Nanofibres in Drug Delivery, UCL Press, 2018, pp. 24–59.
[83] Q. Yang, Z. Li, Y. Hong, Y. Zhao, S. Qiu, C. Wang, Y. Wei, Influence of solvents on the formation of ultrathin uniform poly(vinyl pyrrolidone) nanofibers with electrospinning, J. Polym. Sci. Part B: Polym. Phys. 42 (2004) 3721–3726.
[84] C.J. Angammana, S.H. Jayaram, Analysis of the effects of solution conductivity on electrospinning process and fiber morphology, IEEE Trans. Ind. Appl. 47 (2011) 1109–1117.
[85] Y. Li, Q. Li, Z. Tan, A review of electrospun nanofiber-based separators for rechargeable lithium-ion batteries, J. Power Sources 443 (2019) 227262.
[86] J. Doshi, D.H. Reneker, Electrospinning process and applications of electrospun fibers, J. Electrost. 35 (1995) 151–160.
[87] C. Zhang, X. Yuan, L. Wu, Y. Han, J. Sheng, Study on morphology of electrospun poly(vinyl alcohol) mats, Eur. Polym. J. 41 (2005) 423–432.
[88] N. Joy, R. Anuraj, A. Viravalli, H.N. Dixit, S. Samavedi, Coupling between voltage and tip-to-collector distance in polymer electrospinning: Insights from analysis of regimes, transitions and cone/jet features, Chem. Eng. Sci. 230 (2021) 116200.
[89] I. Shepa, E. Mudra, J. Dusza, Electrospinning through the prism of time, Mater. Today Chem. 21 (2021) 100543.
[90] Z.-M. Huang, Y.Z. Zhang, M. Kotaki, S. Ramakrishna, A review on polymer nanofibers by electrospinning and their applications in nanocomposites, Compos. Sci. Technol. 63 (2003) 2223–2253.
[91] D. Mailley, A. Hébraud, G. Schlatter, A review on the impact of humidity during electrospinning: from the nanofiber structure engineering to the applications, Macromol. Mater. Eng. 306 (2021) 2100115.
[92] M.S. Peresin, Y. Habibi, J.O. Zoppe, J.J. Pawlak, O.J. Rojas, Nanofiber composites of polyvinyl alcohol and cellulose nanocrystals: manufacture and characterization, Biomacromolecules 11 (2010) 674–681.
[93] H. Utkarsh, M. Hegab, N.A. Tariq, G. Syed, R. Rizvi, Pop-Iliev, towards analysis and optimization of electrospun PVP (Polyvinylpyrrolidone) nanofibers, Adv. Polym. Technol. 2020 (2020) 4090747.
[94] Y. Cai, M. Gevelber, The effect of relative humidity and evaporation rate on electrospinning: fiber diameter and measurement for control implications, J. Mater. Sci. 48 (2013) 7812–7826.
[95] N. Khanam, C. Mikoryak, R.K. Draper, K.J. Balkus, Electrospun linear polyethyleneimine scaffolds for cell growth, Acta Biomater. 3 (2007) 1050–1059.
[96] L. Li, Y.-L. Hsieh, Ultra-fine polyelectrolyte fibers from electrospinning of poly (acrylic acid), Polymer 46 (2005) 5133–5139.
[97] R. Casasola, N.L. Thomas, A. Trybala, S. Georgiadou, Electrospun poly lactic acid (PLA) fibres: Effect of different solvent systems on fibre morphology and diameter, Polymer 55 (2014) 4728–4737.
[98] M.J. Mochane, T.S. Motsoeneng, E.R. Sadiku, T.C. Mokhena, J.S. Sefadi, Morphology and properties of electrospun pcl and its composites for medical applications: a mini review, Appl. Sci. 9 (2019) 2205.
[99] L.Quoc Pham, M.V. Uspenskaya, R.O. Olekhnovich, R.A. Olvera Bernal, A review on electrospun PVC nanofibers: fabrication, properties, and application, Fibers 9 (2021) 12.
[100] M.M. Demir, I. Yilgor, E. Yilgor, B. Erman, Electrospinning of polyurethane fibers, Polymer 43 (2002) 3303–3309.
[101] L. Kalluri, M. Satpathy, Y. Duan, Effect of electrospinning parameters on the fiber diameter and morphology of PLGA nanofibers, Dent, Oral. Biol. Craniofacial Res. 4 (2021) 20.

[102] M. Ma, H. Zhou, S. Gao, N. Li, W. Guo, Z. Dai, Analysis and prediction of electrospun nanofiber diameter based on artificial neural network, Polymers 15 (2023) 2813.
[103] T.Y. Chee, A.R. Mohd Yusoff, F. Abdullah, W.M. Asyraf Wan Mahmood, M.J. Fathi Jasni, N.A. Nizam Nik Malek, N.A. Buang, M. Govarthanan, Fabrication, characterization and application of electrospun polysulfone membrane for phosphate ion removal in real samples, Chemosphere 303 (2022) 135228.
[104] J. Lasprilla-Botero, M. Álvarez-Láinez, J.M. Lagaron, The influence of electrospinning parameters and solvent selection on the morphology and diameter of polyimide nanofibers, Mater. Today Commun. 14 (2018) 1–9.
[105] A.S. Motamedi, H. Mirzadeh, F. Hajiesmaeilbaigi, S. Bagheri-Khoulenjani, M. Shokrgozar, Effect of electrospinning parameters on morphological properties of PVDF nanofibrous scaffolds, Prog. Biomater. 6 (2017) 113–123.
[106] T. Uyar, F. Besenbacher, Electrospinning of uniform polystyrene fibers: the effect of solvent conductivity, Polymer 49 (2008) 5336–5343.
[107] J. Matulevicius, L. Kliucininkas, D. Martuzevicius, E. Krugly, M. Tichonovas, J. Baltrusaitis, Design and characterization of electrospun polyamide nanofiber media for air filtration applications, J. Nanomater. 2014 (2014) 859656.
[108] S.J. Kim, Y.S. Nam, D.M. Rhee, H.-S. Park, W.H. Park, Preparation and characterization of antimicrobial polycarbonate nanofibrous membrane, Eur. Polym. J. 43 (2007) 3146–3152.
[109] D.P. Ura, J.E. Karbowniczek, P.K. Szewczyk, S. Metwally, M. Kopyściański, U. Stachewicz, Cell integration with electrospun PMMA nanofibers, microfibers, ribbons, and films: a microscopy study, Bioengineering 6 (2019) 41.
[110] I.N. Strain, Q. Wu, A.M. Pourrahimi, M.S. Hedenqvist, R.T. Olsson, R. L. Andersson, Electrospinning of recycled PET to generate tough mesomorphic fibre membranes for smoke filtration, J. Mater. Chem. A 3 (2015) 1632–1640.
[111] Y. Zhang, C. Zhang, Y. Wang, Recent progress in cellulose-based electrospun nanofibers as multifunctional materials, Nanoscale Adv. 3 (2021) 6040–6047.
[112] N. Angel, L. Guo, F. Yan, H. Wang, L. Kong, Effect of processing parameters on the electrospinning of cellulose acetate studied by response surface methodology, J. Agric. Food Res. 2 (2020) 100015.
[113] M. Borrego, J.E. Martín-Alfonso, C. Valencia, J.M. M.d.C. Sánchez Carrillo, Franco, Developing electrospun ethylcellulose nanofibrous webs: an alternative approach for structuring castor oil, ACS Appl. Polym. Mater. 4 (2022) 7217–7227.
[114] J.X. Law, L.L. Liau, A. Saim, Y. Yang, R. Idrus, Electrospun collagen nanofibers and their applications in skin tissue engineering, Tissue Eng. Regen. Med. 14 (2017) 699–718.
[115] H. Homayoni, S.A.H. Ravandi, M. Valizadeh, Electrospinning of chitosan nanofibers: processing optimization, Carbohydr. Polym. 77 (2009) 656–661.
[116] Z.-M. Huang, Y.Z. Zhang, S. Ramakrishna, C.T. Lim, Electrospinning and mechanical characterization of gelatin nanofibers, Polymer 45 (2004) 5361–5368.
[117] B.-M. Min, G. Lee, S.H. Kim, Y.S. Nam, T.S. Lee, W.H. Park, Electrospinning of silk fibroin nanofibers and its effect on the adhesion and spreading of normal human keratinocytes and fibroblasts in vitro, Biomaterials 25 (2004) 1289–1297.
[118] H. Chen, J. Su, C.S. Brennan, P. Van der Meeren, N. Zhang, Y. Tong, P. Wang, Recent developments of electrospun zein nanofibres: strategies, fabrication and therapeutic applications, Mater. Today Adv. 16 (2022) 100307.
[119] M. Khraisheh, F. AlMomani, M. Al-Ghouti, Electrospun Al2O3 hydrophobic functionalized membranes for heavy metal recovery using direct contact membrane distillation, Int J. Energy Res 45 (2021) 8151–8167.
[120] L. Meng, F. Niu, P. Deng, N. Li, Y. Lv, M. Huang, Electrospun nanofiber supports with bio-inspired modification enabled high-performance forward osmosis composite membranes, Compos. Commun. 22 (2020) 100473.
[121] S. Karki, G. Hazarika, D. Yadav, P.G. Ingole, Polymeric membranes for industrial applications: recent progress, challenges and perspectives, Desalination 573 (2024) 117200.
[122] S. Steven, M. Mulyono, A. Yustisia, E.S.A. Soekotjo, G. Otivriyanti, M.L. D. Wardani, Z. Murti, R.Y.H. Sinaga, N.S. Laili, G. Suantika, K. Khoiruddin, I. G. Wenten, M. Sudiono, V. Lukitari, A.A. Soedarsono, Perspectives and research direction on polymeric membrane integration for sustainable aquaculture industries, J. Environ. Chem. Eng. 12 (2024) 111691.
[123] H. Chan, K. Fang, T. Li, L. Zhang, Q. Zheng, Y. Liang, Green preparation of water-stable coptidis-dyeing composite nanofiber filters with ultraviolet shielding and antibacterial activity and biodegradability, Sep. Purif. Technol. 336 (2024) 126289.
[124] Z. Wang, M. Guan, X. Yang, H. Li, Y. Zhao, Y. Chen, A trifecta membrane modified by multifunctional superhydrophilic coating for Oil/Water separation and simultaneous absorption of dyes and heavy metal, Sep. Purif. Technol. 333 (2024) 125904.
[125] W. Shao, S. Liu, K. Wang, J. Niu, L. Zhu, S. Zhu, G. Ren, X. Wang, Y. Cao, H. Zhang, Y. Wang, X. Sun, F. Liu, J. He, Using modified raw materials to fabricate electrospun, superhydrophobic poly(lactic acid) multiscale nanofibrous membranes for air-filtration applications, Sep. Purif. Technol. 333 (2024) 125872.
[126] Q. Wu, J. Zhou, Y. Li, L. Zhang, X. Wang, X. Lu, Superhydrophobic nanofiber membranes with 3D-network reinforced pore structure for membrane distillation, Sep. Purif. Technol. 335 (2024) 126145.
[127] Q. Zhao, S. Yu, J. Zhu, G. Gong, Y. Hu, Beads-on-string structural nanofiber membrane with ultrahigh flux for membrane distillation, Sep. Purif. Technol. 334 (2024) 125999.
[128] Y. Tang, Z. Cai, X. Sun, C. Chong, X. Yan, M. Li, J. Xu, Electrospun nanofiber-based membranes for water treatment, Polymers 14 (2022) 2004.
[129] C. Liu, P.C. Hsu, H.W. Lee, M. Ye, G. Zheng, N. Liu, W. Li, Y. Cui, Transparent air filter for high-efficiency PM 2.5 capture, Nat. Commun. 6 (2015) 6205.
[130] X. Mao, Y. Si, Y. Chen, L. Yang, F. Zhao, B. Ding, J. Yu, Silica nanofibrous membranes with robust flexibility and thermal stability for high-efficiency fine particulate filtration, RSC Adv. 2 (2012) 12216–12223.
[131] A. Stanishevsky, W.A. Brayer, P. Pokorny, T. Kalous, D. Lukáš, Nanofibrous alumina structures fabricated using high-yield alternating current electrospinning, Ceram. Int. 42 (2016) 17154–17161.
[132] H. Liu, Y. Zhu, C. Zhang, Y. Zhou, D.-G. Yu, Electrospun nanofiber as building blocks for high-performance air filter: A review, Nano Today 55 (2024) 102161.
[133] H. El-Sayed, C. Vineis, A. Varesano, S. Mowafi, R.A. Carletto, C. Tonetti, M. A. Taleb, A critique on multi-jet electrospinning: state of the art and future outlook, Nanotechnol. Rev. 8 (2019) 236–245.
[134] H.S. SalehHudin, E.N. Mohamad, A.M. Afifi, W.N.L.W. Mahadi, Simulation and experimental study of parameters in multiple-nozzle electrospinning: effects of voltage and nozzle configuration on the electric field and electrospun jet attributes, J. Manuf. Process. 85 (2023) 544–555.
[135] A. Ahmed, J. Yin, L. Xu, F. Khan, High-throughput free surface electrospinning using solution reservoirs with different radii and its preparation mechanism study, J. Mater. Res. Technol. 9 (2020) 9059–9072.
[136] G. Jiang, L. Johnson, S. Xie, Investigations into the mechanisms of electrohydrodynamic instability in free surface electrospinning, Open Phys. 17 (2019) 313–319.
[137] K.M. Forward, A. Flores, G.C. Rutledge, Production of core/shell fibers by electrospinning from a free surface, Chem. Eng. Sci. 104 (2013) 250–259.
[138] Y. Xing, W. Dan, Y. Fan, Xa Li, Low temperature synthesis of high-entropy (Y0.2Yb0.2Sm0.2Eu0.2Er0.2)2O3 nanofibers by a novel electrospinning method, J. Mater. Sci. Technol. 103 (2022) 215–220.
[139] W. Shi, Z. Peng, S. Chen, X. Yan, H. Xu, L. Liu, Low-temperature fabrication of Pr-doped In2O3 electrospun nanofibers for flexible field-effect transistors, J. Mater. Chem. C. 10 (2022) 15996–16003.
[140] D. Abbas, M.S. Mu'min, M. Bonanno, S. Thiele, T. Böhm, Active solution heating and cooling in electrospinning enabling spinnability from various solvents, J. Appl. Polym. Sci. 139 (2022) e52730.
[141] K. Kalantari, A.M. Afifi, H. Jahangirian, T.J. Webster, Biomedical applications of chitosan electrospun nanofibers as a green polymer – review, Carbohydr. Polym. 207 (2019) 588–600.
[142] J.V. Patil, S.S. Mali, A.S. Kamble, C.K. Hong, J.H. Kim, P.S. Patil, Electrospinning: a versatile technique for making of 1D growth of nanostructured nanofibers and its applications: An experimental approach, Appl. Surf. Sci. 423 (2017) 641–674.
[143] M.N. Pervez, G.K. Stylios, Y. Liang, F. Ouyang, Y. Cai, Low-temperature synthesis of novel polyvinylalcohol (PVA) nanofibrous membranes for catalytic dye degradation, J. Clean. Prod. 262 (2020) 121301.
[144] S. Zargham, S. Bazgir, A. Tavakoli, A.S. Rashidi, R. Damerchely, The effect of flow rate on morphology and deposition area of electrospun Nylon 6 nanofiber, J. Eng. Fibers Fabr. 7 (2012) 42–49, 155892501200700414.
[145] R. Kyselica, E.T. Enikov, P. Polyvas, R. Anton, Electrostatic focusing of electrospun Polymer(PEO) nanofibers, J. Electrost. 94 (2018) 21–29.
[146] Z. Li, Y. Liu, J. Yan, K. Wang, B. Xie, Y. Hu, W. Kang, B. Cheng, Electrospun polyvinylidene fluoride/fluorinated acrylate copolymer tree-like nanofiber membrane with high flux and salt rejection ratio for direct contact membrane distillation, Desalination 466 (2019) 68–76.
[147] P. Kallem, F. Banat, L. Yejin, H. Choi, High performance nanofiber-supported thin film composite forward osmosis membranes based on continuous thermal-rolling pretreated electrospun PES/PAN blend substrates, Chemosphere 261 (2020) 127687.
[148] O.G. Apul, N. Hoogesteijn von Reitzenstein, J. Schoepf, D. Ladner, K. D. Hristovski, P. Westerhoff, Superfine powdered activated carbon incorporated into electrospun polystyrene fibers preserve adsorption capacity, Sci. Total Environ. 592 (2017) 458–464.
[149] Z. Wang, R. Sahadevan, C. Crandall, T.J. Menkhaus, H. Fong, Hot-pressed PAN/PVDF hybrid electrospun nanofiber membranes for ultrafiltration, J. Membr. Sci. 611 (2020) 118327.
[150] S.K. Ghorai, T. Roy, S. Maji, P. Guha Ray, K. Sarkar, A. Dutta, A. De, S. Bandyopadhyay, S. Dhara, S. Chattopadhyay, A judicious approach of exploiting polyurethane-urea based electrospun nanofibrous scaffold for stimulated bone tissue regeneration through functionally nobbled nanohydroxyapatite, Chem. Eng. J. 429 (2022) 132179.
[151] N. Chailek, D. Daranarong, W. Punyodom, R. Molloy, P. Worajittiphon, Crosslinking assisted fabrication of ultrafine poly (vinyl alcohol)/functionalized graphene electrospun nanofibers for crystal violet adsorption, J. Appl. Polym. Sci. 135 (2018) 46318.
[152] H. Zhang, B. Li, D. Sun, X. Miao, Y. Gu, SiO2-PDMS-PVDF hollow fiber membrane with high flux for vacuum membrane distillation, Desalination 429 (2018) 33–43.
[153] M. Herrero-Herrero, J.A. Gomez-Tejedor, A. Vallés-Lluch, Role of electrospinning parameters on poly (lactic-co-glycolic acid) and poly (caprolactone-co-glycolic acid) membranes, Polymers 13 (2021) 695.
[154] U.Y. Karatepe, T. Ozdemir, Improving mechanical and antibacterial properties of PMMA via polyblend electrospinning with silk fibroin and polyethyleneimine towards dental applications, Bioact. Mater. 5 (2020) 510–515.
[155] R. Zhang, K. Huang, M. Zhu, G. Chen, Z. Tang, Y. Li, H. Yu, B. Qiu, X. Li, Corrosion resistance of stretchable electrospun SEBS/PANi micro-nano fiber membrane, Eur. Polym. J. 123 (2020) 109394.
[156] Z. Zhu, L. Zhong, X. Chen, W. Zheng, J. Zuo, G. Zeng, W. Wang, Monolithic and self-roughened Janus fibrous membrane with superhydrophilic/omniphobic surface for robust antifouling and antiwetting membrane distillation, J. Membr. Sci. 615 (2020) 118499.

[157] Z. Temoçin, M. İnal, M. Gökgöz, M. Yiğitoğlu, Immobilization of horseradish peroxidase on electrospun poly(vinyl alcohol)–polyacrylamide blend nanofiber membrane and its use in the conversion of phenol, Polym. Bull. 75 (2018) 1843–1865.
[158] S.-F. Li, Y.-H. Fan, J.-F. Hu, Y.-S. Huang, W.-T. Wu, Immobilization of Pseudomonas cepacia lipase onto the electrospun PAN nanofibrous membranes for transesterification reaction, J. Mol. Catal. B: Enzym. 73 (2011) 98–103.
[159] I. Yezer, D.O. Demirkol, Cellulose acetate–chitosan based electrospun nanofibers for bio-functionalized surface design in biosensing, Cellulose 27 (2020) 10183–10197.
[160] X. Lu, M. Li, H. Wang, C. Wang, Advanced electrospun nanomaterials for highly efficient electrocatalysis, Inorg. Chem. Front. 6 (2019) 3012–3040.
[161] L.A. Mercante, K.B.R. Teodoro, D.M. dos Santos, F.V. dos Santos, C.A. S. Ballesteros, T. Ju, G.R. Williams, D.S. Correa, Recent progress in stimuli-responsive antimicrobial electrospun nanofibers, Polymers 15 (2023) 4299.
[162] A. Camposeo, M. Moffa, L. Persano, Electrospun fluorescent nanofibers and their application in optical sensing, in: A. Macagnano, E. Zampetti, E. Kny (Eds.), Electrospinning for High Performance Sensors, Springer International Publishing, Cham, 2015, pp. 129–155.
[163] I. Salahshoori, A. Seyfaee, A. Babapoor, F. Neville, R. Moreno-Atanasio, Evaluation of the effect of silica nanoparticles, temperature and pressure on the performance of PSF/PEG/SiO2 mixed matrix membranes: a molecular dynamics simulation (MD) and design of experiments (DOE) study, J. Mol. Liq. 333 (2021) 115957.
[164] X. Yin, Z. Zhang, H. Ma, S. Venkateswaran, B.S. Hsiao, Ultra-fine electrospun nanofibrous membranes for multicomponent wastewater treatment: filtration and adsorption, Sep. Purif. Technol. 242 (2020) 116794.
[165] F. Zhan, X. Yan, F. Sheng, B. Li, Facile in situ synthesis of silver nanoparticles on tannic acid/zein electrospun membranes and their antibacterial, catalytic and antioxidant activities, Food Chem. 330 (2020) 127172.
[166] L. Zhang, L. Li, L. Wang, J. Nie, G. Ma, Multilayer electrospun nanofibrous membranes with antibacterial property for air filtration, Appl. Surf. Sci. 515 (2020) 145962.
[167] C.-G. Yuan, S. Guo, J. Song, C. Huo, Y. Li, B. Gui, X. Zhang, One-step fabrication and characterization of a poly (vinyl alcohol)/silver hybrid nanofiber mat by electrospinning for multifunctional applications, RSC Adv. 7 (2017) 4830–4839.
[168] J. Kujawa, S. Al-Gharabli, T.M. Muzioł, K. Knozowska, G. Li, L.F. Dumée, W. Kujawski, Crystalline porous frameworks as nano-enhancers for membrane liquid separation – recent developments, Coord. Chem. Rev. 440 (2021) 213969.
[169] A. Chen, H. Guo, J. Luan, Y. Li, X. He, L. Chen, Y. Zhang, The electrospun polyacrylonitrile/covalent organic framework nanofibers for efficient enrichment of trace sulfonamides residues in food samples, J. Chromatogr. A 1668 (2022) 462917.
[170] Z. Zha, P. He, S. Zhao, R. Guo, Z. Wang, J. Wang, Interlayer-modulated polyamide composite membrane for organic solvent nanofiltration, J. Membr. Sci. 647 (2022) 120306.
[171] M. Qian, X. Yan, Y. Chen, X.-J. Guo, W.-Z. Lang, Covalent organic framework membrane on electrospun polyvinylidene fluoride substrate with a hydrophilic intermediate layer, J. Colloid Interface Sci. 622 (2022) 11–20.
[172] Y. Wang, R. Cao, C. Wang, X. Song, R. Wang, J. Liu, M. Zhang, J. Huang, T. You, Y. Zhang, D. Yan, W. Han, L. Yan, J. Xiao, P. Li, In situ embedding hydrogen-bonded organic frameworks nanocrystals in electrospinning nanofibers for ultrastable broad-spectrum antibacterial activity, Adv. Funct. Mater. 33 (2023) 2214388.
[173] N. Lu, L. Yan, Y. Ma, H. Sun, Z. Zhu, W. Liang, J. Li, A. Li, Electrospun modified SiO2 nanofiber membranes as superamphiphobic self-cleaning filters with high heat stability for efficient particle matter capture, ACS Appl. Nano Mater. 5 (2022) 9871–9881.
[174] H. Wang, L. Chen, Y. Yi, Y. Fu, J. Xiong, N. Li, Durable polyurethane/SiO2 nanofibrous membranes by electrospinning for waterproof and breathable textiles, ACS Appl. Nano Mater. 5 (2022) 10686–10695.
[175] J. Song, Q. Deng, M. Huang, Z. Kong, Carbon nanotube enhanced membrane distillation for salty and dyeing wastewater treatment by electrospinning technology, Environ. Res. 204 (2022) 111892.
[176] L. Francis, N. Hilal, Electrohydrodynamic atomization of CNT on PTFE membrane for scaling resistant membranes in membrane distillation, npj Clean. Water 6 (2023) 15.
[177] H. Dai, X. Liu, C. Zhang, K. Ma, Y. Zhang, Electrospinning polyacrylonitrile/graphene oxide/polyimide nanofibrous membranes for high-efficiency PM2.5 filtration, Sep. Purif. Technol. 276 (2021) 119243.
[178] M.A. Kanjwal, A.A. Ghaferi, Graphene incorporated electrospun nanofiber for electrochemical sensing and biomedical applications: a critical review, Sensors 22 (2022) 8661.
[179] S.R. Haque, M.A. Chowdhury, M.M. Rana, N. Hossain, Fabrication of PVA/graphene nanofibrous membrane infused with neem extraction for packaging and biomedical applications, SN Appl. Sci. 5 (2023) 177.
[180] A. Rasekh, A. Raisi, Electrospun nanofibrous polyether-block-amide membrane containing silica nanoparticles for water desalination by vacuum membrane distillation, Sep. Purif. Technol. 275 (2021) 119149.
[181] R. Zhao, Y. Li, B. Sun, S. Chao, X. Li, C. Wang, G. Zhu, Highly flexible magnesium silicate nanofibrous membranes for effective removal of methylene blue from aqueous solution, Chem. Eng. J. 359 (2019) 1603–1616.
[182] D. Hou, D. Lin, C. Ding, D. Wang, J. Wang, Fabrication and characterization of electrospun superhydrophobic PVDF-HFP/SiNPs hybrid membrane for membrane distillation, Sep. Purif. Technol. 189 (2017) 82–89.
[183] Y. Yang, Y. Xu, Z. Liu, H. Huang, X. Fan, Y. Wang, Y. Song, C. Song, Preparation and characterization of high-performance electrospun forward osmosis membrane by introducing a carbon nanotube interlayer, J. Membr. Sci. 616 (2020) 118563.
[184] J. Yan, W. Xiao, L. Chen, Z. Wu, J. Gao, H. Xue, Superhydrophilic carbon nanofiber membrane with a hierarchically macro/meso porous structure for high performance solar steam generators, Desalination 516 (2021) 115224.
[185] M.Q. Seah, W.J. Lau, P.S. Goh, A.F. Ismail, Greener synthesis of functionalized-GO incorporated TFN NF membrane for potential recovery of saline water from salt/dye mixed solution, Desalination 523 (2022) 115403.
[186] Y.C. Woo, L.D. Tijing, W.-G. Shim, J.-S. Choi, S.-H. Kim, T. He, E. Drioli, H. K. Shon, Water desalination using graphene-enhanced electrospun nanofiber membrane via air gap membrane distillation, J. Membr. Sci. 520 (2016) 99–110.
[187] Q. Zhao, S. Yu, J. Zhu, G. Gong, Y. Hu, Beads-on-string structural nanofiber membrane with ultrahigh flux for membrane distillation, Sep. Purif. Technol. 334 (2024) 125999.
[188] Q. Wu, J. Zhou, Y. Li, L. Zhang, X. Wang, X. Lu, Superhydrophobic nanofiber membranes with 3D-network reinforced pore structure for membrane distillation, Sep. Purif. Technol. 335 (2024) 126145.
[189] X.-Q. Wu, X. Wu, T.-Y. Wang, L. Zhao, Y.B. Truong, D. Ng, Y.-M. Zheng, Z. Xie, Omniphobic surface modification of electrospun nanofiber membrane via vapor deposition for enhanced anti-wetting property in membrane distillation, J. Membr. Sci. 606 (2020) 118075.
[190] C. Liu, X. Li, T. Liu, Z. Liu, N. Li, Y. Zhang, C. Xiao, X. Feng, Microporous CA/PVDF membranes based on electrospun nanofibers with controlled crosslinking induced by solvent vapor, J. Membr. Sci. 512 (2016) 1–12.
[191] Q. Su, J. Zhang, L.-Z. Zhang, Fouling resistance improvement with a new superhydrophobic electrospun PVDF membrane for seawater desalination, Desalination 476 (2020) 114246.
[192] H.N. Doan, P.P. Vo, K. Hayashi, K. Kinashi, W. Sakai, N. Tsutsumi, Recycled PET as a PDMS-Functionalized electrospun fibrous membrane for oil-water separation, J. Environ. Chem. Eng. 8 (2020) 103921.
[193] X. Wang, B.S. Hsiao, Electrospun nanofiber membranes, Curr. Opin. Chem. Eng. 12 (2016) 62–81.
[194] K. Yoon, B.S. Hsiao, B. Chu, Functional nanofibers for environmental applications, J. Mater. Chem. 18 (2008) 5326–5334.
[195] S.S. Ray, S.S. Chen, C.W. Li, N.C. Nguyen, H.T. Nguyen, A comprehensive review: electrospinning technique for fabrication and surface modification of membranes for water treatment application, RSC Adv. 6 (2016) 85495–85514.
[196] W. Ma, Q. Zhang, D. Hua, R. Xiong, J. Zhao, W. Rao, S. Huang, X. Zhan, F. Chen, C. Huang, Electrospun fibers for oil-water separation, RSC Adv. 6 (2016) 12868–12884.
[197] L. Shen, C. Cheng, X. Yu, Y. Yang, X. Wang, M. Zhu, B.S. Hsiao, Low pressure UV-cured CS-PEO-PTEGDMA/PAN thin film nanofibrous composite nanofiltration membranes for anionic dye separation, J. Mater. Chem. A 4 (2016) 15575–15588.
[198] L. Shen, X. Yu, C. Cheng, C. Song, X. Wang, M. Zhu, B.S. Hsiao, High filtration performance thin film nanofibrous composite membrane prepared by electrospraying technique and hot-pressing treatment, J. Membr. Sci. 499 (2016) 470–479.
[199] J. Guo, Q. Zhang, Z. Cai, K. Zhao, Preparation and dye filtration property of electrospun polyhydroxybutyrate–calcium alginate/carbon nanotubes composite nanofibrous filtration membrane, Sep. Purif. Technol. 161 (2016) 69–79.
[200] D. Li, Y. Yan, H. Wang, Recent advances in polymer and polymer composite membranes for reverse and forward osmosis processes, Prog. Polym. Sci. 61 (2016) 104–155.
[201] E.L. Tian, H. Zhou, Y.W. Ren, Z. mirza, X.Z. Wang, S.W. Xiong, Novel design of hydrophobic/hydrophilic interpenetrating network composite nanofibers for the support layer of forward osmosis membrane, Desalination 347 (2014) 207–214.
[202] M. Tian, Y.N. Wang, R. Wang, A.G. Fane, Synthesis and characterization of thin film nanocomposite forward osmosis membranes supported by silica nanoparticle incorporated nanofibrous substrate, Desalination 401 (2017) 142–150.
[203] P.J. Blankestijn, I. Ledebo, B. Canaud, Hemodiafiltration: clinical evidence and remaining questions, Kidney Int 77 (2010) 581–587.
[204] M. Irfan, A. Idris, Overview of PES biocompatible/hemodialysis membranes: PES-blood interactions and modification techniques, Mater. Sci. Eng. C. 56 (2015) 574–592.
[205] W.S. Hung, C.L. Lai, Q. An, M. De Guzman, T.J. Shen, Y.H. Huang, K.C. Chang, C. H. Tsou, C.C. Hu, K.R. Lee, A study on high-performance composite membranes comprising heterogeneous polyamide layers on an electrospun substrate for ethanol dehydration, J. Membr. Sci. 470 (2014) 513–523.
[206] T.M. Yeh, Z. Wang, D. Mahajan, B.S. Hsiao, B. Chu, High flux ethanol dehydration using nanofibrous membranes containing graphene oxide barrier layers, J. Mater. Chem. A 1 (2013) 12998–13003.
[207] Q. Wang, N. Li, B. Bolto, M. Hoang, Z. Xie, Desalination by pervaporation: a review, Desalination 387 (2016) 46–60.
[208] C. Cheng, L. Shen, X. Yu, Y. Yang, X. Li, X. Wang, Robust construction of a graphene oxide barrier layer on a nanofibrous substrate assisted by the flexible poly(vinylalcohol) for efficient pervaporation desalination, J. Mater. Chem. A 5 (2017) 3558–3568.
[209] Y. Jiang, J. Hou, J. Xu, B. Shan, Switchable oil/water separation with efficient and robust Janus nanofiber membranes, Carbon 115 (2017) 477–485.
[210] R. Zhao, X. Li, B. Sun, H. Ji, C. Wang, Diethylenetriamine-assisted synthesis of amino-rich hydrothermal carbon-coated electrospun polyacrylonitrile fiber adsorbents for the removal of Cr (VI) and 2, 4-dichlorophenoxyacetic acid, J. Colloid Interface Sci. 487 (2017) 297–309.

[211] A. Vanangamudi, L.F. Dumée, E. Des Ligneris, M. Duke, X. Yang, Thermo-responsive nanofibrous composite membranes for efficient self-cleaning of protein foulants, J. Membr. Sci. 574 (2019) 309–317.
[212] E. Tian, X. Wang, Y. Zhao, Y. Ren, Middle support layer formation and structure in relation to performance of three-tier thin film composite forward osmosis membrane, Desalination 421 (2017) 190–201.
[213] S. Shokrollahzadeh, S. Tajik, Fabrication of thin film composite forward osmosis membrane using electrospun polysulfone/polyacrylonitrile blend nanofibers as porous substrate, Desalination 425 (2018) 68–76.
[214] D. Teng, Y. Xu, T. Zhao, X. Zhang, Y. Li, Y. Zeng, Zein adsorbents with micro/nanofibrous membrane structure for removal of oils, organic dyes, and heavy metal ions in aqueous solution, J. Hazard. Mater. 425 (2022) 128004.
[215] N. Rosli, W.Z.N. Yahya, M.D.H. Wirzal, Crosslinked chitosan/poly(vinyl alcohol) nanofibers functionalized by ionic liquid for heavy metal ions removal, Int. J. Biol. Macromol. 195 (2022) 132–141.
[216] W. Guo, R. Guo, H. Pei, B. Wang, N. Liu, Z. Mo, Electrospinning PAN/PEI/MWCNT-COOH nanocomposite fiber membrane with excellent oil-in-water separation and heavy metal ion adsorption capacity, Colloids Surf. A Physicochem. Eng. Asp. 641 (2022) 128557.
[217] Y.A.Y.A. Mohammed, A.M. Abdel-Mohsen, Q.-J. Zhang, M. Younas, L.-B. Zhong, J.-C.E. Yang, Y.-M. Zheng, Facile synthesis of ZIF-8 incorporated electrospun PAN/PEI nanofibrous composite membrane for efficient Cr(VI) adsorption from water, Chem. Eng. J. 461 (2023) 141972.
[218] S. Wu, W. Shi, K. Li, J. Cai, C. Xu, L. Gao, J. Lu, F. Ding, Chitosan-based hollow nanofiber membranes with polyvinylpyrrolidone and polyvinyl alcohol for efficient removal and filtration of organic dyes and heavy metals, Int. J. Biol. Macromol. 239 (2023) 124264.
[219] H. Wang, Y. Wang, C. Li, L. Jia, Fabrication of eco-friendly calcium crosslinked alginate electrospun nanofibres for rapid and efficient removal of Cu(II), Int. J. Biol. Macromol. 219 (2022) 1–10.
[220] N. Torasso, A. Vergara-Rubio, R. Pereira, J. Martinez-Sabando, J.R.V. Baudrit, S. Cerveny, S. Goyanes, An in situ approach to entrap ultra-small iron oxide nanoparticles inside hydrophilic electrospun nanofibers with high arsenic adsorption, Chem. Eng. J. 454 (2023) 140168.
[221] B.S. Rathi, P.S. Kumar, A review on sources, identification and treatment strategies for the removal of toxic Arsenic from water system, J. Hazard. Mater. 418 (2021) 126299.
[222] F. Zhu, Y.-M. Zheng, B.-G. Zhang, Y.-R. Dai, A critical review on the electrospun nanofibrous membranes for the adsorption of heavy metals in water treatment, J. Hazard. Mater. 401 (2021) 123608.
[223] C. Jiang, Z. Ling, Y. Xu, J. Bao, L. Feng, H. Cheng, W. Zhao, C. Zhao, Long-term, synergistic and high-efficient antibacterial polyacrylonitrile nanofibrous membrane prepared by "one-pot" electrospinning process, J. Colloid Interface Sci. 609 (2022) 718–733.
[224] S. Miao, J. Guo, Z. Deng, J. Yu, Y. Dai, Adsorption and reduction of Cr(VI) in water by iron-based metal-organic frameworks (Fe-MOFs) composite electrospun nanofibrous membranes, J. Clean. Prod. 370 (2022) 133566.
[225] D. Chen, X. Zhao, X. Jing, R. Zhao, G. Zhu, C. Wang, Bio-inspired functionalization of electrospun nanofibers with anti-biofouling property for efficient uranium extraction from seawater, Chem. Eng. J. 465 (2023) 142844.
[226] W.-b Tan, D. Luo, W. Song, Y.-y Lu, N. Cheng, J.-b Zhang, T. Huang, Y. Wang, Polydopamine-assisted polyethyleneimine grafting on electrospun cellulose acetate/TiO2 fibers towards highly efficient removal of Cr(VI), Eur. Polym. J. 180 (2022) 111632.
[227] C. Yee Foong, X. Ling Lau, M. Dzul Hakim Wirzal, M.A. Bustam, M. Syaamil Bin Saad, N. Syakinah Abd Halim, Blended nylon 6,6 and choline glycinate-ionic liquid for adsorptive nanofiber membrane on the removal of Fe(III) from synthetic wastewater, J. Mol. Liq. 368 (2022) 120677.
[228] H.H. Eom, Y. Kim, D. Harbottle, J.W. Lee, Immobilization of KTS-3 on an electrospun fiber membrane for efficient removal of Cs+ and Sr2+, J. Environ. Chem. Eng. 9 (2021) 105991.
[229] S. Karimzadeh, R. Hmtshirazi, T. Mohammadi, A.A. Asadi, Polyacrylonitrile (PAN)/Freeze-dried Chitosan (FCS)-NaY zeolite triple layer nanostructure fibrous adsorptive membrane (PAN/FCS-NaY TNAM) for Cu(II) and Pb(II) ions removal from aqueous solutions, Sep. Purif. Technol. 327 (2023) 124885.
[230] X. Xu, M. Zhang, H. Lv, Y. Zhou, Y. Yang, D.-G. Yu, Electrospun polyacrylonitrile-based lace nanostructures and their Cu(II) adsorption, Sep. Purif. Technol. 288 (2022) 120643.
[231] R. Wang, Q.-h Hu, Q.-y Wang, Y.-l Xiang, S.-h Huang, Y.-z Liu, S.-y Li, Q.-l Chen, Q.-h Zhou, Efficiently selective removal of Pb(II) by magnetic ion-imprinted membrane based on polyacrylonitrile electro-spun nanofibers, Sep. Purif. Technol. 284 (2022) 120280.
[232] N.S. Surgutskaia, A.D. Martino, J. Zednik, K. Ozaltin, L. Lovecká, E.D. Bergerová, D. Kimmer, J. Svoboda, V. Sedlarik, Efficient Cu2+ , Pb2+ and Ni2+ ion removal from wastewater using electrospun DTPA-modified chitosan/polyethylene oxide nanofibers, Sep. Purif. Technol. 247 (2020) 116914.
[233] M.E. Talukder, M.N. Pervez, W. Jianming, Z. Gao, G.K. Stylios, M.M. Hassan, H. Song, V. Naddeo, Chitosan-functionalized sodium alginate-based electrospun nanofiber membrane for As (III) removal from aqueous solution, J. Environ. Chem. Eng. 9 (2021) 106693.
[234] A. Kakoria, S. Sinha-Ray, S. Sinha-Ray, Industrially scalable Chitosan/Nylon-6 (CS/N) nanofiber-based reusable adsorbent for efficient removal of heavy metal from water, Polymer 213 (2021) 123333.
[235] R. Khalili, M.M. Sabzehmeidani, M. Parvinnia, M. Ghaedi, Removal of hexavalent chromium ions and mixture dyes by electrospun PAN/graphene oxide nanofiber decorated with bimetallic nickel–iron LDH, Environ. Nanotechnol., Monit. Manag. 18 (2022) 100750.
[236] I. Mahar, F.K. Mahar, N. Mahar, A.A. Memon, A.A.A. Pirzado, Z. Khatri, K. H. Thebo, A. Ali, Fabrication and characterization of MXene/carbon composite-based nanofibers (MXene/CNFs) membrane: an efficient adsorbent material for removal of Pb+ 2 and As+ 3 ions from water, Chem. Eng. Res. Des. 191 (2023) 462–471.
[237] Q. Ran, D. Zhao, Y. Ji, Z. Fan, G. Lin, X. Liu, K. Jia, Recyclable adsorption removal and fluorescent monitoring of hexavalent chromium by electrospun nanofibers membrane derived from Tb3+ coordinating polyarylene ether amidoxime, Talanta 266 (2024) 125058.
[238] A. Herath, M. Salehi, S. Jansone-Popova, Production of polyacrylonitrile/ionic covalent organic framework hybrid nanofibers for effective removal of chromium (VI) from water, J. Hazard. Mater. 427 (2022) 128167.
[239] Y. Ding, J. Wu, J. Wang, J. Wang, J. Ye, F. Liu, Superhydrophilic carbonaceous-silver nanofibrous membrane for complex oil/water separation and removal of heavy metal ions, organic dyes and bacteria, J. Membr. Sci. 614 (2020) 118491.
[240] D. Cao, Z. Cao, G. Wang, X. Dong, Y. Dong, Y. Ye, S. Hu, Plasma induced graft co-polymerized electrospun polyethylene terephalate membranes for removal of Cu2 + from aqueous solution, Chem. Phys. 536 (2020) 110832.
[241] E.A. Mwafy, A.M. Mostafa, Tailored MWCNTs/SnO2 decorated cellulose nanofiber adsorbent for the removal of Cu (II) from waste water, Radiat. Phys. Chem. 177 (2020) 109172.
[242] Q. Zia, M. Tabassum, J. Meng, Z. Xin, H. Gong, J. Li, Polydopamine-assisted grafting of chitosan on porous poly (L-lactic acid) electrospun membranes for adsorption of heavy metal ions, Int. J. Biol. Macromol. 167 (2021) 1479–1490.
[243] D. Picón, N. Torasso, J.R.V. Baudrit, S. Cerveny, S. Goyanes, Bio-inspired membranes for adsorption of arsenic via immobilized L-Cysteine in highly hydrophilic electrospun nanofibers, Chem. Eng. Res. Des. 185 (2022) 108–118.
[244] A.R. Esfahani, Z. Zhang, Y.Y.L. Sip, L. Zhai, A.H.M.A. Sadmani, Removal of heavy metals from water using electrospun polyelectrolyte complex fiber mats, J. Water Process Eng. 37 (2020) 101438.
[245] X. Zhang, Q. Dong, Y. Wang, Z. Zhu, Z. Guo, J. Li, Y. Lv, Y.T. Chow, X. Wang, L. Zhu, G. Zhang, D. Xu, Water-stable metal–organic framework (UiO-66) supported on zirconia nanofibers membrane for the dynamic removal of tetracycline and arsenic from water, Appl. Surf. Sci. 596 (2022) 153559.
[246] X.-H. Li, H.-J. Yang, Y.-X. Ma, T.-Z. Li, W.-L. Meng, X.-M. Zhong, A novel PAN/GO electrospun nanocomposite fibrous membranes with rich amino groups for highly efficient adsorption of Au(III), Diam. Relat. Mater. 137 (2023) 110175.
[247] X. Yang, Y. Zhou, Z. Sun, C. Yang, D. Tang, Effective strategy to fabricate ZIF-8@ZIF-8/polyacrylonitrile nanofibers with high loading efficiency and improved removing of Cr(VI), Colloids Surf. A Physicochem. Eng. Asp. 603 (2020) 125292.
[248] M. Mousakhani, N. Sarlak, Electrospun composite nanofibre adsorbents for effective removal of Cd2+ from polluted water, Mater. Chem. Phys. 256 (2020) 123578.
[249] Q.-H. Li, M. Dong, R. Li, Y.-Q. Cui, G.-X. Xie, X.-X. Wang, Y.-Z. Long, Enhancement of Cr(VI) removal efficiency via adsorption/photocatalysis synergy using electrospun chitosan/g-C3N4/TiO2 nanofibers, Carbohydr. Polym. 253 (2021) 117200.
[250] M. Kumar, A. Tiwari, J.K. Randhawa, Electrospun nanofibers of α-hematite/polyacrylonitrile/calcium carbonate/cellulose triacetate as a multifunctional platform in, wastewater treatment and remineralisation, Desalination 541 (2022) 116030.
[251] Y.-X. Ma, H.-J. Yang, X.-F. Shi, X.-H. Li, W.-L. Meng, Recovery of Ag(I) from aqueous solution by hyperbranched polyethyleneimine grafted polyacrylonitrile/graphene oxide electrospun nanocomposite fiber membrane for catalytic reduction of toxic P-nitrophenol, Diam. Relat. Mater. 127 (2022) 109161.
[252] H. Zandavar, S.M. Pourmortazavi, S. Mirsadeghi, Highly-efficient capture of chromium (VI) ions on electrospun polyacrylonitrile/diaminoglyoxime nanofiber: thermal stability, decomposition kinetics and tensile strength, J. Mater. Res. Technol. 13 (2021) 25–37.
[253] R. Guo, W. Guo, H. Pei, B. Wang, X. Guo, N. Liu, Z. Mo, Polypyrrole deposited electrospun PAN/PEI nanofiber membrane designed for high efficient adsorption of chromium ions (VI) in aqueous solution, Colloids Surf. A Physicochem. Eng. Asp. 627 (2021) 127183.
[254] N. Mohammad, Y. Atassi, Enhancement of removal efficiency of heavy metal ions by polyaniline deposition on electrospun polyacrylonitrile membranes, Water Sci. Eng. 14 (2021) 129–138.
[255] S.K. Sahoo, G.K. Panigrahi, J.K. Sahoo, A.K. Pradhan, A.K. Purohit, J.P. Dhal, Electrospun magnetic polyacrylonitrile-GO hybrid nanofibers for removing Cr(VI) from water, J. Mol. Liq. 326 (2021) 115364.
[256] I. Khan Rind, A. Sarı, M. Tuzen, M. Farooque Lanjwani, I. Karaman, T.A. Saleh, Bacteria immobilized onto carbon nanofiber as a composite for effective removal of arsenic from wastewater, Mater. Sci. Eng. B 297 (2023) 116809.
[257] R. Hmtshirazi, T. Mohammadi, A.A. Asadi, Incorporation of amine-grafted halloysite nanotube to electrospun nanofibrous membranes of chitosan/poly (vinyl alcohol) for Cd (II) and Pb(II) removal, Appl. Clay Sci. 220 (2022) 106460.
[258] S. Wu, K. Li, W. Shi, J. Cai, Preparation and performance evaluation of chitosan/polyvinylpyrrolidone/polyvinyl alcohol electrospun nanofiber membrane for heavy metal ions and organic pollutants removal, Int. J. Biol. Macromol. 210 (2022) 76–84.
[259] Y. Lu, Z. Liu, S.W. You, L. McLoughlin, B. Bridgers, S. Hayes, X. Wang, R. Wang, Z. Guo, E.K. Wujcik, Electrospun carbon/iron nanofibers: the catalytic effects of iron and application in Cr(VI) removal, Carbon 166 (2020) 227–244.

[260] H.Y. Choi, J.H. Bae, Y. Hasegawa, S. An, I.S. Kim, H. Lee, M. Kim, Thiol-functionalized cellulose nanofiber membranes for the effective adsorption of heavy metal ions in water, Carbohydr. Polym. 234 (2020) 115881.
[261] S. Li, D. Thiyagarajan, B.-K. Lee, Efficient removal of methylene blue from aqueous solution by ZIF-8-decorated helicoidal electrospun polymer strips, Chemosphere 333 (2023) 138961.
[262] M. Narayan, R. Sadasivam, G. Packirisamy, S. Pichiah, Electrospun polyacrylonitrile-Moringa Olifera based nanofibrous bio-sorbent for remediation of Congo red dye, J. Environ. Manag. 317 (2022) 115294.
[263] X. Wang, J. Dong, C. Gong, S. Zhang, J. Yang, A. Zhang, Z. Feng, Bendable poly (vinylidene fluoride)/polydopamine/β-cyclodextrin composite electrospun membranes for highly efficient and bidirectional adsorption of cation and anion dyes from aqueous media, Compos. Sci. Technol. 219 (2022) 109256.
[264] Q. Zia, M. Tabassum, M. Umar, H. Nawaz, H. Gong, J. Li, Cross-linked chitosan coated biodegradable porous electrospun membranes for the removal of synthetic dyes, React. Funct. Polym. 166 (2021) 104995.
[265] A. Ghaffar, M. Mehdi, A.A. Otho, U. Tagar, R.A. Hakro, S. Hussain, Electrospun silk nanofibers for numerous adsorption-desorption cycles on Reactive Black 5 and reuse dye for textile coloration, J. Environ. Chem. Eng. 11 (2023) 111188.
[266] R.-S. Juang, C.-A. Liu, C.-C. Fu, Polyaminated electrospun chitosan fibrous membranes for highly selective removal of anionic organics from aqueous solutions in continuous operation, Sep. Purif. Technol. 319 (2023) 124043.
[267] S.B. Kang, Z. Wang, W. Zhang, K.-Y. Kim, S.W. Won, Removal of short- and long-chain PFAS from aquatic systems using electrostatic attraction of polyethylenimine-polyvinyl chloride electrospun nanofiber adsorbent, Sep. Purif. Technol. 326 (2023) 124853.
[268] J. Zhu, X. Wang, L. Mao, X. Chen, J. Han, X. Li, S. Xia, H. Wang, Electrospun nanofibrous poly(ether-block-amide) membrane for removing biogenic amines in acidic wastewater from the yellow rice wine factory, Sci. Total Environ. 862 (2023) 160720.
[269] P. Abi Younes, S. Sayegh, A.A. Nada, M. Weber, I. Iatsunskyi, E. Coy, N. Abboud, M. Bechelany, Elaboration of porous alumina nanofibers by electrospinning and molecular layer deposition for organic pollutant removal, Colloids Surf. A Physicochem. Eng. Asp. 628 (2021) 127274.
[270] H.A. Altaleb, B.M. Thamer, M.M. Abdulhameed, H. El-Hamshary, S. Z. Mohammady, A.M. Al-Enizi, Efficient electrospun terpolymer nanofibers for the removal of cationic dyes from polluted waters: A non-linear isotherm and kinetic study, J. Environ. Chem. Eng. 9 (2021) 105361.
[271] B.M. Thamer, A.A. Shaker, M.M. Abdul Hameed, A.M. Al-Enizi, Highly selective and reusable nanoadsorbent based on expansive clay-incorporated polymeric nanofibers for cationic dye adsorption in single and binary systems, J. Water Process Eng. 54 (2023) 103918.
[272] H. Sun, B. Yu, X. Pan, Z. Liu, MOF Nanosheets-decorated electrospun nanofiber membrane with Ultra-high adsorption capacity for dye removal from aqueous solutions, J. Mol. Liq. 367 (2022) 120367.
[273] S.J. Kim, W.H. Park, Polydopamine- and polyDOPA-coated electrospun poly(vinyl alcohol) nanofibrous membranes for cationic dye removal, Polym. Test. 89 (2020) 106627.
[274] B.M. Thamer, A. Aldalbahi, A. M. Moydeen, A.M. Al-Enizi, H. El-Hamshary, M. H. El-Newehy, Synthesis of aminated electrospun carbon nanofibers and their application in removal of cationic dye, Mater. Res. Bull. 132 (2020) 111003.
[275] H. Pakalapati, P.L. Show, J.-H. Chang, B.-L. Liu, Y.-K. Chang, Removal of dye waste by weak cation-exchange nanofiber membrane immobilized with waste egg white proteins, Int. J. Biol. Macromol. 165 (2020) 2494–2507.
[276] W. Zhu, Z. Wu, S. Zhao, F. Lv, Y. Zhang, S. Guo, Selective adsorption and separation of methylene blue from wastewater by self-standing polyvinylpyrrolidone and SiO2 electrospun membranes, Chem. Eng. Sci. 280 (2023) 119009.
[277] A.A. Sitab, F. Tujjohra, T.U. Rashid, M.M. Rahman, Thermally crosslinked electrospun nanofibrous mat from chrome-tanned solid wastes for cationic dye adsorption in wastewater treatment, Clean. Eng. Technol. 13 (2023) 100621.
[278] X. Li, K. Yi, Q. Ran, Z. Fan, C. Liu, X. Liu, K. Jia, Selective removal of cationic organic dyes via electrospun nanofibrous membranes derived from polyarylene ethers containing pendent nitriles and sulfonates, Sep. Purif. Technol. 301 (2022) 121942.
[279] N.M. Mahmoodi, M. Oveisi, A. Taghizadeh, M. Taghizadeh, Synthesis of pearl necklace-like ZIF-8@chitosan/PVA nanofiber with synergistic effect for recycling aqueous dye removal, Carbohydr. Polym. 227 (2020) 115364.
[280] J.H. Lim, K. Goh, D.Y.F. Ng, J. Chew, R. Wang, Layer-by-layer hierarchically structured nanofibrous membrane scaffolds incorporating metal-organic framework and carbon nanotube adsorbents for high-performance versatile organic solvent recovery, J. Clean. Prod. 404 (2023) 136925.
[281] Z. Wang, S.B. Kang, E. Yang, S.W. Won, Preparation of adsorptive polyethyleneimine/polyvinyl chloride electrospun nanofiber membrane: characterization and application, J. Environ. Manag. 316 (2022) 115155.
[282] K. Kadirvelu, N.N. Fathima, Keratin functionalized electrospun PEI/PAN microfiltration system as a simple and sustainable approach for anionic dye removal, J. Environ. Chem. Eng. 10 (2022) 107791.
[283] J.H. Lim, K. Goh, D.Y.F. Ng, X. Jiang, C.Y. Chuah, J.W. Chew, R. Wang, Alternating spin-and-spray electrospun scaffold membranes with fractionated MIL-101(Cr) adsorbent for high-performance single-pass dye adsorption process, Chem. Eng. J. 450 (2022) 137963.
[284] X. Lu, H. Wang, J. Chen, L. Yang, T. Hu, F. Wu, J. Fu, Z. Chen, Negatively charged hollow crosslinked aromatic polymer fiber membrane for high-efficiency removal of cationic dyes in wastewater, Chem. Eng. J. 433 (2022) 133650.
[285] N. Li, W. Wang, L. Zhu, W. Cui, X. Chen, B. Zhang, Z. Zhang, A novel electro-cleanable PAN-ZnO nanofiber membrane with superior water flux and electrocatalytic properties for organic pollutant degradation, Chem. Eng. J. 421 (2021) 127857.
[286] Z. Hussain, S. Ullah, J. Yan, Z. Wang, I. Ullah, Z. Ahmad, Y. Zhang, Y. Cao, L. Wang, M. Mansoorianfar, R. Pei, Electrospun tannin-rich nanofibrous solid-state membrane for wastewater environmental monitoring and remediation, Chemosphere 307 (2022) 135810.
[287] K. Venkatesh, G. Arthanareeswaran, A.C. Bose, P.S. Kumar, Hydrophilic hierarchical carbon with TiO2 nanofiber membrane for high separation efficiency of dye and oil-water emulsion, Sep. Purif. Technol. 241 (2020) 116709.
[288] H. Piao, J. Zhao, M. Liu, S. Zhang, Q. Huang, Y. Liu, C. Xiao, Ultra-low power light driven lycopodium-like nanofiber membrane reinforced by PET braid tube with robust pollutants removal and regeneration capacity based on photo-Fenton catalysis, Chem. Eng. J. 450 (2022) 138204.
[289] H.M.A. Hassan, I.H. Alsohaimi, M.R. El-Aassar, M.A. El-Hashemy, M.Y. El-Sayed, N.F. Alotaibi, M.A. Betiha, M. Alsuhybani, R.A. Alenazi, Electrospun TiO2-GO/PAN-CA nanofiber mats: A novel material for remediation of organic contaminants and nitrophenol reduction, Environ. Res. 234 (2023) 116587.
[290] H. Lv, M. Zhang, P. Wang, X. Xu, Y. Liu, D.-G. Yu, Ingenious construction of Ni (DMG)2/TiO2-decorated porous nanofibers for the highly efficient photodegradation of pollutants in water, Colloids Surf. A Physicochem. Eng. Asp. 650 (2022) 129561.
[291] G.-Y. Huang, W.-J. Chang, T.-W. Lu, I.L. Tsai, S.-J. Wu, M.-H. Ho, F.-L. Mi, Electrospun CuS nanoparticles/chitosan nanofiber composites for visible and near-infrared light-driven catalytic degradation of antibiotic pollutants, Chem. Eng. J. 431 (2022) 134059.
[292] G. El-Barbary, M.K. Ahmed, M.M. El-Desoky, A.M. Al-Enizi, A.A. Alothman, A. M. Alotaibi, A. Nafady, Cellulose acetate nanofibers embedded with Ag nanoparticles/CdSe/graphene oxide composite for degradation of methylene blue, Synth. Met. 278 (2021) 116824.
[293] C. Porwal, S. Verma, V. Singh Chauhan, R. Vaish, Bismuth zinc borate-Polyacrylonitrile nanofibers for photo-piezocatalysis, J. Ind. Eng. Chem. 124 (2023) 358–367.
[294] S. Yu, Y. Gao, R. Khan, P. Liang, X. Zhang, X. Huang, Electrospun PAN-based graphene/SnO2 carbon nanofibers as anodic electrocatalysis microfiltration membrane for sulfamethoxazole degradation, J. Membr. Sci. 614 (2020) 118368.
[295] A. Moradi, M. Khamforoush, F. Rahmani, H. Ajamein, Synthesis of 0D/1D electrospun titania nanofibers incorporating CuO nanoparticles for tetracycline photodegradation and modeling and optimization of the removal process, Mater. Sci. Eng.: B 297 (2023) 116711.
[296] H. Zhang, J. Zhao, H. Piao, Q. Huang, J. Hu, Y. Xia, M. Zhang, Necklace-like hybrid nanofiber as an enhanced and recyclable intrinsic photocatalyst for tetracycline removal and hydrogen evolution, Mater. Today Commun. 29 (2021) 102761.
[297] Q. Pan, J. Wang, H. Chen, P. Yin, Q. Cheng, Z. Xiao, Y.-z Zhao, H.-B. Liu, Piezo-photocatalysis of Sr-doped Bi4O5Br2/Bi2MoO6 composite nanofibers to simultaneously remove inorganic and organic contaminants, J. Water Process Eng. 56 (2023) 104330.
[298] W. Liu, J. Wang, N. Cai, J. Wang, L. Shen, H. Shi, D. Yang, X. Feng, F. Yu, Porous carbon nanofibers loaded with copper-cobalt bimetallic particles for heterogeneously catalyzing peroxymonosulfate to degrade organic dyes, J. Environ. Chem. Eng. 9 (2021) 106003.
[299] B. Li, B. Qi, Z. Guo, D. Wang, T. Jiao, Recent developments in the application of membrane separation technology and its challenges in oil-water separation: a review, Chemosphere 327 (2023) 138528.
[300] H.M. Mousa, H.S. Fahmy, G.A.M. Ali, H.N. Abdelhamid, M. Ateia, Membranes for oil/water separation: a review, Adv. Mater. Interfaces 9 (2022) 2200557.
[301] N. Yanar, Y. Liang, E. Yang, M. Kim, H. Kim, J. Byun, M. Son, H. Choi, Robust and fouling-resistant ultrathin membranes for water purification tailored via semi-dissolved electrospun nanofibers, J. Clean. Prod. 418 (2023) 138056.
[302] F. Yalcinkaya, A. Gunduz, E. Boyraz, M. Bryjak, Nanofibers for oil-water separation and coalescing filtration, in: A. Kargari, T. Matsuura, M.M.A. Shirazi (Eds.), Electrospun and Nanofibrous Membranes, Elsevier, 2023, pp. 409–432.
[303] D. Ettel, O. Havelka, S. Isik, D. Silvestri, S. Wacławek, M. Urbánek, V.V.T. Padil, M. Černík, F. Yalcinkaya, R. Torres-Mendieta, Laser-synthesized Ag/TiO nanoparticles to integrate catalytic pollutant degradation and antifouling enhancement in nanofibrous membranes for oil–water separation, Appl. Surf. Sci. 564 (2021) 150471.
[304] R. Sarbatly, C.-K. Chiam, An overview of recent progress in nanofiber membranes for oily wastewater treatment, Nanomaterials 12 (2022) 2919.
[305] T. Diwan, Z.N. Abudi, M.H. Al-Furaiji, A. Nijmeijer, A competitive study using electrospinning and phase inversion to prepare polymeric membranes for oil removal, Membranes 13 (2023) 474.
[306] C. Ma, Y. Tian, X. Liu, Y. Li, P. Zhang, X. Chu, L. Wang, B. Zhao, Z. Zhang, Preparation and characterization of double-skinned FO membranes: comparative performance between nanofiber and phase conversion membranes as supporting layers, Process Saf. Environ. Prot. 164 (2022) 807–817.
[307] L.T. Choong, Y.-M. Lin, G.C. Rutledge, Separation of oil-in-water emulsions using electrospun fiber membranes and modeling of the fouling mechanism, J. Membr. Sci. 486 (2015) 229–238.
[308] A. Tanvir, V.P. Ting, S.J. Eichhorn, Nanoporous electrospun cellulose acetate butyrate nanofibres for oil sorption, Mater. Lett. 261 (2020) 127116.
[309] Y. Chen, L. Jiang, Incorporation of UiO-66-NH2 into modified PAN nanofibers to enhance adsorption capacity and selectivity for oil removal, J. Polym. Res. 27 (2020) 69.

[310] F. Yalcinkaya, B. Yalcinkaya, J. Hruza, P. Hrabak, Effect of nanofibrous membrane structures on the treatment of wastewater microfiltration, Sci. Adv. Mater. 9 (2017) 747–757.
[311] K. Lee, G. Kwon, Y. Jeon, S. Jeon, C. Hong, J.W. Choung, J. You, Toward millimeter thick cellulose nanofiber/epoxy laminates with good transparency and high flexural strength, Carbohydr. Polym. 291 (2022) 119514.
[312] J.V. Sanchaniya, I. Lasenko, S.P. Kanukuntla, A. Mannodi, A. Viluma-Gudmona, V. Gobins, Preparation and characterization of non-crimping laminated textile composites reinforced with electrospun nanofibers, Nanomaterials 13 (2023) 1949.
[313] A. Evangelou, K. Loizou, M. Georgallas, E. Sarris, O. Marangos, L. Koutsokeras, S. Yiatros, G. Constantinides, C. Doumanidis, V. Drakonakis, Evaluation of a thermal consolidation process for the production of enhanced technical fabrics, Machines 9 (2021) 143.
[314] C. Su, C. Lu, T. Horseman, H. Cao, F. Duan, L. Li, M. Li, Y. Li, Dilute solvent welding: a quick and scalable approach for enhancing the mechanical properties and narrowing the pore size distribution of electrospun nanofibrous membrane, J. Membr. Sci. 595 (2020) 117548.
[315] D. Li, Y. Shen, L. Wang, F. Liu, B. Deng, Q. Liu, Hierarchical structured polyimide–silica hybrid nano/microfiber filters welded by solvent vapor for air filtration, Polymers 12 (2020) 2494.
[316] K. Shanmugam, Cellulose Nanofiber, Lamination of the Paper Substrates via Spray Coating – Proof of Concept and Barrier Performance, Online Journal of Materials Science 1 (2022) 30–51.
[317] E. Boyraz, F. Yalcinkaya, J. Hruza, J. Maryska, Surface-modified nanofibrous PVDF membranes for liquid separation technology, Materials 12 (2019) 2702.
[318] X. Yang, L. Li, W. Zhao, M. Wang, W. Yang, Y. Tian, R. Zheng, S. Deng, Y. Mu, X. Zhu, Characteristics and functional application of cellulose fibers extracted from cow dung wastes, Materials 16 (2023) 648.
[319] Y. Nie, S. Zhang, Y. He, L. Zhang, Y. Wang, S. Li, N. Wang, One-step modification of electrospun PVDF nanofiber membranes for effective separation of oil-water emulsion, N. J. Chem. 46 (2022) 4734–4745.
[320] R. Su, L. Li, J. Kang, X. Ma, D. Chen, X. Fan, Y. Yu, AgNPs-thiols modified PVDF electrospun nanofiber membrane with a highly rough and pH-responsive surface for controllable oil/ water separation, J. Environ. Chem. Eng. 10 (2022) 108235.
[321] K. Venkatesh, G. Arthanareeswaran, A. Chandra Bose, P. Suresh Kumar, J. Kweon, Diethylenetriaminepentaacetic acid-functionalized multi-walled carbon nanotubes/titanium oxide-PVDF nanofiber membrane for effective separation of oil/water emulsion, Sep. Purif. Technol. 257 (2021) 117926.
[322] X. Huang, S. Zhang, W. Xiao, J. Luo, B. Li, L. Wang, H. Xue, J. Gao, Flexible PDA@ACNTs decorated polymer nanofiber composite with superhydrophilicity and underwater superoleophobicity for efficient separation of oil-in-water emulsion, J. Membr. Sci. 614 (2020) 118500.
[323] Y. Ye, T. Li, Y. Zhao, J. Liu, D. Lu, J. Wang, K. Wang, Y. Zhang, J. Ma, E. Drioli, X. Cheng, Engineering environmentally friendly nanofiber membranes with superhydrophobic surface and intrapore interfaces for ultrafast Oil-water separation, Sep. Purif. Technol. 317 (2023) 123885.
[324] Z. Chu, Y. Li, A. Zhou, L. Zhang, X. Zhang, Y. Yang, Z. Yang, Polydimethylsiloxane-decorated magnetic cellulose nanofiber composite for highly efficient oil-water separation, Carbohydr. Polym. 277 (2022) 118787.
[325] D. Son, S. Kim, J. Kim, D. Kim, S. Ryu, Y. Lee, M. Kim, H. Lee, Surface grafting of a zwitterionic copolymer onto a cellulose nanofiber membrane for oil/water separation, Cellulose 30 (2023) 9635–9645.
[326] Z. Wu, T. Zhang, H. Zhang, R. Liu, H. Chi, X. Li, S. Wang, Y. Zhao, One-pot fabrication of hydrophilic-oleophobic cellulose nanofiber-silane composite aerogels for selectively absorbing water from oil–water mixtures, Cellulose 28 (2021) 1443–1453.
[327] L. Bai, X. Wang, X. Guo, F. Liu, H. Sun, H. Wang, J. Li, Superhydrophobic electrospun carbon nanofiber membrane decorated by surfactant-assisted in-situ growth of ZnO for oil–water separation, Appl. Surf. Sci. 622 (2023) 156938.
[328] Y. Liang, E. Yang, M. Kim, S. Kim, H. Kim, J. Byun, N. Yanar, H. Choi, Lotus leaf-like SiO2 nanofiber coating on polyvinylidene fluoride nanofiber membrane for water-in-oil emulsion separation and antifouling enhancement, Chem. Eng. J. 452 (2023) 139710.
[329] H. Xu, H. Liu, Y. Huang, C. Xiao, Three-dimensional structure design of tubular polyvinyl chloride hybrid nanofiber membranes for water-in-oil emulsion separation, J. Membr. Sci. 620 (2021) 118905.
[330] S. Jiang, X. Meng, B. Chen, N. Wang, G. Chen, Electrospinning superhydrophobic–superoleophilic PVDF-SiO2 nanofibers membrane for oil–water separation, J. Appl. Polym. Sci. 137 (2020) 49546.
[331] Z. Guo, B. Long, S. Gao, J. Luo, L. Wang, X. Huang, D. Wang, H. Xue, J. Gao, Carbon nanofiber based superhydrophobic foam composite for high performance oil/water separation, J. Hazard. Mater. 402 (2021) 123838.
[332] H. Yin, J. Zhao, Y. Li, Y. Liao, L. Huang, H. Zhang, L. Chen, Electrospun SiNPs/ZnNPs-SiO2/TiO2 nanofiber membrane with asymmetric wetting: ultra-efficient separation of oil-in-water and water-in-oil emulsions in multiple extreme environments, Sep. Purif. Technol. 255 (2021) 117687.
[333] D. Gao, B. Xin, M.A.A. Newton, Preparation and characterization of electrospun PVDF/PVP/SiO2 nanofiber membrane for oil-water separation, Colloids Surf. A Physicochem. Eng. Asp. 676 (2023) 132153.
[334] Q. Geng, Y. Pu, Y. Li, X. Yang, H. Wu, S. Dong, D. Yuan, X. Ning, Multi-component nanofiber composite membrane enabled high PM0.3 removal efficiency and oil/water separation performance in complex environment, J. Hazard. Mater. 422 (2022) 126835.
[335] X. Jiang, B. Zhou, J. Wang, Super-wetting and self-cleaning polyvinyl alcohol/sodium alginate nanofiber membrane decorated with MIL-88A(Fe) for efficient oil/water emulsion separation and dye degradation, Int. J. Biol. Macromol. 253 (2023) 127205.
[336] X. Zhang, Y. Liu, F. Zhang, W. Fang, J. Jin, Y. Zhu, Nanofibrous Janus membrane with improved self-cleaning property for efficient oil-in-water and water-in-oil emulsions separation, Sep. Purif. Technol. 308 (2023) 122914.
[337] S. Tian, Y. He, L. Zhang, S. Li, Y. Bai, Y. Wang, J. Wu, J. Yu, X. Guo, CNTs/TiO2-loaded carbonized nanofibrous membrane with two-type self-cleaning performance for high efficiency oily wastewater remediation, Colloids Surf. A Physicochem. Eng. Asp. 656 (2023) 130306.
[338] A. Gul, J. Hruza, F. Yalcinkaya, Fouling and chemical cleaning of microfiltration membranes: a mini-review, Polymers 13 (2021) 846.
[339] A. Gul, J. Hruza, L. Dvorak, F. Yalcinkaya, Chemical cleaning process of polymeric nanofibrous membranes, Polymers 14 (2022) 1102.
[340] J. Kujawa, W. Kujawski, Driving force and activation energy in air-gap membrane distillation process, Chem. Pap. 69 (2015) 1438–1444.
[341] A.S. Jönsson, R. Wimmerstedt, A.C. Harrysson, Membrane distillation - a theoretical study of evaporation through microporous membranes, Desalination 56 (1985) 237–249.
[342] K.W. Lawson, D.R. Lloyd, Membrane distillation, J. Membr. Sci. 124 (1997) 1–25.
[343] W. Jankowski, W. Kujawski, J. Kujawa, Spicing up membrane distillation: enhancing PVDF membrane performance with cinnamic acid, Desalination 575 (2024) 117304.
[344] L.D. Tijing, J.-S. Choi, S. Lee, S.-H. Kim, H.K. Shon, Recent progress of membrane distillation using electrospun nanofibrous membrane, J. Membr. Sci. 453 (2014) 435–462.
[345] L. Meng, L. Wang, Z. Wang, Membrane distillation with electrospun omniphobic membrane for treatment of hypersaline chemical industry wastewater, Desalination 564 (2023) 116782.
[346] Y. Xu, Y. Yang, X. Fan, Z. Liu, Y. Song, Y. Wang, P. Tao, C. Song, M. Shao, In-situ silica nanoparticle assembly technique to develop an omniphobic membrane for durable membrane distillation, Desalination 499 (2021) 114832.
[347] M. Xu, J. Cheng, X. Du, Q. Guo, Y. Huang, Q. Huang, Amphiphobic electrospun PTFE nanofibrous membranes for robust membrane distillation process, J. Membr. Sci. 641 (2022) 119876.
[348] C. Xu, S. Xu, J. Song, N. Jiang, M. Yan, J. Li, M. Huang, Janus C-PAN/PH membrane for simulated shale gas wastewater (SGW) treatment in membrane distillation: integrating surface property and catalytic degradation for anti-fouling, J. Membr. Sci. 683 (2023) 121785.
[349] M.R.S. Kebria, A. Rahimpour, S.K. Salestan, S.F. Seyedpour, A. Jafari, F. Banisheykholeslami, N. Tavajohi, Hassan Kiadeh, Hyper-branched dendritic structure modified PVDF electrospun membranes for air gap membrane distillation, Desalination 479 (2020) 114307.
[350] S. Ding, T. Zhang, M. Wu, X. Wang, Photothermal dual-layer hydrophilic/hydrophobic composite nanofibrous membrane for efficient solar-driven membrane distillation, J. Membr. Sci. 680 (2023) 121740.
[351] Z. Chen, J. Li, J. Zhou, X. Chen, Photothermal Janus PPy-SiO2@PAN/F-SiO2@PVDF-HFP membrane for high-efficient, low energy and stable desalination through solar membrane distillation, Chem. Eng. J. 451 (2023) 138473.
[352] V. Sangeetha, N.J. Kaleekkal, Investigation of the performance of dual-layered omniphobic electrospun nanofibrous membranes for direct contact membrane distillation, J. Environ. Chem. Eng. 10 (2022) 108661.
[353] G.-R. Xu, X.-C. An, R. Das, K. Xu, Y.-L. Xing, Y.-X. Hu, Application of electrospun nanofibrous amphiphobic membrane using low-cost poly (ethylene terephthalate) for robust membrane distillation, J. Water Process Eng. 36 (2020) 101351.
[354] C. Ji, Z. Zhu, L. Zhong, W. Zhang, W. Wang, Design of firm-pore superhydrophobic fibrous membrane for advancing the durability of membrane distillation, Desalination 519 (2021) 115185.
[355] J. Li, L.-F. Ren, H.S. Zhou, J. Yang, J. Shao, Y. He, Fabrication of superhydrophobic PDTS-ZnO-PVDF membrane and its anti-wetting analysis in direct contact membrane distillation (DCMD) applications, J. Membr. Sci. 620 (2021) 118924.
[356] P. Yadav, R. Farnood, V. Kumar, Superhydrophobic modification of electrospun nanofibrous Si@PVDF membranes for desalination application in vacuum membrane distillation, Chemosphere 287 (2022) 132092.
[357] O. Mutlu-Salmanli, B. Eryildiz, V. Vatanpour, Z. Deliballi, B. Kiskan, I. Koyuncu, Fabrication of novel hydrophobic electrospun nanofiber membrane using polybenzoxazine for membrane distillation application, Desalination 546 (2023) 116203.
[358] E. Koh, Y.T. Lee, Preparation of an omniphobic nanofiber membrane by the self-assembly of hydrophobic nanoparticles for membrane distillation, Sep. Purif. Technol. 259 (2021) 118134.
[359] J. Ju, K. Fejjari, Y. Cheng, M. Liu, Z. Li, W. Kang, Y. Liao, Engineering hierarchically structured superhydrophobic PTFE/POSS nanofibrous membranes for membrane distillation, Desalination 486 (2020) 114481.
[360] R. Ding, S. Chen, H. Xuan, B. Li, Y. Rui, Green-solvent-processed amphiphobic polyurethane nanofiber membranes with mechanically stable hierarchical structures for seawater desalination by membrane distillation, Desalination 516 (2021) 115223.
[361] Y.-H. Chiao, M.B.M. Yap Ang, Y.-X. Huang, S.S. DePaz, Y. Chang, J. Almodovar, S. R. Wickramasinghe, A "Graft to" electrospun zwitterionic bilayer membrane for the separation of hydraulic fracturing-produced water via membrane distillation, Membranes 10 (2020) 402.
[362] J. Cai, Z. Liu, F. Guo, Transport analysis of anti-wetting composite fibrous membranes for membrane distillation, Membranes 11 (2021) 14.

[363] L. Zhao, Z. Liu, Z. Wang, S.J.D. Smith, X. Lu, C. Wu, D. Ng, J. Zhang, Q.J. Niu, Z. Xie, MOF incorporated adsorptive nanofibrous membranes for enhanced ammonia removal by membrane distillation, Desalination 568 (2023) 117018.
[364] M.R. Elmarghany, A.H. El-Shazly, S. Rajabzadeh, M.S. Salem, M.A. Shouman, M. Nabil Sabry, H. Matsuyama, N. Nady, Triple-layer nanocomposite membrane prepared by electrospinning based on modified PES with carbon nanotubes for membrane distillation applications, Membranes 10 (2020) 15.
[365] C. Lu, C. Su, H. Cao, T. Horseman, F. Duan, Y. Li, Nanoparticle-free and self-healing amphiphobic membrane for anti-surfactant-wetting membrane distillation, J. Environ. Sci. 100 (2021) 298–305.
[366] L. Jiao, K. Yan, J. Wang, S. Lin, G. Li, F. Bi, L. Zhang, Low surface energy nanofibrous membrane for enhanced wetting resistance in membrane distillation process, Desalination 476 (2020) 114210.
[367] H. Abdelrazeq, M. Khraisheh, F. Al Momani, J.T. McLeskey, M.K. Hassan, M. Gad-el-Hak, H.V. Tafreshi, Performance of electrospun polystyrene membranes in synthetic produced industrial water using direct-contact membrane distillation, Desalination 493 (2020) 114663.
[368] M. Huang, J. Song, Q. Deng, T. Mu, J. Li, Novel electrospun ZIF/PcH nanofibrous membranes for enhanced performance of membrane distillation for salty and dyeing wastewater treatment, Desalination 527 (2022) 115563.
[369] M. Afsari, Q. Li, E. Karbassiyazdi, H.K. Shon, A. Razmjou, L.D. Tijing, Electrospun nanofiber composite membranes for geothermal brine treatment with lithium enrichment via membrane distillation, Chemosphere 318 (2023) 137902.
[370] J. Zhao, Q. Huang, S. Gao, H. Piao, Q. Quan, C. Xiao, In situ photo-thermal conversion nanofiber membrane consisting of hydrophilic PAN layer and hydrophobic PVDF-ATO layer for improving solar-thermal membrane distillation, J. Membr. Sci. 635 (2021) 119500.
[371] A.S. Niknejad, A. Kargari, M. Namdari, M. Pishnamazi, M. Barani, E. Ranjbari, R. Sallakhniknezhad, S. Bazgir, M. Rasouli, D. McAvoy, A scalable dual-layer PAN/SAN nanofibrous membrane for treatment of saline oily water using membrane distillation, Desalination 566 (2023) 116895.
[372] X. Hu, X. Chen, M. Giagnorio, C. Wu, Y. Luo, C. Hélix-Nielsen, P. Yu, W. Zhang, Beaded electrospun polyvinylidene fluoride (PVDF) membranes for membrane distillation (MD), J. Membr. Sci. 661 (2022) 120850.
[373] B. Ozbey-Unal, E. Gezmis-Yavuz, B. Eryildiz, D.Y. Koseoglu-Imer, B. Keskinler, I. Koyuncu, Boron removal from geothermal water by nanofiber-based membrane distillation membranes with significantly improved surface hydrophobicity, J. Environ. Chem. Eng. 8 (2020) 104113.
[374] D. Liu, J. Cao, M. Qiu, G. Zhang, Y. Hong, Enhanced properties of PVDF nanofibrous membrane with liquid-like coating for membrane distillation, Sep. Purif. Technol. 295 (2022) 121282.
[375] L. Zhou, C.L. Li, P.T. Chang, S.H. Tan, A.L. Ahmad, S.C. Low, Intrinsic microspheres structure of electrospun nanofibrous membrane with rational superhydrophobicity for desalination via membrane distillation, Desalination 527 (2022) 115594.
[376] X.-Q. Wu, N.R. Mirza, Z. Huang, J. Zhang, Y.-M. Zheng, J. Xiang, Z. Xie, Enhanced desalination performance of aluminium fumarate MOF-incorporated electrospun nanofiber membrane with bead-on-string structure for membrane distillation, Desalination 520 (2021) 115338.
[377] A.S. Niknejad, S. Bazgir, A. Kargari, Desalination by direct contact membrane distillation using a superhydrophobic nanofibrous poly (methyl methacrylate) membrane, Desalination 511 (2021) 115108.
[378] T. Pan, J. Liu, N. Deng, Z. Li, L. Wang, Z. Xia, J. Fan, Y. Liu, ZnO Nanowires@PVDF nanofiber membrane with superhydrophobicity for enhanced anti-wetting and anti-scaling properties in membrane distillation, J. Membr. Sci. 621 (2021) 118877.
[379] J. Li, D. Wang, J. Zhang, N. Zhang, Y. Chen, Z. Wang, High performance membrane distillation membranes with thermo-responsive self-cleaning capacities, Desalination 555 (2023) 116544.
[380] Y.-H. Chiao, Y. Cao, M.B.M.Y. Ang, A. Sengupta, S.R. Wickramasinghe, Application of superomniphobic electrospun membrane for treatment of real produced water through membrane distillation, Desalination 528 (2022) 115602.
[381] G. Tan, D. Xu, Z. Zhu, X. Zhang, J. Li, Tailoring pore size and interface of superhydrophobic nanofibrous membrane for robust scaling resistance and flux enhancement in membrane distillation, J. Membr. Sci. 658 (2022) 120751.
[382] H.F. Juybari, M. Karimi, R. Srivastava, J. Swaminathan, D.M. Warsinger, Superhydrophobic composite asymmetric electrospun membrane for sustainable vacuum assisted air gap membrane distillation, Desalination 553 (2023) 116411.
[383] W.U. Rehman, A. Khan, N. Mushtaq, M. Younas, X. An, M. Saddique, S. Farrukh, Y. Hu, M. Rezakazemi, Electrospun hierarchical fibrous composite membrane for pomegranate juice concentration using osmotic membrane distillation, J. Environ. Chem. Eng. 8 (2020) 104475.
[384] J. Lee, C. Boo, W.-H. Ryu, A.D. Taylor, M. Elimelech, Development of omniphobic desalination membranes using a charged electrospun nanofiber scaffold, ACS Appl. Mater. Interfaces 8 (2016) 11154–11161.
[385] L. Deng, K. Liu, P. Li, D. Sun, S. Ding, X. Wang, B.S. Hsiao, Engineering construction of robust superhydrophobic two-tier composite membrane with interlocked structure for membrane distillation, J. Membr. Sci. 598 (2020) 117813.
[386] W. Qing, Y. Wu, X. Li, X. Shi, S. Shao, Y. Mei, W. Zhang, C.Y. Tang, Omniphobic PVDF nanofibrous membrane for superior anti-wetting performance in direct contact membrane distillation, J. Membr. Sci. 608 (2020) 118226.
[387] M. Fouladivanda, J. Karimi-Sabet, F. Abbasi, M.A. Moosavian, Step-by-step improvement of mixed-matrix nanofiber membrane with functionalized graphene oxide for desalination via air-gap membrane distillation, Sep. Purif. Technol. 256 (2021) 117809.
[388] H.-S. Park, Y.O. Park, Filtration properties of electrospun ultrafine fiber webs, Korean J. Chem. Eng. 22 (2005) 165–172.
[389] F. Cengiz, O. Jirsak, The effect of salt on the roller electrospinning of polyurethane nanofibers, Fibers Polym. 10 (2009) 177–184.
[390] Top 5 Reasons a Nanofiber Performance Layer Filter is Worth It https://astcanada.ca/resources/technical-articles/filters-parts-articles/top-5-reasons-a-nanofiber-performance-layer-filter-is-worth-it/ AST Canada.
[391] I. Manisalidis, E. Stavropoulou, A. Stavropoulos, E. Bezirtzoglou, Environmental and health impacts of air pollution: a review, Front. Public Health 8 (2020) 14.
[392] G. Wang, J. Deng, Y. Zhang, Q. Zhang, L. Duan, J. Hao, J. Jiang, Air pollutant emissions from coal-fired power plants in China over the past two decades, Sci. Total Environ. 741 (2020) 140326.
[393] M. Zhang, W. Qin, X. Ma, A. Liu, C. Yan, P. Li, M. Huang, C. He, An environmentally friendly technology of metal fiber bag filter to purify dust-laden airflow, Atmosphere 13 (2022) 485.
[394] D. Wei, F. Nielsen, L. Ekberg, A. Löfvendahl, M. Bernander, J.-O. Dalenbäck, PM 2.5 and ultrafine particles in passenger car cabins in Sweden and northern China—the influence of filter age and pre-ionization, Environ. Sci. Pollut. Res. 27 (2020) 30815–30830.
[395] M. Alavy, T. Li, J.A. Siegel, Energy use in residential buildings: analyses of high-efficiency filters and HVAC fans, Energy Build. 209 (2020) 109697.
[396] W.-M. Lu, K.-L. Tung, C.-H. Pan, K.-J. Hwang, The effect of particle sedimentation on gravity filtration, Sep. Sci. Technol. 33 (1998) 1723–1746.
[397] Y. Chuanfang, Aerosol filtration application using fibrous media—an industrial perspective, Chin. J. Chem. Eng. 20 (2012) 1–9.
[398] E.A. Ramskill, W.L. Anderson, The inertial mechanism in the mechanical filtration of aerosols, J. Colloid Sci. 6 (1951) 416–428.
[399] S. Adanur, A. Jayswal, Filtration mechanisms and manufacturing methods of face masks: An overview, J. Ind. Text. 51 (2022) 3683S–3717S.
[400] C.-S. Wang, Electrostatic forces in fibrous filters—a review, Powder Technol. 118 (2001) 166–170.
[401] M.P. Sikka, M. Mondal, A critical review on cleanroom filtration, Res. J. Text. Appar. 26 (2022) 452–467.
[402] A. Vaseashta, N. Bölgen, Electrospun Nanofibers, Springer, 2022.
[403] L. Zhang, Q. Zheng, X. Ge, H. Chan, G. Zhang, K. Fang, Y. Liang, Preparation of nylon-6 micro-nanofiber composite membranes with 3D uniform gradient structure for high-efficiency air filtration of ultrafine particles, Sep. Purif. Technol. 308 (2023) 122921.
[404] R. Chen, H. Zhang, M. Wang, X. Zhang, Z. Gan, Thermoplastic polyurethane nanofiber membrane based air filters for efficient removal of ultrafine particulate matter PM0, ACS Appl. Nano Mater. 4 (1) (2020) 182–189.
[405] A. Sanyal, S. Sinha-Ray, Ultrafine PVDF nanofibers for filtration of air-borne particulate matters: A comprehensive review, Polymers 13 (2021) 1864.
[406] D.S. de Almeida, E.H. Duarte, E.M. Hashimoto, F.R.B. Turbiani, E.C. Muniz, P. R. de Souza, M.L. Gimenes, L.D. Martins, Development and characterization of electrospun cellulose acetate nanofibers modified by cationic surfactant, Polym. Test. 81 (2020) 106206.
[407] G.Cd Mata, M.S. Morais, W.Pd Oliveira, M.L. Aguiar, Composition effects on the morphology of PVA/chitosan electrospun nanofibers, Polymers 14 (2022) 4856.
[408] Z. Sarac, A. Kilic, C. Tasdelen-Yucedag, Optimization of electro-blown polysulfone nanofiber mats for air filtration applications, Polym. Eng. Sci. 63 (2023) 723–737.
[409] V.S. Naragund, P.K. Panda, Electrospun polyacrylonitrile nanofiber membranes for air filtration application, Int. J. Environ. Sci. Technol. (2021) 1–12.
[410] J. Avossa, T. Batt, T. Pelet, S.P. Sidjanski, K. Schönenberger, R.M. Rossi, Polyamide nanofiber-based air filters for transparent face masks, ACS Appl. Nano Mater. 4 (2021) 12401–12406.
[411] Z. Shao, J. Jiang, X. Wang, W. Li, L. Fang, G. Zheng, Self-powered electrospun composite nanofiber membrane for highly efficient air filtration, Nanomaterials 10 (2020) 1706.
[412] J. Johnson, M. Muzwar, S. Ramakrishnan, R. Chetty, A.P. Karaiyan, Electrospun nylon-66 nanofiber coated filter media for engine air filtration applications, J. Appl. Polym. Sci. 140 (2023) e54618.
[413] X. Cheng, L. Zhao, Z. Zhang, C. Deng, C. Li, Y. Du, J. Shi, M. Zhu, Highly efficient, low-resistant, well-ordered PAN nanofiber membranes for air filtration, Colloids Surf. A Physicochem. Eng. Asp. 655 (2022) 130302.
[414] Y. Xiao, E. Wen, N. Sakib, Z. Yue, Y. Wang, S. Cheng, J. Militky, M. Venkataraman, G. Zhu, Performance of electrospun polyvinylidene fluoride nanofibrous membrane in air filtration, Autex Res. J. 20 (2020) 552–559.
[415] J. Xiong, W. Shao, L. Wang, C. Cui, Y. Gao, Y. Jin, H. Yu, P. Han, F. Liu, J. He, High-performance anti-haze window screen based on multiscale structured polyvinylidene fluoride nanofibers, J. Colloid Interface Sci. 607 (2022) 711–719.
[416] M. Kwon, J. Kim, J. Kim, Photocatalytic activity and filtration performance of hybrid TiO2-cellulose acetate nanofibers for air filter applications, Polymers 13 (2021) 1331.
[417] R. Chueachot, V. Promarak, S. Saengsuwan, Enhancing antibacterial activity and air filtration performance in electrospun hybrid air filters of chitosan (CS)/AgNPs/PVA/cellulose acetate: effect of CS/AgNPs ratio, Sep. Purif. Technol. 338 (2024) 126515.
[418] G. Ungur, J. Hrůza, Modified nanofibrous filters with durable antibacterial properties, Molecules 26 (2021) 1255.
[419] Z. Yao, M. Xia, Z. Xiong, Y. Wu, P. Cheng, Q. Cheng, J. Xu, D. Wang, K. Liu, A hierarchical structure of flower-like zinc oxide and poly (vinyl alcohol-co-ethylene) nanofiber hybrid membranes for high-performance air filters, ACS Omega 7 (2022) 3030–3036.

[420] S.F. Dehghan, F. Golbabaei, T. Mousavi, H. Mohammadi, M.H. Kohneshahri, R. Bakhtiari, Production of nanofibers containing magnesium oxide nanoparticles for the purpose of bioaerosol removal, Pollution 6 (2020) 185–196.
[421] M. Chen, J. Jiang, S. Feng, Z.-X. Low, Z. Zhong, W. Xing, Graphene oxide functionalized polyvinylidene fluoride nanofibrous membranes for efficient particulate matter removal, J. Membr. Sci. 635 (2021) 119463.
[422] Q. Wang, O. Yildiz, A. Li, K. Aly, Y. Qiu, Q. Jiang, D.Y.H. Pui, S.-C. Chen, P. D. Bradford, High temperature carbon nanotube–nanofiber hybrid filters, Sep. Purif. Technol. 236 (2020) 116255.
[423] H. Lee, S. Jeon, Polyacrylonitrile nanofiber membranes modified with Ni-based conductive metal organic frameworks for air filtration and respiration monitoring, ACS Appl. Nano Mater. 3 (2020) 8192–8198.
[424] Z. Niu, C. Xiao, J. Mo, L. Zhang, C. Chen, Investigating the influence of metal–organic framework loading on the filtration performance of electrospun nanofiber air filters, ACS Appl. Mater. Interfaces 14 (2022) 27096–27106.
[425] J.H. Lee, H.J. Oh, Y.K. Park, Y. Kim, G. Lee, S.J. Doh, W. Lee, S.-J. Choi, K. R. Yoon, Multi-scale nanofiber membrane functionalized with metal-organic frameworks for efficient filtration of both PM2. 5 and CH3CHO with colorimetric NH3 detection, Chem. Eng. J. 464 (2023) 142725.
[426] L. Wang, Y. Bian, C.K. Lim, Z. Niu, P.K.H. Lee, C. Chen, L. Zhang, W.A. Daoud, Y. Zi, Tribo-charge enhanced hybrid air filter masks for efficient particulate matter capture with greatly extended service life, Nano Energy 85 (2021) 106015.
[427] W. Zhao, M. Wang, Y. Yao, Z. Cheng, Y. Zhang, J. Tao, J. Xiong, H. Lin, Y. Chen, H. Cao, Hyperbranched Quaternary Ammonium Salt Induced Antibacterial Tree-Like Nanofibrous Membrane for High Effective Air Filtration, Available at SSRN 4462989.
[428] W. Shao, J. Niu, R. Han, S. Liu, K. Wang, Y. Cao, P. Han, X. Li, H. Zhang, H. Yu, Electrospun multiscale poly (lactic acid) nanofiber membranes with a synergistic antibacterial effect for air-filtration applications, ACS Appl. Polym. Mater. 5 (2023) 9632–9641.
[429] M.S. Rafique, M.B. Tahir, M. Rafique, M. Shakil, Photocatalytic nanomaterials for air purification and self-cleaning. in: Nanotechnology and Photocatalysis for Environmental Applications, Elsevier, 2020, pp. 203–219.
[430] S. Sepahvand, A. Ashori, M. Jonoobi, Application of cellulose nanofiber as a promising air filter for adsorbing particulate matter and carbon dioxide, Int. J. Biol. Macromol. 244 (2023) 125344.
[431] Y. Liu, H. Shao, H. Wang, Z. Ji, R. Bai, F. Chen, B. Li, C. Chang, T. Lin, Improvement of air filtration performance using nanofibrous membranes with a periodic variation in packing density, Adv. Mater. Interfaces 9 (2022) 2101848.
[432] F. Xie, Y. Wang, L. Zhuo, F. Jia, D. Ning, Z. Lu, Electrospun wrinkled porous polyimide nanofiber-based filter via thermally induced phase separation for efficient high-temperature PMs capture, ACS Appl. Mater. Interfaces 12 (2020) 56499–56508.
[433] F. Xie, Y. Wang, L. Zhuo, D. Ning, N. Yan, J. Li, S. Chen, Z. Lu, Multiple hydrogen bonding self-assembly tailored electrospun polyimide hybrid filter for efficient air pollution control, J. Hazard. Mater. 412 (2021) 125260.
[434] F. Lopresti, I. Keraite, A.E. Ongaro, N.M. Howarth, V. La Carrubba, M. Kersaudy-Kerhoas, Engineered membranes for residual cell trapping on microfluidic blood plasma separation systems: a comparison between porous and nanofibrous membranes, Membranes 11 (2021) 680.
[435] A. Mamun, T. Blachowicz, L. Sabantina, Electrospun nanofiber mats for filtering applications—technology, structure and materials, Polymers 13 (2021) 1368.
[436] M.V. Rodrigues, M.A.S. Barrozo, J.A.S. Gonçalves, J.R. Coury, Effect of particle electrostatic charge on aerosol filtration by a fibrous filter, Powder Technol. 313 (2017) 323–331.
[437] S. Habibi, A. Ghajarieh, Application of nanofibers in virus and bacteria filtration, Russ. J. Appl. Chem. 95 (2022) 486–498.
[438] A.B. Alayande, Y. Kang, J. Jang, H. Jee, Y.-G. Lee, I.S. Kim, E. Yang, Antiviral nanomaterials for designing mixed matrix membranes, Membranes 11 (2021) 458.
[439] A.K. Selvam, G. Nallathambi, Polyacrylonitrile/silver nanoparticle electrospun nanocomposite matrix for bacterial filtration, Fibers Polym. 16 (2015) 1327–1335.
[440] V. Felix Swamidoss, M. Bangaru, G. Nalathambi, D. Sangeetha, A.K. Selvam, Silver-incorporated poly vinylidene fluoride nanofibers for bacterial filtration, Aerosol Sci. Technol. 53 (2019) 196–206.
[441] Y. Liu, S. Li, W. Lan, M.A. Hossen, W. Qin, K. Lee, Electrospun antibacterial and antiviral poly(ε-caprolactone)/zein/Ag bead-on-string membranes and its application in air filtration, Mater. Today Adv. 12 (2021) 100173.
[442] G. Pullangott, U. Kannan, S. G, D.V. Kiran, S.M. Maliyekkal, A comprehensive review on antimicrobial face masks: an emerging weapon in fighting pandemics, RSC Adv. 11 (2021) 6544–6576.
[443] R. Bai, Q. Zhang, L. Li, P. Li, Y.-J. Wang, O. Simalou, Y. Zhang, G. Gao, A. Dong, N-halamine-containing electrospun fibers kill bacteria via a contact/release co-determined antibacterial pathway, ACS Appl. Mater. Interfaces 8 (2016) 31530–31540.
[444] H. Ma, B.S. Hsiao, B. Chu, Functionalized electrospun nanofibrous microfiltration membranes for removal of bacteria and viruses, J. Membr. Sci. 452 (2014) 446–452.
[445] A. Sato, R. Wang, H. Ma, B.S. Hsiao, B. Chu, Novel nanofibrous scaffolds for water filtration with bacteria and virus removal capability, J. Electron Microsc. 60 (2011) 201–209.
[446] S.P. Sundaran, C.R. Reshmi, P. Sagitha, O. Manaf, A. Sujith, Multifunctional graphene oxide loaded nanofibrous membrane for removal of dyes and coliform from water, J. Environ. Manag. 240 (2019) 494–503.
[447] D. Hussain, S.T. Raza Naqvi, M.N. Ashiq, M. Najam-ul-Haq, Analytical sample preparation by electrospun solid phase microextraction sorbents, Talanta 208 (2020) 120413.
[448] Q. Wu, D. Wu, Y. Guan, Fast equilibrium micro-extraction from biological fluids with biocompatible core–sheath electrospun nanofibers, Anal. Chem. 85 (2013) 5924–5932.
[449] R.D. Katigbak, L.F. Dumée, L. Kong, Isolating motile sperm cell sorting using biocompatible electrospun membranes, Sci. Rep. 12 (2022) 6057.
[450] F. Barati, A.M. Farsani, M. Mahmoudifard, A promising approach toward efficient isolation of the exosomes by core–shell PCL-gelatin electrospun nanofibers, Bioprocess Biosyst. Eng. 43 (2020) 1961–1971.
[451] B. Subeshan, A. Atayo, E. Asmatulu, Machine learning applications for electrospun nanofibers: a review, J. Mater. Sci. 59 (2024) 14095–14140.